Identification and Characterization of a Novel Voltage Gating Mechanism in Extracellular-pH-sensitive K2P Channels

Dissertation

zur Erlangung des Doktorgrades
der Mathematisch-Naturwissenschaftlichen Fakultät
der Christian-Albrechts-Unversität
zu Kiel

vorgelegt von
Ehsanollah Nematian Ardestani

Kiel, Juli 2017

Erster Gutachter: Prof. Dr. rer. nat. Thomas Baukrowitz

Zweiter Gutachter: Prof. Dr. rer. nat. Eric Beitz

Tag der Disputation: 29.09.2017

To my mother

Acknowledgements

First and foremost I would like to thank my supervisor Prof. Thomas Baukrowitz for his support and guidance during my time in his lab as a PhD candidate. Furthermore his trust and patience was very encouraging and inspirational for doing science.

This work is part of a shared project between my colleague, Dr. Marcus Schewe, and myself, as we were both doing our PhD studies, through which we shared and discussed experience, data and results. I would like to extend special thanks to him for his support and collaboration during years of our research. I would also like to extend my gratitude to my other colleagues in the lab and the institute of physiology, especially Dr. Hariolf Fritzenschaft, Mrs. Ria Neumann and Mrs. Michaela Unmack, without whose support this work would be impossible.

Finally I would like to thank Prof. Stephen J. Tucker, Prof. Bert de Groot and Dr. Han Sun for their positive feedbacks, answering my questions and providing supportive data.

Abstract

By contributing to the establishment of the resting membrane potential and repolarization after an action potential, K2P channels play a major role in the electrical excitability and activity of the cells. In this work I investigated the voltage-dependent gating properties of extracellular pH (pH_{ex}) sensitive K2P channels (TASK, TALK and TWIK subfamilies) and discovered a novel voltage-sensing mechanism. Unlike the canonical voltage-activated ion channels (Ca_V, K_V and Na_V) that use a charged membrane domain to sense voltage, the voltage sensor in K2P channels is formed by the selectivity filter which gates open or close in response to rearrangement of the ions within it. The rearrangement is determined by both the permeant ion species and direction of the ion flow. Outward flow of the ions leads to opening of filter whereas the inward flow shots the filter closed. To explain the underlining structural mechanisms of this "ion-flux check valve" gating, in this study, two distinct but intertwined mechanisms are introduced, namely the "Pause-and-Turn" and the "Ion-Zipper" models. I also show that mutations within the selectivity filter can abolish the voltage gating of the pH_{ex} sensitive K2P channel and make them permanently open at all voltages, which emphasizes the role of the selectivity filter for voltage gating. In addition to voltage, various other stimuli including membrane stretch, temperature, intracellular H^+ and numerous lipids are known to induce strong activation in some K2P channels (e.g. in TREK-1, TREK-2 and TRAAK). Remarkably, these activators abolish voltage activation and convert these K2P channels into open leak channels, but for the pH_{ex} sensitive K2P channels such activators are not known. This suggests that ion-flux voltage activation described here is the predominant gating mechanism in these K2P channels.

Unlike most other K2P channels TWIK-1 channels exhibit very little activity in cells. This is explained in part by strong retention of these channels in the ER. However, even when the responsible retention motif is removed and channels translocate to the plasma membrane their activity is still very low. To understand this better I investigated the voltage gating properties in TWIK-1, which revealed a number of significant differences to the other K2P channels. Firstly, in TWIK-1 ion-flux activation occurs only at very positive voltages and, thus, outside the physiological range. Secondly, with non-physiological ions such as Rb^+ strong activation at physiological voltages was observed as in other K2P channels but this voltage activation was independent of the ion flow direction and blocked by unusual low K^+ concentrations. Finally, TWIK-1 activity was inhibited by intracellular

H^+ resulting in low activity at physiological pH. In summary, these unusual gating features in TWIK-1 can explain the low activity of these channels in the plasma membrane.

Kurzreferat

Die Familie der K2P Kanäle zählt 15 humane Mitglieder, die in sechs Unterfamilien eingeteilt werden und maßgeblich an der Etablierung des Ruhemembranpotentials und der Repolarisation von Aktionspotentialen beteiligt sind. In dieser Arbeit wurde die Aktivierung von Mitgliedern der TASK, TALK und TWIK Unterfamilien durch Veränderung der Membranspannung untersucht. Diese Kanäle werden alle durch den extrazellulären pH reguliert und hier als pH_{ex}-regulierte K2P Kanäle zusammengefasst. Ich konnte zeigen, dass diese Kanäle durch einen neuartigen Mechanismus auf Änderungen der Spannung reagieren. Kanonische spannungsabhängige Ionenkanälen (Ca_V, K_V und Na_V Kanäle) benutzen eine geladene Membrandomäne, die sich in Abhängigkeit von der Spannung bewegt und dadurch die Öffnung der Kanalpore kontrolliert. Der Spannungssensor in K2P Kanälen befindet sich hingegen im Selektivitätsfilter,dessen Ionenbesatz sich in Abhängigkeit der permierenden Ionenspezies und der Membranspannung ändert. Dabei zeigte sich, dass die Auswärtsbewegung von Ionen den Filter öffnet, während Einwärtsbewegung den Filter schließt. Um diesen stromrichtungsabhängigen „Ventilklappenmechanismus“ zu erklären, werden zwei unterschiedliche, aber miteinander verwobene Mechanismen dargestellt – ein „Pause-and-Turn“ und ein „Ion-Zipper“ Mechanismus. Außerdem konnte ich zeigen, dass Mutationen im Selektivitätsfilter den „Ventilklappenmechanismus“ ausschalten und zu permanent geöffneten Kanälen führen. Einige K2P Kanäle (z.B. TREK-1, TREK-2 und TRAAK) werden neben Membrandepolarisation durch verschiedene anderer physiologischer Stimuli aktiviert (z.B. mechanischer Stress, Temperatur und verschiedene Lipide) und verlieren dabei das spannungsabhängige Schaltverhalten. Solche Aktivatoren sind für die pHex-regulierten K2P Kanäle nicht bekannt. Dies impliziert, dass der hier beschriebene „Ventilklappenmechanismus“ der physiologisch wichtigste Regulationsmechanismus dieser Kanäle ist (neben der extrazellulären pH Empfindlichkeit).

Im Gegensatz zu den meisten anderen K2P Kanälen zeigen TWIK-1 Kanäle nur kleine Ströme in Zellen. Dies ist zum Teil dadurch erklärt, dass TWIK-1 Kanäle durch ein “ER-retention motif” im ER zurückgehalten werden. Aber auch wenn TWIK-1 Kanäle in hoher Konzentration in die Zellmembran translozieren (nach Entfernung des “ER-retention motif`s”) zeigen sie nur eine geringe Aktivität (d.h. Offenwahrscheinlichkeit). Um dieses

Eigenschaft besser zu verstehen, habe ich das spannungsabhängige Schaltverhalten der TWIK-1 Kanälen untersucht. Dabei zeigten sich eine Reihe deutlicher Unterschiede zum Schaltverhalten der anderen K2P Kanäle. Erstens, TWIK-1 werden zwar durch Membrandepolarisation aktiviert, aber die notwendigen positiven Spannungen waren viel höher und weit außerhalb des physiologischen Spannungsbereichs. Zweitens, TWIK-1 Kanäle werden ebenso wie viele andere K2P Kanäle durch nicht-physiologische Ionen wie Rb^+ stark aktiviert, aber die aktivierten Ströme zeigten keine Abhängigkeit von der Stromrichtung (fehlender „Ventilklappenmechanismus“) und wurden außerdem durch ungewöhnlich niedrige K^+ Konzentration blockiert. Des Weiteren zeigen TWIK-1 Kanäle eine deutlich Inhibition durch intrazelluläre H^+ im physiologischen pH Bereich (was in anderen K2P Kanälen nicht beobachtet wurde). Diese ungewöhnlichen Schalteigenschaften der TWIK-Kanäle (d.h. geringe Spannungsaktivierung und starke intrazelluläre pH Inhibition) erklären die sehr niedrige Aktivität von TWIK-1 Kanälen in der Zellmembran.

Table of contents

Table of figures

1. Introduction

1.1. Prologue

All living cells use the membrane potential to generate and maintain ion and water homeostasis, absorb nutrients like amino acids and glucose, and to generate, process and transfer information. Ion channels play a crucial role in this process. Among the ensemble of ion channels in the plasma membrane there are many types of K^+ channels that function together with other components of the cell to finely tune cellular processes. They are involved in setting the resting membrane potential, volume regulation, enzyme and hormone secretion, cell proliferation and differentiation, and control of the frequency and duration of action potentials. Therefore, it is essential to understand the mechanisms that govern K^+ channels function in order to understand the role that these channels play in both normal physiology as well as pathophysiological conditions.

In their pioneering work Hodgkin and Huxley recognized that in addition to the major components of sodium and potassium currents, a minor current component also existed which was a small relatively voltage-independent background conductance of undetermined ionic basis. This component was dubbed the leak current [1]. Typically, the resting membrane potential is close to E_K, because K^+ channels densely populate most cell membranes. Therefore cellular leak currents are attributed to open K^+ channels. These include K^+ currents passed by inwardly rectifying K^+ (K_{ir}) channels. It has been suggested that K_{ir} channels determine the inward-rectifying branch of the background K^+ current [2]. However these channels are closed at positive potentials due to block by intracellular polyamines such as spermine, as well as intracellular Mg^{2+}. Therefore strongly rectifying K_{ir} channels are conductive when excitable cells are at rest, and nonconductive during excitation i.e. when depolarized. However there is an outwardly-rectifying component to these leak currents and also K^+ leak currents during a typical action potential. Both of which are attributed to the Two-Pore Domain family of K^+ channels, the last discovered family of mammalian K^+ channels.

The Two-Pore Domain (K2P) K^+ channels are the predominant contributors to background (leak) K^+ currents. However as it may first imply, K2P channels are not simple passive permanently open channels. If K2P channels were open at any voltage, then during depolarization they would short-circuit the membrane potential. However, K2P channels open and close in response to a variety of stimuli, such as neurotransmitters, volatile anesthetics and changes in pH. Therefore as mentioned above, they are not just passive permanently open leak channels.

Encoded by 15 *KCNK* genes in human and divided into 6 subfamilies (Fig. 1.11), K2P channels are subject to alternative transcription initiation, splicing, translation initiation, heteromerization and post-translational modifications to add to their diversity and functionality [3]. In this work, I have studied the voltage regulation of three subfamilies of K2P channels, namely; TWIK, TASK and TALK channels. Later on, these channels are referred to as pH_{ex}-sensitive K2P channels, since all of them are regulated by extracellular pH changes. First I discuss the general and common structural features of K2P channels based on the solved structures of TWIK-1, TRAAK, and TREK-2 and then look at regulation of the K2P channels followed by physiological and pathological roles of three K2P channels subfamilies that were studied in this work. At the end of this chapter pharmacological modulation of these channels is also discussed.

1.2. Structure of K2P channels

1.2.1. General information.

K2P channels possess four distinct structural features that separate them from all other K^+ channels. Specific structural features of K2P channels are:

1- Two pore domains in one subunit
2- An extracellular structure (CAP domain) that spans about 35 Å over selectivity filter (SF). This is a segment in the first pore domain that connects the outer transmembrane helix to the pore helix.
3- Unusual selectivity filter
4- Open cytoplasmic side to the intracellular cavity.

All K^+ channels' pores are composed of four pore-forming (P) domains. Each P domain contains an outer transmembrane helix, a pore helix, a SF signature sequence, and an inner transmembrane helix [4]. The crystal structures of K^+ channels determined to date are of tetrameric channels, with four identical subunits that each contain one P domain. In contrast to this general structure each subunit of dimeric K2P channels contains two P domain sequences (P domain 1 and P domain 2) arranged in tandem [5, 6]. As a result each K2P channel subunit contains four transmembrane helices M1 to M4 (Fig 1.1). M1 is the outer helix of P1 domain and M2 is the inner helix. In the same manner M3 and M4 are the outer and inner helices of P2 domain, receptively (Fig.1.1). Pore helices span about 35 Å in a lipid membrane [5, 6]. Despite this unique structural assembly, the crystal structures of TWIK-1 and TRAAK show that although K2P channels are dimeric, they also recapitulate the fundamental architecture of tetrameric K^+ channels [5, 6]. This suggests that each subunit could have been evolved from duplication of an ancestral gene. As each domain of the gene can evolve independent from other sections, the two pore domains are not identical and show differences that can provide insights into the gating and permeation of these channels.

The two pore domains in each subunit are distinct from each other in 3 features;

1- In P1 the linker between the first transmembrane helix (M1) and the pore helix consists of two extracellular helices of about 56 residues. These helices intertwine with those of the adjacent subunit and together make the extracellular domain, CAP structure, which is stabilized via a disulfide bridge by a conserved cysteine residue at the apex of each subunit, except for in TASK-1 and TASK-3 channels [3]. However the linker in P2 is like other K^+ channels; short (5-20 residues) and makes a turret (Fig 1.1 and 1.2).
2- In P1 the linker between the SF and inner transmembrane helix (M2) is shorter than that in P2 and like other K^+ channels interacts with the outer transmembrane helix (M1) which as a result tethers the extracellular ends of M1 and M2. However the corresponding linker in P2 is longer and pushes the inner transmembrane helix (M4) away from the channel core. Therefore the existing interactions in P1 are not observed in P2 and the extracellular ends of M3 and M4 do not connect together (Fig 1.3). As we learn later this feature of K2P channels have a key role in the response of this family of K^+ channels to regulatory signals.

3- In P1, on M2, two residues downstream of the hinge glycine, that is conserved in all K^+ channels, there is a conserved proline (except for the THIK subfamily) where the inner transmembrane helix kinks halfway through the membrane and goes down toward the cytoplasmic side of the membrane less sharply than M4, about 20° in TWIK-1 at Pro143 and 25° in TRAAK at Pro155 (Fig 1.3 and 1.4) [5, 6]. In contrast to that, like in other K^+ channels the inner transmembrane helix (M4) in P2 lacks the kink due to the absence of the corresponding proline, although the hinge glycine is also preserved in P2. (Fig 1.3) [5, 6]. In TREK-2 these glycines are involved in transduction of signals from C-terminus to the SF and vice versa [7].

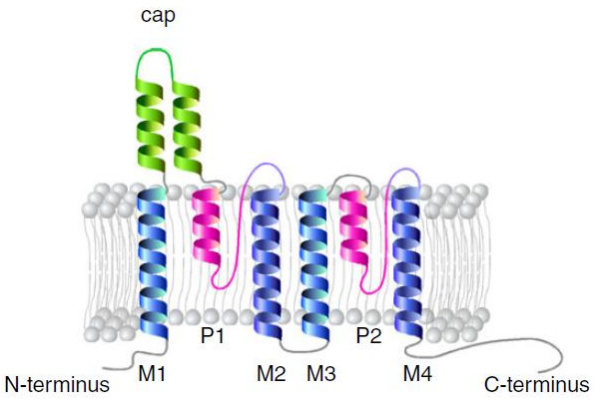

Fig. 1.1. The schematic constituent assembly of a typical subunit from the K2P family. Two subunits join to make a functional channel [3].

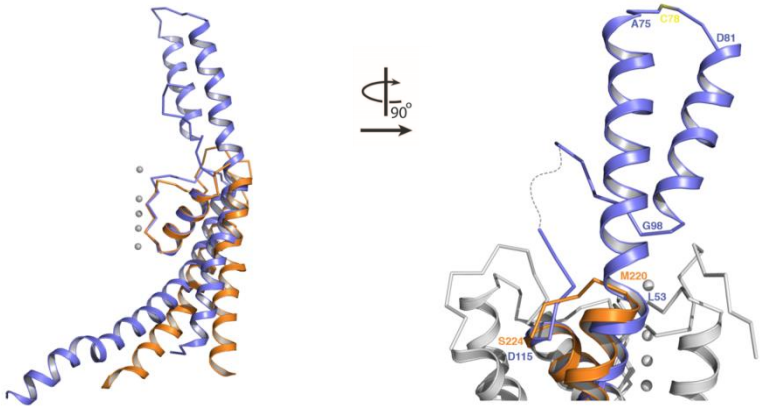

Fig. 1.2. P1 (blue) and P2 (orange) superimposed to compare the long extracellular linkers between M1 and pore helix1 in P1 and the short linker between M3 and pore helix2 in P2. [6].

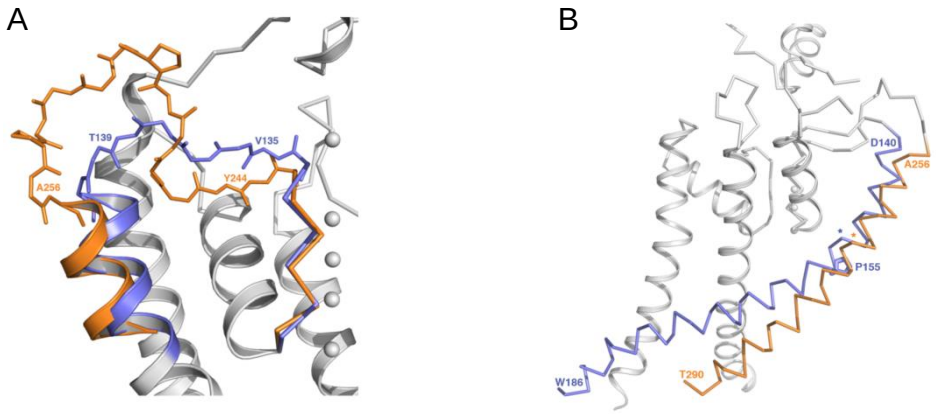

Fig.1.3. (A); P1 (blue) and P2 (orange) superimposed to compare the linker between the SF sequence and M2 in P1 and the linker between the SF sequence and M4 in P2. Note that M4 (orange) is pushed away in comparison to M2 (blue). (B); M2 from P1 (blue) and M4 from P2 are superimposed to show the kink on M2 due to the Pro155 [6].

1.2.2. Structural components of K2P channels.

The overall structure of the K2P channel can be dissected into four distinct sections. However TWIK-1 has an additional helix at cytoplasmic side of the channel that does not exist in other K2P channels. In the following these structural features are discussed in more detail.

1.2.2.1. Cap structure and extracellular ion pathways.

Early studies before the structures of K2P channels were resolved showed that these channels are generally resistant to blockers (e.g. Tetraethylammonium (TEA)) and toxins which inhibit ion flow through other K^+ channels when applied from extracellular side, however these compounds are still capable of inhibiting these channels from the intracellular side [8]. Even mutation of residues around the upper mouth of the SF to those found in K_V channels did not made K2P channels sensitive to these blockers [9]. The first crystal structures of K2P channels showed that, unlike tetrameric K^+ channels, K2P channels have an extracellular region of about 55 amino acids within the P1 domain, between M1 and pore helix 1, which extends about 35 Å above the membrane, that neither is present in the P2 domain of K2P channels nor is found in tetrameric K^+ channels (Fig. 1.4) [5]. These residues comprise two helices E1 and E2 which extend upward and downward, respectively. At the apex of this structure there is a conserved cysteine that makes a covalent bond with the adjacent subunit [5, 6]. The rest of the cap structure is held

together via a hydrophobic core that is constituted from interaction of highly conserved hydrophobic residues from two adjacent subunits [6].

The existence of the cap structure restricts direct access of extracellular ions to the SF. Ion flow is therefore funneled in and out through two side pathways that join together above the SF (Fig. 1.5). The walls through the two side pathways are covered by residues which contribute negative charges to them. In addition the C-terminus of the E2 helices also contribute to negative charges within the ion pathway in the cap just above the SF, causing an increase in the local concentration of cations over the SF [5]. Moreover in acid sensitive K2P channels like TASK-1 and TASK-3 and also TWIK-1 that has similar pH sensitivity to that of TASK subfamily, the restricted space ensures a higher concentration of H^+ near the extracellular pH sensor. On the other hand, the existence of the cap structure and the two side pathways inside it explains why many K^+ channel blockers cannot inhibit K2P channels from the extracellular side, although they can if applied from intracellular side.

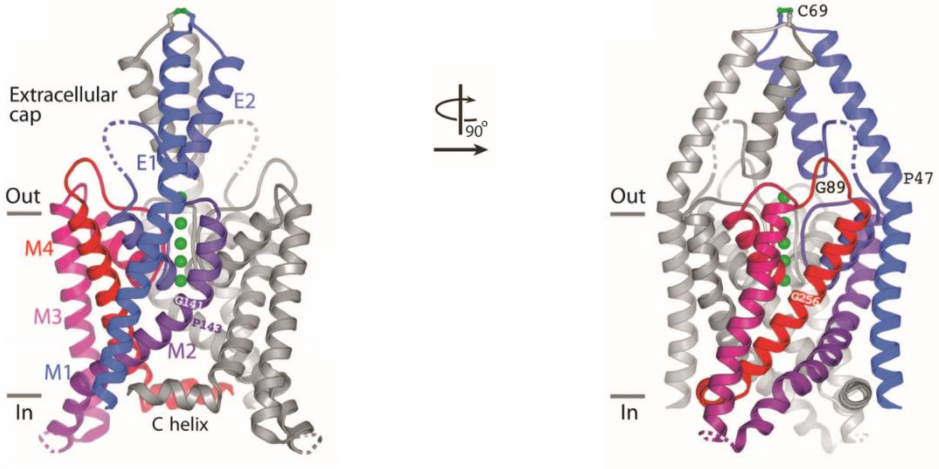

Fig.1.4. TWIK-1 cartoon presentation. Transmembrane helices M1-M4 are color coded and hinge glycines (Gly141 and Gly256) and kink proline (Pro143) are marked. K^+ ions in the SF are presented as green spheres. Dotted lines present areas with unsolved structure [5].

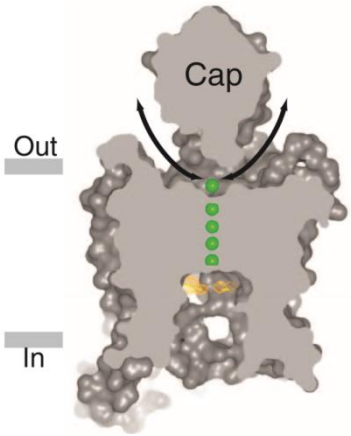

Fig.1.5. Ion pathways on two sides of the cap structure that function like funnels, connecting the SF to the extracellular medium through the cap. The ion pathways are shown with black arrows [5].

1.2.2.2. Pore structure and the lower gate:

In general, potassium channel gating is controlled by two separate gates; one is the C-type or outer gate that involves the SF and directly interacts with permeating ions whilst the second gate is at the cytoplasmic side of the channel, which is made from flexible pore lining transmembrane helices, structurally equivalent to M2 and M4 of K2P channels. However in the crystal structure of both TWIK-1 and TRAAK the inner helices resemble the open state of other K^+ channels, distanced from each other more than 11Å, which suggests that the crystalized channel is in the open state (Fig. 1.6 and 1.7) [5, 6]. As in tetrameric K^+ channels, a central cavity is located just below the SF, near the center of the membrane (Fig. 1.1 and 1.6)

In non-K2P K^+ channels, a glycine residue that is located on the inner helices near the midpoint of the membrane serves as a gating hinge that permits the inner helices to bend as they constrict and dilate the pore near the intracellular side. In K2P channels the equivalent glycine residues are strictly conserved in both inner helices (Fig. 1.7). This suggests that the inner helices may move in an analogous fashion. However it has been shown that in TREK-1 channels both quaternary ammonium (QA) ions such as tetrahexylammonium (THA) which binds in the pore under the SF to block ion flux and also chemically reactive QAs such as 8-(Tributylammonium)octyl Methanethiosulfonate (MTS-TBAO) which covalently bind to an introduced cysteine in the pore and permanently blocks the channels, can freely access the central cavity even when the channels are functionally closed [8, 10]. Moreover, as crystal structures of the TRAAK channel were resolved, Brohawn *et. al.*

proposed that structural features of the channel in P1, such as the conserved kink at P155, interaction of M2 with the membrane after the kink, and the peptide linker between M2 to M3, together restrict the ability of the pore-lining TMs to constrict the entrance to the inner cavity [6]. We have also recently showed that the rate of modification-block by MTS-TBAO is very similar in both closed and open states, which confirms that during gating the inner helices do not move and the pore is wide open [126].

The crystal structures of K2P channels show that the transmembrane helices (M1-M4) are rather flexible and can move or rearrange the side chains of the residues in response to various regulatory stimuli. [11,12]. It has been suggested that these movements couple these regulatory signals to gating at the SF [11]. This is particularly relevant in TREK channels where M4 is followed by a large C-terminal regulatory domain which is the target for pH sensing, arachidonic acid binding and phosphorylation [11]. Indeed, using gain of function mutants, it has been shown that the SF is the common gate used in K2P channels to respond to different inhibitory or stimulatory inputs [13]. Based on these experiments it has also been suggested that the movement of the N-terminal region of M4 may have a central role to integrate signals from different sensors throughout the channel structure towards the SF [13]. Recent crystal structures of TRAAK and TREK-2 supports such movements of M4, and suggest that ion occupancy of the SF would be changed accordingly [11, 14]. The long linker between the SF and M4 (in comparison to that of P1) possibly gives flexibility to the N-terminus of M4 which supports that idea.

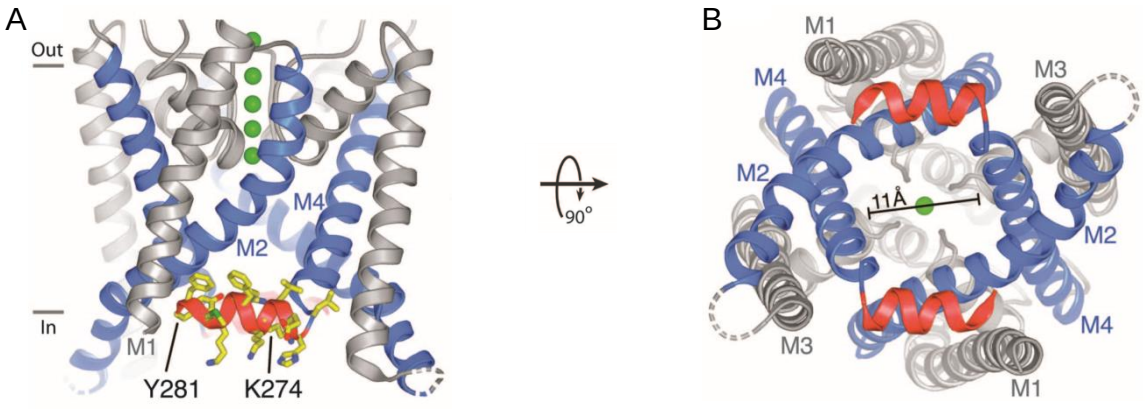

Fig. 1.6. TWIK-1. The inner helices are colored blue, the C-helices are red, and the remaining portions are gray. K^+ ions are shown as green spheres. In (A), residues on the C-helix in the foreground are drawn as sticks (yellow, carbon; blue, nitrogen; red, oxygen; green, sulfur) [5].

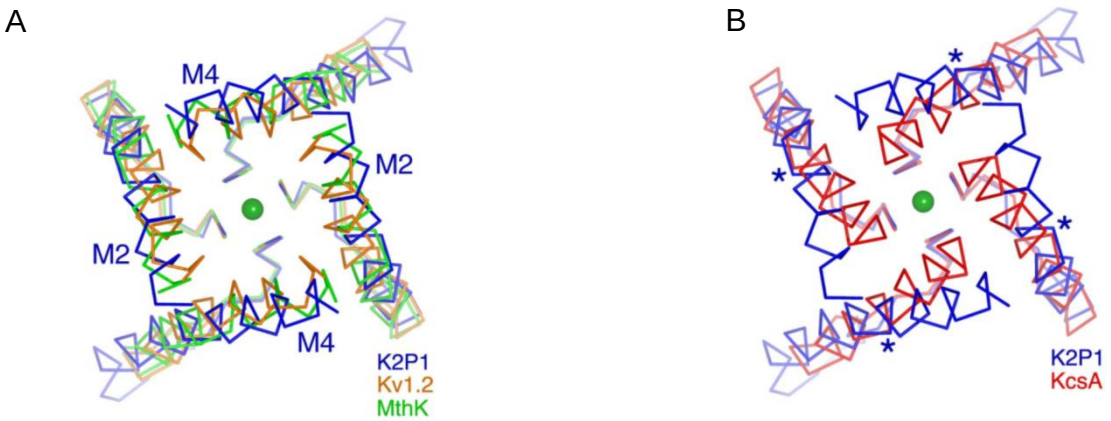

Fig. 1.7. (A); superimposition of TWIK-1 (K2P1), K_V1.2 and MthK channels in the open state from intracellular side. (B); superimposition of TWIK-1 in open and KcsA in closed states from the intercellular side. Notice that in the open state they overlay nicely but in the closed state KcsA is moved inside. Asterisks indicate the location of glycines 141 and 256 of TWIK-1[5].

1.2.2.3. Selectivity filter

As mentioned in the last section, the SF is the common gate for different regulatory input signals. It was shown some time ago that the *Drosophila* KCNKØ K2P channel exhibits properties that are identical to C-type inactivation of K_V channels, including the effect of extracellular K^+ concentration, residues near the SF at the extracellular side and the effect of blockers like TEA on decrease of inactivation [15]. Also it has been shown that the C-type gate responds to both extracellular pH and temperature in both TREK-1 and

TREK-2 [13]. In general, the existence of a C-type inactivation gate in K2P channels is widely accepted [16]. Therefore the K2P channel SF should have structural properties that are very similar to canonical K^+ channels.

The pore helix and filter are the most conserved domains in K^+ channels. The canonical SF signature in non-K2P channels is TXGYGDX where X can be any amino acid (Fig. 1.8). Dehydrated K^+ ions are coordinated by the side chain of the threonine and carbonyl oxygen atoms of the other residues [26]. Since in K^+ channels every subunit contributes one pore domain to the tetramer, in homomeric K^+ channels all pore domains and SF sequences are identical and changes are often not tolerated. For instance; in $K_V2.1$ mutating SF GYGD for Y and D at each position, only one substitution gave rise to functional channels. The tyrosine could only be mutated to a leucine without losing function, while for the aspartate, only the charge conserving mutation to glutamate was tolerated [17]. However in case of K2P channels each subunit possesses two pore domains that can have different SF sequences. All K2P channels and those that were studied in this work have a conserved threonine in both P1 and P2 SF sequences, which suggests that the threonine is crucial to the selectivity of these K^+ channels. In the second position where any amino acid can be substituted there are isoleucine or valine residues within both P1 and P2 SF sequences, except for TWIK-1 which in P1 there is a threonine. It has been suggested that this residue (Thr118) is responsible for Na^+ conductivity of TWIK-1 in low extracellular K^+ concentration [18]. This shift happens during hypokalemia when extracellular K^+ concentration goes bellow 3 mM [5]. Next, there are GYG and GFG motifs present in P1 and P2 respectively. However in the P2 domain of TWIK-1 a leucine is replacing phenylalanine of the GFG motif [5, 19, 20, 21 & 22]. The last conserved residue in the filter is an aspartate. However in acid sensitive K2P channels like TASK-1 and TASK-3 this residue is replaced by histidine which contributes to the extracellular acid sensitivity of these channels [23, 24]. Likewise in TWIK-1 there is a histidine in this position that contributes to inhibition of TWIK-1 channels by low extracellular pH [25].

These differences in the SF of K2P channels creates a two-fold symmetry instead of the four-fold symmetry in other K^+ channels. However crystal structures of both TWIK-1 and TRAAK suggest that their filter adopts a four-fold symmetry in the presence of K^+ ions [5, 6]. Although minor deviations due to existence of different side chains within the two pore domains are observed, the K^+ coordinating oxygen atoms in the SF of TRAAK align

well with those from KcsA [6] which confirms existence of a four-fold symmetry in K2P channels. However it is worth noting that the contribution of the two pore domains to the function of K2P channels is not equal. For instance in TASK-1 channels while replacement of phenylalanine in the GFG motif from P2 with a few amino acids is tolerated, that of tyrosine in GYG is restricted to phenylalanine [9].

How are all the components of the SF arranged in order to coordinate and conduct K^+ ions? In both structures of TWIK-1 and TRAAK, carbonyl oxygens from the second glycine in GYG are directed straight out into solution, making a ring surrounding the perimeter of the pore entryway. Thus, the extracellular pore entryway is fairly electronegative and attracts K^+ ions and therefore this glycine assists in the hydration and dehydration of a K^+ ion at the extracellular entryway [26]. The crystal structures of TWIK-1 and TRAAK also show that carbonyl groups of the rest of the residues are pointing toward the inner axes. Dehydrated K^+ ions can bind to these carbonyl groups since their charge is counter balanced by partial negative charge of the groups. Unlike the rest of the residues in the SF, in addition to its carbonyl oxygen, the side chain of threonine is oriented toward the axis of the SF with its oxygen atom pointing to K^+ ions. This arrangement suggests that this residue has a very important role in the function of the SF of K2P channels.

Next it might be asked, what is the role of side chains in the SF? Both crystal structures of TWIK-1 and TRAAK show that the SF side changes interact with pore helices that surround them. These interactions can stabilize the filter and play a role in gating [5, 6].

It is also interesting to note that in the crystal structures, four K^+ ions are observed in the SF, which are closely interacting with each other and no water molecules. It is widely believed that the distribution of ions in the filter is restricted to 2 or 3 K^+ ions binding simultaneously to their binding sites while separated from each other by water molecules [27]. However, recent MD simulations contradict this arrangement and suggest that K^+ interact directly with each other which in turn provide coulombic repulsions that facilitate a more efficient ion translocation across the SF, causing an increase in ion conductance from the K^+ channel [28].

1.2.2.4. Fenestrations

In contrast to tetrameric K^+ channels (except for KcsA) the interface between two dimers of a K2P channel is not totally sealed. This causes openings (fenestrations) (Fig. 1.9) that connect the intracellular cavity of the channel to alkyl region of the lipid bilayer. This feature of K2P channels is due to preserved prolines on M2, the same prolines that cause an upward kink in M2, which is unique to K2P channels (Pro143 in TWIK-1 and Pro155 in TRAAK, Fig. 1.8). The bending causes separation of M2 from M4 of the adjacent subunit [5, 6] and hence a horizontal hole, i.e. fenestration in the channel (Fig. 1.9). The crystal structures of TWIK-1, TRAAK and TREK-2 channels suggest that alkyl chains of lipid bilayer can enter these fenestrations [5, 11 & 12]. Indeed, in these crystal structures of TRAAK the channels are in the nonconductive state due to physical block of conductive pathway by alkyl chains positioned in the pore. In another conformation of the channel, it has been proposed that the upward movement and rotation of M4 closes this fenestration so that alkyl chains cannot block the ion pathway in the channel [11, 12]. However, this 'lipid occlusion' model of gating remains controversial.

1.2.2.5. C-helix in TWIK-1

In TWIK-1, unlike the other K2P channels, the residues that follow M4 (His271-Tyr281) form an amphipathic helix (the C-helix) at the membrane/cytosol interface. The C-helix lays roughly parallel to the membrane, following a bend of about 80° at Leu270 from M4 (Fig. 1.6). The C-helix extends to the other subunit and its C-terminus positions between M1 and M2 of adjacent (counterpart) subunit. [5]. The counterpart region to the C-helix in other K2P channels is known to be important for channel gating [5].

The structure of TWIK-1 suggests that C-helix can be involved in stabilization of the gate by keeping the inner helices apart from each other [5]. Also Lys274 where putative sumoylation and silencing of the channel happens is located on the C-helix [25].

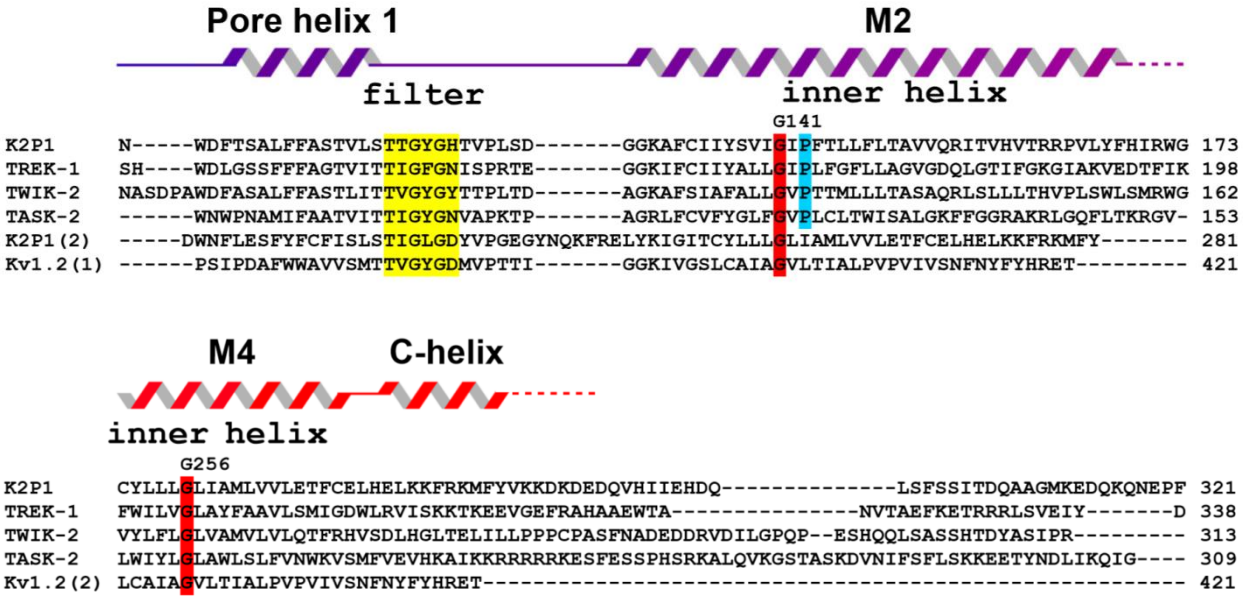

Fig. 1.8. Alignment of a few of K2P channels with K_V1.2. The conserved SF signature is marked in yellow and conserved hinge glycine residues are marked in red. Kink proline residues which are only conserved in K2P channels are marked in cyan [5].

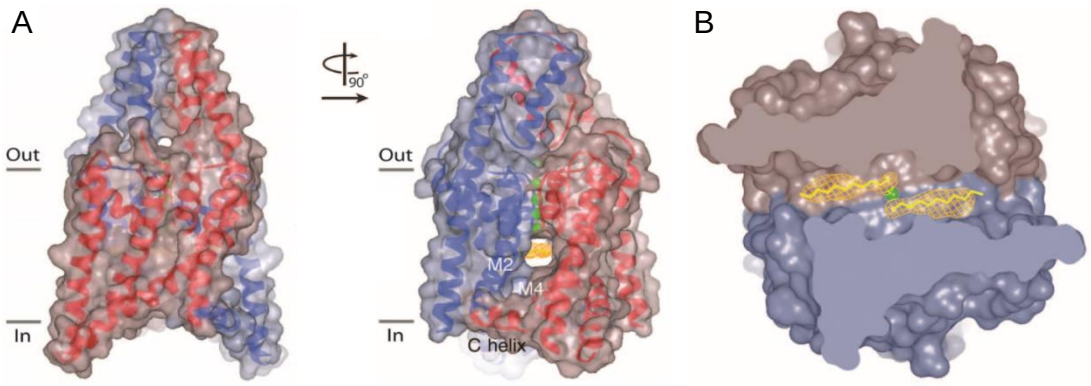

Fig. 1.9. (A); molecular density view of TWIK-1 to show interface between two subunits, blue and red. The fenestration is seen in the middle view and lies almost at the center of the lipid bilayer. Alkyl chains are shown in yellow. (B); cutaway view of the channel from the intracellular side. Green sphere is K^+ ion in S4 and yellow lines represent alkyl chains of the lipids [5].

1.2.2.6. Domain swapping.

In dimeric K2P channels, M1 and M2 of the core channel and E1 and E2 from cap structure are close to each other and interacting, as expected. However a higher resolution crystal structure of TRAAK channels showed that M1-E1 segment of two subunits are swapped between them (Fig. 1.10) [14]. In the sense that after formation of the dimer channel M1-E1 from each subunit rotates along vertical axis that goes through the SF and positions along the E2-M2 of the other subunit. It should be mentioned that it is not yet exactly clear whether all the channels have the domain swapped features or just a fraction of them. However based on the evidence it is suspected that the domain swapped architecture is correct for TRAAK channels [14] and also for the TREK-1 and TREK-2 channels [11].

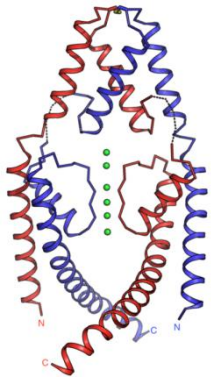

Fig. 1.10. TRAAK channel in swapped domain configuration. Two subunits are depicted in blue and red and K^+ ions in the SF are the green spheres. P2 is removed for clarity. Note that M2 (the inner helix) of a subunit is located next to M1 (the outer helix) of the other, instead of being next the helix from the same subunit [14].

1.3. General attributes of K2P channels studied in this work.

Based on their sequence similarity and functional features, K2P channels are classified into six subfamilies (Fig. 1.11); the weak rectifying group (TWIK-1, TWIK-2, and KCNK7), the mechano-gated group (TREK-1, TREK-2, and TRAAK), the acid-sensing group (TASK-1, TASK-3, and TASK-5), the alkaline-sensitive group (TALK-1, TALK-2, and TASK-2), the halothane-sensitive group (THIK-1 and THIK-2), and the spinal cord-expressed TRESK channel [29].

In this work I have studied TASK-1, TASK-2, TASK-3, TALK-1 TALK-2 and TWIK-1 channels. Therefore the following sections mainly focus on these channels and features of other K2P channels are mentioned where appropriate.

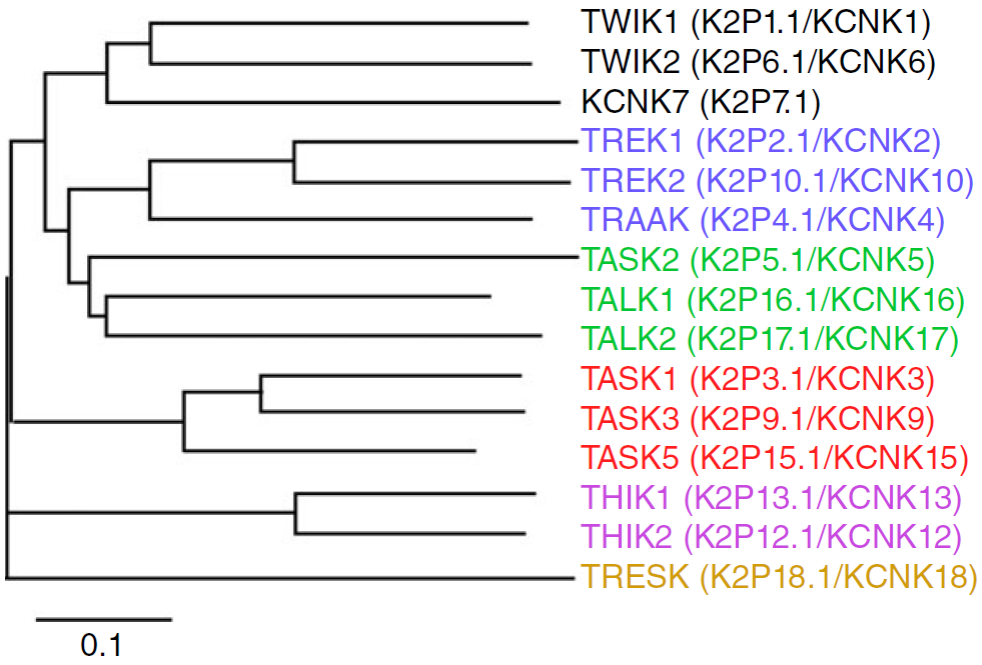

Fig.1.11. A dendrogram of K2P channels subfamilies with their conventional and systematic names [3]. The more similar the amino acid sequences for two channels, the shorter is the path connecting them.

1.3.2. TASK channels

TWIK-related Acid-Sensitive K^+ subfamily members are TASK-1, TASK-3 and TASK-5. TASK-1 and TASK-3 show sensitivity to extracellular pH in the physiological range and are inhibited by increase of extracellular H^+ concentration. TASK-5 is regarded as a silent channel and is included in this subfamily solely due to structural similarity [30]. With the exception of M3 segment which has 64% amino acid identity with that of TASK-1, the pore and transmembrane sequences of TASK-3 are nearly identical to those of TASK-1 [21]. The conserved cysteine that is responsible for covalent binding of two subunits in most of K2P channels is not present in TASK-1 and TASK-3 channels [19, 23].

TASK-1 mRNA is expressed in many human tissues, including the brain, lungs, prostate, heart, kidneys, uterus, small intestine and colon, but particularly is found in pancreas and placenta. While in mice, the highest expression is seen in the heart and brain. [19]. In the

rat brain, TASK-1 and TASK-3 are almost always co-expressed in the same cells. Exceptions are in some parts of amygdala and striatum in basal forebrain [31]. In guinea pigs, TASK-3 is exclusively expressed in the brain while very weakly in the heart. In contrast TASK-1 is strongly expressed in the heart [21, 23]. TASK-3 mRNA is expressed in many rat tissues including the brain, kidneys, liver, lungs, colon, stomach, spleen, testes, and skeletal muscle, and at very low levels in the heart and small intestine [21] In contrast, human TASK-3 is mostly expressed in cerebellum [32]. Therefore TASK-3 should have different roles in different spices.

Functional expression of TASK channels in heterologous expression systems like *Xenopus* oocytes and HEK cells endows them with negative potentials [32, 33], indicating an outward K^+ current from these channels and that in native cells TASK and other K2P channels serve as regulators of resting membrane potential.

At the single channel level TASK-3 channel is inward rectifying within symmetrical K^+ concentrations. However, depolarization increases the open probability (P_O) of the channel 5-fold, with constant P_O in the range of -100 to -40 mV and stepwise increase for potentials from 40 to 100 mV [21, 23], clearly indicating they are voltage-activated. It also explains why the macroscopic currents are outwardly rectifying. TASK-3 channels expressed in *Xenopus* oocytes show time-dependent activation kinetics with a rise time of 2–4 ms for voltages -20 to 60 mV.

TASK-1 and TASK-3 are also activated by halothane [43], suggesting they can also have a role in general anesthetic action.

1.3.3. TALK channels

Twik related **AL**kaline pH activated $\mathbf{K}^+$ subfamily members consist of TALK-1, TALK-2 and TASK-2. The TALK-1 and TALK-2 genes are separated by less than 1 kb from each other. Moreover the structures of genes regarding combination of exons and introns are very similar; with the only difference that it seems TALK-2 has lost the last intron and that flanking exons are connected to each other to form one single exon [22]. The gene organizations of TALK-1 and TALK-2 are very similar to those of TASK-2, TREK-1

TREK-2 and TRAAK suggesting these channels are variants of a common ancestral gene which duplicated several times.

1.3.3.1. TALK-1 and TALK-2 channels

In humans, TALK-1 is mainly expressed in the pancreas [34] while TALK-2 is expressed highest in the liver, lungs, pancreas, placenta, aorta and heart [35]. TALK-1 channels are active at physiological pH 7.4, however become much more activated as extracellular pH increases. In contrast TALK-2 channels are closed at physiological pH and are activated by extracellular pH 8.5 [22]. They also show time-dependent voltage activated currents [35]. TALK-1 single channels also show inward rectification [34].

1.3.3.2. TASK-2 channel

In humans TASK-2 is mainly expressed in the kidneys and localized in cortical distal tubules and collecting ducts, but it is also identified to a lesser extent in the pancreas, the liver, the placenta, and the small intestine and seems to be preferentially present in epithelia. However it is essentially absent in the brain. Based on this localization pattern, it has been suggested that TASK-2 could play an important role in renal K^+ transport [20]. TASK-2 is more related to TALK-1 and TALK-2 than to any other K2P channel [22]. However upon cloning it was named TASK-2 to emphasize its inhibition in low pH, like that of TASK-1 [20]. These three channels also share the same chromosome position; 6p21 [22].

In symmetrical ion conditions TASK-2 single channels are also slightly inwardly rectifying. It also shows time-dependent voltage activation at all voltages positive to reversal potential [20], which indicates an increase of the P_O due to depolarization. Increase of extracellular K^+ from 5 to 155 mM increases the overall conductance of TASK-2 channels [20]. In the original work that led to cloning of TASK-2 it is described as the K2P channel with the slowest activation kinetics [20].

1.3.4. TWIK-1 channel

Human TWIK-1 channel was the first member of mammalian K2P channel family to be discovered and the second after TOK-1. The channel is widely distributed in human body, including the brain, kidneys, liver, lungs, pancreas and placenta, chondrocytes but most abundant in the brain and the heart [36, 37 & 38]. In the heart, TWIK-1 is highly expressed in the atrium and Purkinje fibers [16]. This wide distribution along with the biophysical properties, including being open at all potentials and time-independent gating, and the fact that expression of TWIK-1 channels in *Xenopus* oocytes led to more hyperpolarized resting membrane potential, led to speculation that TWIK-1 channels represent a well-described leak (background) currents of previously unknown origin [37].

TWIK-1 produces modest currents in whole-cell two electrode voltage clamp in *Xenopus* oocytes and almost no currents in cultured mammalian cells [36]. One feature of this channel is fast inactivation of its currents. Inactivation causes inward rectification of steady-state IV in physiological ion condition, while other K2P channels show outward rectification [36]. Although TWIK-1 channels expressed in *Xenopus* oocytes are described as weakly inward rectifying a study on dentate gyrus granule cells suggests the channel is outwardly rectifying [39]. But another study suggests that serotonin-activated TWIK-1 currents in the cortex are inwardly rectifying [40].

TWIK-1 channel subunits self-assemble to form a functional K^+ channel. The Cys69 located on top of cap structure is necessary for dimerization and formation of functional channels from TWIK-1 subunits [5, 41]. However, once formed, reducing the disulfide bond had no effect on the function of the channel [41]. This may explain why TASK channels which do not poses a disulfide bond in the cap structure are still functional.

Unlike other K2P channels that possess a GYG/GFG motif in P2, in TWIK-1 this is GLG. Mutating the leucine to isoleucine or even a tyrosine cause loss of activity of TWIK-1, however phenylalanine replacement produces functional channels [41].

One of the interesting features of TWIK-1 channel is the ability to change the ion selectivity. If extracellular K^+ concentration falls below 3 mM, TWIK-1 channels slowly become Na^+ permeable and resting membrane potential becomes more depolarized due to

inward Na^+ conductance of the channel. When K^+ is then increased back to its normal concentration TWIK-1 channels gain the K^+ selectivity back again, however this process is much slower than becoming Na^+ permeable. Thr118 within the SF (TTGYG) of P1 is recognized to be responsible for this unique feature of TWIK-1 channels, where in other K2P channels it is a valine or isoleucine exists. The mutation T118I eliminates the ability to change the ion selectivity in low extracellular K^+ condition [16].

1.4. Regulation of K2P channels

Mechanical force, temperature, lipid interaction, voltage, pH, posttranslational modification, accessory protein interaction, heterodimerization and mechanisms that control the expression of K2P channels together regulate functionality of K2P channels. In the following sections those that are relevant to the K2P channels which were subject to this study are discussed.

1.4.1. pH regulation

K2P channels of TASK and TALK subfamilies are primarily regulated by extracellular pH. TASK channels are inhibited by extracellular acidic pH and are active at neutral pH. While TALK channels are activated at alkaline pH. Different members of each subfamily react differently to pH; at neutral pH, TALK-1 channels are largely inhibited, TALK-2 channels are totally inhibited, while TASK-2 channels are less active at neutral pH [3]. On the other hand while extracellular acidification apparently inhibits K^+ currents from TWIK-1 channels, it changes the selectivity of these channels from solely K^+ selective to Na^+ permeable.

1.4.1.1. TASK channels

TASK-1 channels are not sensitive to internal pH changes. However with a pK_a of 7.24 to 7.34 they are extremely sensitive to external H^+ concentration at physiological pH range (6.5-7.8) with 90% of maximum current at pH 7.66 and fully activated currents at pH 8.0 while they conduct just about 10% of maximum currents at pH 6.68 and are completely inhibited at pH 6.0 [19, 42]. Likewise TASK-3 channels are just sensitive to extracellular

pH change. With a pK_a of about 6.0 to 6.7 which is lower than that of TASK-1. They show 74% inhibition of the currents when pH drops from 7.2 to 6.4 and 96% at pH 6 [23, 43]. In other words TASK-3 channels are most sensitive to extracellular pH changes between pH 6 and 7 which occurs during cerebral ischemia and can lead to cell depolarization due to TASK-3 inhibition [23].

pH inhibition of TASK channels is not due to proton block rather it is due to decrease of the P_O with the increase of extracellular H^+ concentration [21]. MD simulations have shown that in both TASK-1 and TASK-3 channels, protonation and deprotonation of His98 next to GYG motif in P1 is responsible for pH sensing. In the unprotonated state that represents the open channel, side chains of two His98 are positioned next to the SF at the extracellular mouth of the pore. In this state the SF is stabilized via a water molecule that makes hydrogen bonds with the His98 and the tyrosine and the second glycine in GYG motif. However as the pH drops, the histidines become protonated and not only the extra positive charges on these residues repel K^+ ions away from the mouth of the SF, but also the hydrogen bonds which stabilize the SF are weakened and break due to the change in orientation of the water molecules. Moreover the histidines move upward and narrow the ion pathway, creating an "electropositive barrier" to K^+ ions at the outer mouth of the channel while the carbonyl oxygen of the phenylalanine/tyrosine can rotate more readily away from the conduction axis. As a result the K^+ ions in S0 and S1 binding sites of the SF would be destabilized and the SF shifts to non-conductive state which is reminiscent of C-type inactivation in other K^+ channels [44, 45]. However, Ma *et.al.* propose that similar to TWIK-1 channels both TASK-1 and TASK-3 become Na^+ permeable at lower pH and the inhibition of K^+ currents is due to reduction of driving force due to Na^+ permeability. They also suggest that the decrease of inhibition of channels in low pH with increase of extracellular K^+ concentration is due to the decrease of Na^+ concentration and hence less decrease in driving force in higher K^+ concentration [46]. However it should be mentioned in their experiments using non-permeable $NMDG^+$ instead of Na^+, still the K^+ currents decrease although to a lesser extent. Moreover, an increase in extracellular K^+ concentration also decreases the driving force and should have the same effect.

In any case, electrophysiology measurements of the H98N mutant in one or both subunits showed that in TASK-3 the protonation of two histidines is cooperative, in a sense that the deprotonation of one effects the pK_a from the other pH sensor and increases the probability

of deprotonation 14-fold. Therefore TASK-3 is more pH sensitive than TASK-1 because this cooperativity does not exists in TASK-1 channels [44]. Moreover despite the fact that His98 is the main pH sensor in TASK-1 channel, but it is not the only residue involved in pH sensing. Not only is the pH sensitivity of the H98N TASK-1 not completely abolished, but also mutating other residues in the pore domain including those of SF alters pH sensitivity of TASK-1 channels [9]. For instance the Asp204 in P2 in equivalent position to the pH sensor is equally important in the pH sensing, since mutating it to histidine or any other amino acid abolishes the pH sensitivity. In other words the His-Asp-His-Asp ring at the mouth of the channel is essential for the pH sensitivity over the physiological range. [47]. Permeant ions also affect the pH sensor, since in higher extracellular K^+ concentration these channels also show the cooperative behavior [42, 44] and TASK-3 channels become less sensitive to pH and open at lower pH values [9, 42].

1.4.1.2. TALK channels

In the TALK subfamily a conserved basic residue (Arg224 in TASK-2, Arg333 in TALK-1 and Arg242 in TALK-2) at the outermost portion of M4 and close to the pore region (P2) is the pH sensor. Replacing this residue with an alanine abolishes pH sensitivity of these channels and produces channels that are open at all pH. It is believed that the pH sensor in its protonated form inhibits the channel through electrostatic repulsions which increase energy barrier for ions moving in the SF. This in turn changes the ion occupancy of the SF [48, 49]. Similar to TASK channels pH sensitivity of TASK-2 is dependent on the extracellular concentration of K^+ and with increase of K^+ concentration pH sensitivity decreases [50]. TASK-2 channels are also activated by intracellular alkalization. A lysine residue (K245) at the cytoplasmic end of M4 is identified as the intracellular pH sensor. Mutation of the pH sensor (K245A) abolishes the intracellular pH sensitivity but has no effect on the response of the channel to extracellular pH change [50].

1.4.1.3. TWIK-1 channel

Upon progressive extracellular acidification from pH 7.5 to pH 6.5, TWIK-1 is first activated and then below pH 6.5 is inhibited [16]. The inhibition is associated with permeability of Na^+ due to acidification and change in driving force for K^+ ions. Indeed unlike TASK channels, protonation of the pH sensor, His122, increases the activity of

TWIK-1 [36]. However the His122, which is equivalent to pH sensor of TASK channels, is not the only factor involved in pH sensing of TWIK-1 channels [36]. Unlike other K2P channels, P1 from TWIK-1 bears a threonine before GY/FG motif (TGYG). Mutating this threonine to isoleucine (T119I) makes the channel resistance to acidification and change in K^+ selectivity at low pH [36]. Indeed TWIK-1 closure at lower pH is similar to C-type inactivation of K_V channels. In this case TWIK-1 becomes Na^+ permeable which corresponds to the narrowing of SF. However unlike K_V channels, with a very slow kinetic [36] and therefore channel stays conductive during the inhibition. Likewise the recovery of the channel after increase of pH to physiological level is very slow [46].

1.4.2. Functional regulation

1.4.2.1. TASK channels.

Heterologous co-expression of TASK-1 together with TRH-R1 receptor, a Gαq/11-coupled receptor expressed in hypoglossal and other motoneurons, causes inhibition of the channels upon application of thyrotropin-releasing hormone (TRH). Also other neurotransmitters and agonists of Gαq coupled receptors like; serotonin, norepinephrine, substance P and 3,5-dihydroxy-phenylglycine inhibit these channels [51]. Indeed, both TASK channels are activated by phosphatidylinositol 4,5-bisphosphate (PIP2) and inhibited by various Gαq coupled receptors that can deplete the membrane from P1P2. However it has been shown that unlike K_V and K_{ir} channels for which activation of phospholipase C by Gαq and consequently depletion of membrane from PIP2 inhibits the channels, TASK channels are directly inhibited by Gαq. Even application of Gαq alone to the PIP2-depleted patches has been shown to inhibit TASK channels. Based on these observations it was proposed that phospholipase C and its substrate PIP2 has no role in inhibition of TASK channels [52]. However a later study showed that in inside out patches diacylglycerol which is produced by activation of phospholipase C and is one of the downstream products of Gαq/11 activation, can also directly inhibit TASK channels. In this regard a VLRFL/MT motif is recognized to be essential for inhibition of the channels [53]. Therefore direct interaction of diacylglycerol with the TASK channels was proposed. However the authors could not rule out the direct interaction of Gαq protein with TASK channels [53].

The VLRFL/MT motif is located in proximal C-terminus of TASK channels and is essential for their activation by halothane and inhibition by G-protein coupled receptor, TRH-R1. Deletion of VLRFMT from TASK-1 and VLRFLT from TASK-3 abolishes both the inhibitory and activation effect of those regulators. Moreover mutations in this motif diminish the effects [43]. In a dimeric channel both motifs are required for the regulators to be effective and deletion of one motif abolishes the effect. While substitution of the C-terminus from TREK-1 which bears this motif too, abolished effects of both halothane and TRH-R1, it had no effect on inhibition of TASK-1 by anandamide and methanandamide [43, 54]. This indicated that these regulators are modulating channel activity in different ways.

1.4.2.2. TALK channels

TASK-2 channels are directly inhibited by Gβγ subunit of G protein, where two lysine residues, K257 and K258 in the C-terminus of the channel are essential for the binding of Gβγ. Based on these observations, it is proposed that TASK-2 channels are involved in regulation of cell response to osmolarity via inhibition by Gβγ subunits [55]. Mouse TASK-2 is directly inhibited by CO_2. The effect is independent from both intra- and extracellular pH sensors and observed in highly buffered solutions as well [56]. Also it is believed that activation of a tyrosine kinase and phosphorylation of TASK-2 directly or due to activation of other regulatory proteins downstream of the tyrosine kinase causes the opening of the channel in response to osmolarity change. On the other hand tyrosine phosphatase inhibits TASK-2 channels in the same fashion [57].

Reactive oxygen species such as singlet oxygen and superoxide ion are by-products of oxidative metabolism. Both TALK-1 and TALK-2 are strongly activated by singlet oxygen, while superoxide activates TALK-2 but not TALK-1 [58].

1.4.2.3. TWIK-1 channel

Most functional data from TWIK-1 channels have been obtained from heterologous expression systems, but even in these systems functional expression only produces low levels of activity. Currently there are three explanations for this low functional expression;

one of them relates to its expression discussed later, the other two are related to functional regulation of the channel that we learn in the following.

SUMO (small ubiquitin-related modifier protein) also known as sentrin, is a ubiquitous posttranslational protein-modifying protein that covalently binds to nuclear proteins. It has been proposed that SUMO silences TWIK-1 channels by binding to the Lys274 in the sequence LKKF which is a variant of the classical ΨKxE/D SUMO binding motif, where Ψ is an aliphatic residue and x can be any residue [25]. It is also believed that sumoylation is reversible and enzymatic desumoylation of TWIK-1 reactivates the channels [25]. Interestingly the K274E mutation which supposedly abolishes sumoylation signal, increased TWIK-1 currents [25] and this idea gained support. It has previously been shown that when expressed in Chinese hamster ovary (CHO) cells in the absence of extracellular K^+, TWIK-1 changes selectivity to conduct large inward Na^+ and outward K^+ currents with a permeability ratio of $Na^+/K^+ \approx 0.53$ [59]. Based on these observations and that TWIK-1 also conducts large inward Rb^+ and NH_4^+ currents, it has been suggested that TWIK-1 reaches the cell membrane and becomes silent by sumoylation. [25, 59]. However, TWIK-1 sumoylation was questioned when the K274R mutation which should also abolish the sumoylation signal and increase the current, was similar to the wild type (WT) channel [60].

Even if TWIK-1 channels are abundant at the plasma membrane they are still functionally silent. More recently it has been proposed that very low activity of TWIK-1 channels is an inherent feature due to existence of a hydrophobic barrier composed from pore lining residues; L146, L261 and L264 under the SF which results in dewetting of the pore and as a consequence weak functional activity of TWIK-1 channels [61]. Although this explanation is plausible, however it does not address why as it has been shown before [59] Rb^+ and NH_4^+ ions can penetrate through a hydrophobic barrier devoid of water. Beside that a former study showed that in K2P channels there are three conserved glycine residues which are important for channel gating. However these residues are replaced by other amino acids in TWIK-1. Mutating them back to glycine (L146G, A151G, V153G), increased TWIK-1 currents more than 3-fold in comparison to the WT [36].

Also TWIK-1 is under the control of G-proteins. Activation of protein kinase C activates TWIK-1. However protein kinase C does not activate TWIK-1 by direct phosphorylation

because mutation of the only putative phosphorylation site (Tl6lA), produces channels that can be still activated by protein kinase C [37].

Functional activity of TWIK-1 is also controlled by ions. Unlike the rest of K2P channels that show intrinsic inward rectification at the single channel level, that of TWIK-1 is due to intracellular inhibition of the channel by Mg^{2+} and in absence of Mg^{2+} the single channels lack any rectification. However, unlike K_{ir} channels even at 10 mM intracellular Mg^{2+} TWIK-1 channels show outward currents, therefore the inward rectification of TWIK-1 is considered to be weak [37].

1.4.3. Expression regulation

1.4.3.1. TASK channels

TASK channel expression is mostly regulated by accessory proteins. Both TASK channels interact with the adaptor protein 14-3-3 which masks a retention signal in the C-terminus of the channels. TASK-1 in addition interacts with the adaptor protein S100A10 and the endosomal SNARE protein, syntaxin-8. S100A10, targets the channel to the endoplasmic reticulum. While syntaxin-8 carries an endocytosis signal that complements an endocytosis signal of the channel that cause cooperative endocytosis of both proteins [62]. Therefore unlike TASK-3, TASK-1 is mainly found in cytoplasm [63]. Despite that in the human atrium TASK-3 is exclusively found in heterodimer of TASK-1 [63].

1.4.3.2. TALK channels

Besides heterodimerization, K2P channels can add to the diversity of K^+ channels by different splice variants. This is best studied in the TALK subfamily.

TASK-2 expression results in two splice variants; TASK-2a which is the full length channel and TASK-2b in which part of the exon 2 and the whole exon 3 are skipped. The exclusion of the exons results in truncation of M1 to M3. TASK-2b acts as a dominant-negative in targeting TASK-2 channels to the plasma membrane and causes down-regulation of the surface expression of TASK-2a channels. In other words TASK-2b acts as the membrane trafficking-defect isoform of TASK-2a [64]. In human myelogenous

leukemia cell line, K562 which overexpress TASK-2a, transfection of TASK-2b inhibits cell proliferation [64], which makes TASK-2b an interesting therapeutic tool in pathological conditions, resulted from overexpression of TASK-2 channel.

Likewise, TALK-1 expresses four splice variants, two of which, TALK-1a and TALK-1b are shown to produce functional channels. These channels are very similar in function and can be identified from each other solely based on the single channel conductance. The other two are lacking M4 and it is not known if the mRNA can be translated to the protein [34].

1.4.3.3. TWIK-1 channel

In section 1.4.2.3. two theories concerning low activity of TWIK-1 channels were discussed; that they are due to the existence of a hydrophobic barrier inherently silent or sumoylation makes the channels silent. However, the fact that K274R mutation which should abolish the sumoylation signal and increase the current like the K274E substitution, showed no difference to the WT channel [60] and identification of high localization of TWIK-1 channels in recycling endosomes [65] led to discovery of a di-isoleucine motif (II293-294AA) in the C-terminus of the channel which via a dynamin-dependent mechanism is responsible for rapid internalization of TWIK-1 [66] and its apparent low functional expression. In the kidney and in transfected cells TWIK-1 is found mainly in recycling endosomes where it is actively and constitutively internalized from the cell surface and is targeted to recycling endosomes. Mutation of the di-isoleucine repeat (II293-294AA) prevents TWIK-1 endocytosis [36]. TWIK-1 is also expressed in dentate gyrus granule cells localized mainly in the cell soma and proximal dendrites [39]. When ARF6 (ADP-ribosylation factor 6), a small G protein which is modulator of endocytosis and its exchange factor, EFA6 bound together, they can interact with TWIK-1, the channel is then rapidly and in a dynamin-dependent manner via clathrin-coated vesicles internalized [65]. It is believed that recycling to the plasma membrane happens via activation of ß2AR and the serotonin receptor 5-HT1R, both of which are G_i-coupled receptors [65]. Also in astrocytes activation of metabotropic glutamate receptor 3 (mGluR3), an G_i/G_o-coupled receptor, by glutamate increases membrane expression of TWIK-1 channels [67].

1.4.4. Heterodimerization of K2P channels

Like members of K_V and K_{ir} channel families that make heteromeric channels with other members inside the family, K2P channels can also assemble heterodimeric channels, which is best documented for TASK-1 and TASK-3 heterodimers in hypoglossal motoneurons. Heterodimeric TASK channels show intermediate properties of homodimeric TASK-1 and TASK-3 channels. For instance the pH sensitivity of heterodimeric TASK channels (pK_a 7.3) is more close to that of TASK-1 channels (pK_a 7.5) than TASK-3 channels (pK_a 6.8). While the single channel conductance of heterodimeric TASK channels is indistinguishable from TASK-3 channels and twice that of TASK-1. On the other hand isoflurane activates both TASK-3 and heterodimeric TASK channels, while TASK-1 channels are slightly inhibited. Likewise, ruthenium red inhibits only TASK-3 channels, but not TASK-1 and heterodimeric TASK channels. Based on these properties it has been estimated that 52% of TASK currents in hypoglossal motoneurons are conducted by heterodimeric TASK channels and the rest by homomeric TAKS-1 and TASK-3 channels [68]. However it should be mentioned that the contribution of heteromeric TASK channels in other tissues and cells that express both TASK-1 and TASK-3 channels can be different. For instance it has been suggested that in adrenal glomerulosa cells and cerebellar granule neurons the whole TASK currents are carried by TASK-3 channels [68]. But, according to another study in the cerebellar granule neurons TWIK-1 is coassembled with both TASK-1 and TASK-3, contributing to acid-sensitive K^+ leak currents from these cells. It has been suggested that about 50% of these currents are silenced by sumoylation of TWIK-1 subunit of heterodimers and shown that application of the desumoylase SENP1 lead to increase of acid-sensitive K^+ leak currents and huge activating effect of halothane on these currents [69].

1.5. Physiological role of K2P channels

K2P channels are present in every organ, tissue and cell, even chondrocytes. Each K2P channel, either alone or with another K2P channels have been proposed to have a physiological role. While much is known about some K2P channels such as the TASK subfamily, the physiological role of some others like those of TALK subfamily are poorly

understood. In the following section we learn about some known physiological roles of K2P channels.

1.5.1. TASK channels

TASK-1 and TASK-3 have a role in wakefulness-sleep behavior. Both channels contribute to the muscarine- and halothane-sensitive conductance in thalamocortical relay neurons, thereby contributing to the change in the activity mode of thalamocortical networks observed during the sleep-wake cycle. The shift from periods of synchronized electroencephalogram (EEG) activity, such as during slow wave sleep, to the desynchronized EEG pattern of wakefulness is associated with tonic depolarization of thalamocortical relay neurons. Activation of mACh receptors is associated with a slow depolarization due to inhibition of TASK-1 and TASK-3 channels [70]. Also inhibition of TASK channels in thalamic neurons and subsequent depolarization of these cells is associated with firing attributed to wakefulness and REMs and therefore the role of these channels in sleep and wakefulness [71]. Indeed, TASK-3 knockout mice are shown to exhibit a slower progression from their waking to sleeping states and, during their sleeping period, the sleep episodes as well as the REM theta oscillations are more fragmented. Moreover the EEG from the TASK-3 knockout mice lack type II theta oscillations (4-9 Hz) which is associated with immobility during the processing of sensory stimuli relevant to initiating, or intending to initiate the motor activity [72]. These oscillations have been shown to increase under influence of halothane which activates TASK-3 channels. Also TASK-3 knockout showed fragmented REMs and exaggerated wake activity [71]. These animals were also more active, showed increased locomotor activity during the dark phase. These animals ate more and were slightly heavier as the control group [73]. They had also higher body temperature during the active periods and showed more resistance in depression tests and unlike the WT animals they showed no response to REM suppressing effect of fluoxetine, suggesting that TASK-3 also can be the target of antidepressant agents [74]. It has been shown that wakefulness-active neurotransmitters, including histamine, noradrenaline, serotonin, and orexin inhibit TASK channels through a Gαq-mediated mechanism. *In vitro* studies have shown that histamine can inhibit both TASK-1 and TASK-3 and also heterodimer TASK-1/TASK-3 channels [75]. Based on this evidence and comparing WT and TASK knockout mice, it has been concluded that TASK channels in

cholinergic neurons contribute to endogenous EEG oscillations as well as the arousal effects of histamine in the γ frequency band [75].

TASK-1 channels have a role in motor coordination and balance since the TASK-1 knockout mice showed modest impairments in motor coordination or balance in Rotarod and walking beam tests [76]. These animals also showed a stronger response in acoustic startle test suggesting role of TASK-1 channels in auditory pathways. Indeed, a large and sustained decrease in the expression of TASK-1 and TASK-5 follows deafness in cochlear nucleus neurons and temporary down regulation of TASK-3 [77]. It has been suggested that TASK-1 channels also have a role in thermal nociception. TASK-1 knockout mice had an increased sensitivity to thermal nociception in the hot-plate test implying the lack of TASK-1 or TASK-1/TASK-3 channels in the thalamus or alterations in ascending pain pathways [76]. It has also been suggested that TASK-3 has a role in balance and motor coordination, despite that TASK-3 deficiency has a subtle effect on both of these, which could be due to lack of TASK-1/TASK-3 heterodimers in motor neurons [73].

TASK channels showed to have a role in learning and memory function. TASK-3 knockout mice shows impaired working memory. It has been suggested that the firing properties of hippocampal neurons are altered in a way that disturbs short-term memory formation and/or retrieval of saved memory [73].

TASK channels in general have a key role in function and excitability of arterial chemoreceptors [78]. The carotid body in carotid artery detects changes in partial pressure of oxygen, carbon dioxide, pH and temperature. TASK-1 and TASK-3 mRNA are expressed in rat carotid body type I cells [79, 80 & 81]. The biophysical and pharmacological properties of leak currents from these cells are strikingly similar to those of TASK-1, TASK-3 and TASK-1/TASK-3 heterodimer, with the later as the major contributor to the leak current from these cells [79, 80]. Therefore it has been suggested that TASK-1/TASK-3 heterodimer is a prime candidate for mediating the oxygen and acid sensitive leak current from these cells and hence detecting the changes in blood components [80]. However another study showed that TASK-1, but not TASK-3 channels are essential for response of this organ to hypoxia and hypercapnia by contributing to the increase in the carotid body discharges in response to a decrease of arterial O_2 pressure or increase in CO_2 pressure and therefore play an important role in the control of ventilation

by the peripheral chemoreceptors [81]. It should be mentioned since human TASK-3 is exclusively expressed in cerebellum [32], TASK-1 alone or other background channels can have the major role in sensitivity of these cells in human.

In addition, TASK channels have crucial role in development. Since, neural activity is important in the early neuronal development, including; proliferation, differentiation and migration, any factor that changes aspects of neuronal function can disrupt neuronal development. In this context TASK-3 channels have a crucial role in migration of cortical pyramidal neurons through stabilization of intracellular calcium concentration [82]. As I will mention in the section for pathological roles of K2P channels, malfunctioning of TASK-3 channels is associated with mental retardation in humans [83]. Programmed cell death is involved in the developing cerebellum to numerically match cerebellar granule cells with the post-synaptic Purkinje neurons. In rat cerebellar granule cells expression of both TASK-1 and TASK-3 significantly increases between post-natal days of 10 to 21 as it does in the cultured cells as well. In cerebellar granule cell cultures, TASK channels play an important role in apoptosis. Indeed, inhibition of TASK channels by pharmaceutical agents or transfection of cells with dominant negative mutants prevents apoptosis and causes cell survival. While transfection of hippocampal neurons with TASK channels make them susceptible to apoptosis in cell culture [84]. These observations suggest that TASK-1 and TASK-3 channels can have a significant role in central nervous system development and physiological function of cells in these areas.

Also TASK channels are involved in development and differentiation of cells in adrenal gland. In TASK-1 knockout mice aldosterone synthesis was absent in the outer cortex normally corresponding to the zona glomerulosa, but abundant in deeper layers of adrenal gland in the reticulo-fasciculata zone [85] which implies that in absence of TASK-1 channels zonation of the adrenal gland is disrupted. It is worth mentioning that TASK-1/TASK-3 heterodimers are involved in regulation of aldosterone secretion, and consequently Na^+ and K^+ homeostasis and blood pressure [85]. Indeed, TASK-1 and TASK-1/TASK-3 knockout mice show severe hyperaldosteronism, hypokalemia, and hypertension [85, 86]. Also an exploratory study in humans showed that single-nucleotide polymorphisms in TASK-3 channels can affect blood pressure through change in aldosterone production [87].

TASK-1 channels but not TASK-3 may have also a neuroprotective role in nervous system after ischemia. TASK-1 knockout mice show more injury after ischemia caused by permanent middle cerebral artery occlusion [88]. Although ischemia conditions would cause lower pH values and inhibition of TASK channels, the authors attributed the neuroprotective role of TASK-1 channels to higher blood pressure of WT mice and therefore facilitated oxygen delivery to the injured area [88].

However the most interesting role of TASK channels for us is their involvement in the regulation of the membrane potential and action potential. For instance TASK-1 and TASK-3 channels in cerebellar granule neurons that are the most populous cells in the mammalian brain are responsible for the standing-outward current [89, 90], which is an outwardly rectifying potassium current that adjusts resting membrane potential of these cells to K^+ reversal potential. Inhibition of TASK-1 in these cells causes inhibition of the current and cell depolarization [89]. Also in rat ventricular muscle inhibition of TASK-1 currents causes increase in action potential duration [91]. The reason for these effects is that unlike K_{ir} channels, K2P channels are also active at potentials more positive than the reversal potential. Therefore they are capable to have a profound effect not only on the resting membrane potential, but on the amplitude and duration of action potentials. Indeed in isolated guinea pig ventricular myocytes where TASK-1 channels express, low pH caused a reduction of leak currents accompanied by a reduction in the resting membrane potential and maximum rate of depolarization, the steady-state outward current and flattening of the plateau but prolongation of the action potential duration [92]. Moreover, TASK-1 has a role in regulation of heart function. TASK-1 knockout mice show a prolongation of the QRS complex, an increase in the QT-interval and action potential duration. Therefore it has been suggested that TASK-1 channels are involved in repolarization of heart ventricles and also involved in the conduction of cardiac excitation. However TASK-1 is not the only channel involved in heart regulation, as these symptoms disappeared by sympathetic stimulation of TASK-1 knockout heart [93]. Moreover in humans TASK-1 is expressed in the atria, auricles and atrio-ventricular node of the heart. Application of the specific TASK-1 blocker, A293 caused prolongation of action potential duration. Therefore it has been suggested that TASK-1 channels are involved in pace making and regulation of the heart rate [94]. Also in permanent atrial fibrillation TASK-1 along with other K^+ channels was upregulated [95].

Na_V channels which are involved in fast firing of neurons are susceptible to slow inactivation that reduces the overall availability of these channels as they enter for several seconds in inactivation mode. After each action potential the membrane potential should be hyperpolarized to prevent Na_V channels to enter the slow inactivation mode and facilitate recovery [1]. Brickley *et. al.* have shown that absence of TASK-3 channels in cerebellar granule neurons, not only caused 10 mV increase of resting membrane potential which in turn induced reduction of action potential threshold, but also shortening of amplitude of pulses and relative widening of them and eventually failure of action potentials much earlier than in presence of TASK-3 channels. Therefore it has been suggested that TASK-3 channels not only reduce the slow inactivation of Na_V channels by hyperpolarization of the membrane but also by increasing the membrane conductance during depolarization they reduce the time constant of the membrane which causes faster membrane hyperpolarization, and as a result fast recovery of Na_V channels from inactivation. This ensures availability of Na_V channels and sustained action potential firing of the membrane [90].

1.5.2. TALK channels

1.5.2.1. TASK-2 channel

TASK-2 channels may have a beneficial role in epilepsy, which is characterized by the presence of spontaneous episodes of neuronal discharge. It is shown that following status epilepticus in model animals, expression of TASK-2 in CA3 pyramidal cell layer of hippocampus gradually increases. It has been suggested that the upregulation of the channel is due to rapid adaptive responses of the cells to the seizures; seizure activity causes an extracellular alkalization which activates TASK-2 channels that in turn can cause hyperpolarization and regulation of seizure activity [96].

The other major role of TASK-2 channels is in respiratory ventilation. The hypoxia-induced reflex consists of an immediate increase of ventilation rate and then a depression of respiratory drive and further slow recovery upon long-term hypoxic exposure. TASK-2 knockout mice show a normal initial respiratory increase in response to hypoxia, suggesting that the peripheral chemoreflex for which carotid bodies, where TASK-1 and TASK-3 channels are expressed, are responsible to be intact. However, the hypoxia-

induced depression of respiration is abolished in TASK-2 knockout mice. This depression is under control of ventral medullary surface in medulla where TASK-2 is also expressed which suggests TASK-2 channels are a key player but not the only one in respiratory reflex under control of central nervous system [97].

Central respiratory chemoreceptors sense CO_2 and H^+ concentrations within the brain and regulate the activity of the respiratory mechanisms to adjust brain and arterial P_{CO2} and pH at physiological levels. TASK-2 is highly expressed in glutamatergic neurons of the retrotrapezoid nucleus, which their inhibition depresses ventilatory responses to CO_2 and raises the CO_2 threshold for breathing. It has been shown that TASK-2 channels contribute to pH sensitivity in glutamatergic neurons of the retrotrapezoid nucleus and they are the molecular sensor for pH sensing in the retrotrapezoid nucleus respiratory chemoreceptor neurons. Indeed TASK-2 knock-out mice show a blunted ventilator response to CO_2 and complete disruption of pH-dependent firing activity of these neurons [98].

TASK-2 channels are involved in cell volume regulation by regulatory volume decrease in hypotonicity induced swelling condition. In Ehrlich cells the swelling-activated K^+ conductance shows functional similarities to TASK-2 currents [99, 100]. Moreover, heterologous expression of TASK-2 channels in HEK cells induces swelling-activated K^+ currents [57]. While proximal convoluted tubules cells from TASK-2 knockout mice do not show these currents and cell volume regulation is completely abolished [99], indicating the role of TASK-2 channels in cell volume regulation. This requires that TASK-2 channels should be osmosensitive. Indeed mouse TASK-2 currents are osmosensitive and are increased by hypotonic cell swelling and decreased by cell shrinkage [100]. However TASK-2 is not a stretch-activated channel. Then how does the channel respond to osmolarity changes? TASK-2 is involved in this process via alkalization of tubular fluid by a chain of reactions that involve activation of an outward Cl^- current due to swelling that in turn activates Cl^-/HCO_3^- exchanger; transporting Cl^- back into the cell in cost of HCO_3^- to exist. Excess HCO_3^- in tubular fluid increase the pH and activates TASK-2 channels [101]. Exit of KCl decreases cytoplasm osmolarity which in turn cause cell volume decrease due to exit of water. It is worth mentioning that the initial Cl^- outward current depolarizes the cell which triggers $Na^+/3HCO_3^-$ cotransport and further depolarization due to exit of HCO_3^- [101]. Therefore TASK-2 channels are engaged in reabsorption of Na^+ and HCO_3^- transport, the latter is important for regulation of blood pH. Indeed TASK-2 knockout mice

suffer from metabolic acidosis caused by renal loss of HCO_3^- [102]. The role of TASK-2 channels in cell volume regulation also implies that they have a role in apoptosis. Apoptotic cell death is preceded by normotonic cell shrinkage which is called apoptotic volume decrease. Moreover enzymes involved in apoptosis are directly controlled by intracellular K^+ concentration, which suggest the role of K^+ channels in this process. In proximal tubule cells TASK-2 channels are directly involved in control of apoptosis. It is believed that reactive oxygen species released from mitochondria open TASK-2 channels and intracellular K^+ concentration decrease triggers apoptosis [103].

TASK-2 channels play also a major role in lymphocyte function. Stimulation of CD4 T cells upregulates TASK-2 expression which in turn increases cell proliferation and interferon gamma (IFNγ) secretion. In contrast, pharmacological inhibition or down regulation of TASK-2 channels by small interfering RNA (siRNA) decreases cell proliferation and IFNγ secretion [104]. The role of TASK-2 in proliferation of T cells is probably due to its involvement in the G1 to S transition. It has been shown that in human K562 cells, a myelogenous leukemia cell line, during the G1 to S transition expression level of TASK-2 protein was increased and was very low in the G0/G1 and G2/M phases [64]. Similar to T cells, stimulation of B cell receptors (BCR ligation) causes upregulation of TASK-2 channels and induction of apoptosis of immature B cells, which is critical to the elimination of self-reactive clones. On the other hand, down regulation of these channels attenuates the cell death. Therefore it has been suggested that TASK-2 channels to be involved in apoptosis and functional regulation of B cells [105].

Both TASK-2 mRNA and protein are detected in human chondrocytes [38]. In osteoarthritis condition a large decrease in TASK-2 expression is observed in osteoarthritis chondrocytes, while these cells have also been shown to be significantly depolarized in comparison to control chondrocytes [106]. It is suggested that TASK-2 channels contribute to the resting membrane potential when joints are at rest and stretch active channels are inactive [38].

1.5.2.2. TALK-1 and TALK-2 channels

The P_O of TALK-2 channels is very low at pH 7.5, so low that TALK-2 currents cannot regulate the resting membrane potential at physiological pH range [35]. Therefore, it is

believed that TALK-2 might be important in tissues, like the bile or pancreas, where physiological pH can range from 7.5 to 8.5 [35]. The acinar cells of exocrine pancreas are the functional units that synthesize, store and secrete digestive enzymes. Secretion of these enzymes is under control of nitric oxide [107]. In humans, both TALK-1 and TALK-2 channels are highly and exclusively expressed in acinar cells of exocrine pancreas. While none of them are present in Langerhans islets in the endocrine pancreas [58]. Duprat *et.al.* have shown that nitric oxide activates both TALK-1 and TALK-2 channels and suggest that they are involved in the regulation of exocrine pancreatic secretion under the control of nitric oxide [58].

1.5.3 TWIK-1 channel

The role of TWIK-1 channels is not yet completely understood and there are some contradictory results in the literature. The reason for this may lie in the fact that measuring TWIK-1 channels in native cells has not been yet possible and the existing results are from comparative studies done in TWIK-1-knockout animals. In the following I mention some of best described roles of TWIK-1 channels.

TWIK-1 channels are highly expressed in the superficial layers of the cortex, including the entorhinal cortex. It is believed TWIK-1 has an inhibitory effect on excitability of stellate and pyramidal neurons in the superficial layers of the entorhinal cortex, by hyperpolarizing the cell membrane, which causes inhibition of hippocampal function. This role of TWIK-1 is mediated by activation of protein kinase A via serotonin activation of Gαi3 [40]. In hippocampal astrocytes TWIK-1 channel is the most abundant K^+ channel expressed. However, TWIK-1 channels are mostly retained in cytoplasm rather than in plasma membrane. It has been suggested that in the astrocytes, TWIK-1 channels may contribute to the homeostasis of intracellular Na^+ and uptake of NH_4^+, rather than contributing to the hyperpolarized resting potential of these cells [67, 108]. On the other hand in the kidneys, surface expression of TWIK-1 is relatively higher than those of astrocytes, which in TWIK-1 knockout mice causes more hyperpolarization of kidney cells in comparison to the astrocytes [108]. Despite that in native kidney and pancreatic cells and heterologous mammalian cells, TWIK-1 is also mainly present in recycling endosomes that have a pH of about 6. It has been proposed that in this acidic environment TWIK-1 shifts to a Na^+

conducting mode and retains it long after returning to the cell membrane. In this case unlike other K2P channels TWIK-1 shifts the cell membrane toward depolarized resting potentials rather than increasing hyperpolarization. Indeed in knockout mice, kidney principal cells and pancreatic β cells are more hyperpolarized than being depolarized [36]. However another study showed that dentate gyrus granule cells in hippocampus from mice lacking TWIK-1 channels have a more depolarized resting membrane potential than the WT cells. Moreover, TWIK-1 channels contribute to outward rectification of the currents evoked from WT cells and cells lacking TWIK-1 have a lower threshold for firing and show more firing events and larger depolarization of cell membrane after excitation in comparison to the control. It has been concluded that TWIK-1 channels contribute to hyperpolarization of dentate gyrus granule cells and set an upper limit to the depolarization and firing rate of these cells [39].

TWIK-1 knockout mice also show impaired renal reabsorption of phosphate in the proximal tubule and as a result impaired stabilization of plasma phosphate concentration in a low phosphate diet. Under normal diet conditions these mice have lower urinary flow rate due to impaired water transport in medullary collecting duct. Both conditions are suggested to be associated with role of TWIK-1 in trafficking of NaPi2a, the transporter that reabsorbs phosphate along Na^+ and also internalization of Aquaporin-2 by regulation of vesicles carrying these transmembrane proteins [109].

1.6. Pathology of K2P channels

Finely tuned expression and function of over 400 ion channels in the human body is involved in many diverse physiological processes, like memory and learning, cell proliferation, hormone secretion, and excitability of neurons and muscles. Consequently, malfunctioning of each ion channel can have serious physiological effects. To date, mutations in over 60 different ion channel genes have been found to cause human diseases [110]. Here I mention some of the known diseases that are consequence of pH_{ex}-sensitive K2P channels malfunctioning.

1.6.1. TASK channels

Birk-Barel Mental Retardation Syndrome (BBMRS), characterized by mental retardation, hypotonia, and characteristic dysmorphism, is currently the only know pathological condition which is caused due to paternal silencing of a K2P channel and mutation in maternal copy of it. The G236R mutation on pore-lining M4 of TASK-3 causes nonfunctional homodimeric channels and acts as a dominant negative mutant with the WT TASK-3 or TASK-1 channels, causing four-fold current reduction [83]. Also, TASK-1 is suggested to be a potential target for the inflammatory therapy and degenerative central nervous system disorders. In animal knockout models suffering from experimental autoimmune encephalomyelitis, that mimics human multiple sclerosis, deletion of TASK-1 or inhibition by anandamide reduced T cell proliferation and cytokine secretion which causes a less inflammatory condition. Moreover, these mice display a considerably lower level of neurodegeneration under these conditions [111].

TASK channels also have a role in pathology relating to the heart. Electric remodeling of human atrial tissue is a hallmark of atrial fibrillation pathophysiology [112]. In human heart TASK-1 is expressed mainly in the atria, especially the paranodal region, and in the atrioventricular node and therefore it is proposed that TASK-1 might have a role in the pathogenesis of atrial fibrillation. Individuals with low expression of TASK-1 channels or a mutation in the channel pore (V123L) which reduces TASK-1 currents, suffer from atrial fibrillation. Heterologous expression of TASK-1 V123L depolarizes the resting membrane potential and increases pH sensitivity of TASK-1 currents. Interestingly, TASK-1 knockout in zebra fish embryos results in a lower heart rate and an increase in atrial and ventricular diameter [113]. On the other hand it has been shown that in patients with chronic atrial fibrillation, TASK-1 mRNA, protein levels and currents are increased. This increase is the cause of shortened action potential duration, while inhibition of TASK-1 prolonged the duration compared to that of control group [112]. Therefore it is plausible that TASK-1 channels are one of the major players in human heart diseases. TASK-1 is also involved in hypertension conditions, since it is expressed in human pulmonary-artery smooth-muscle cells and by setting resting membrane potential is important in the regulation of pulmonary vascular tone. In familial and idiopathic pulmonary arterial hypertension several mutations in TASK-1 gene are identified to be responsible for the

symptoms. All mutations, two of which are located in the SF consensus sequence (G97R and G203D) cause a loss of function in TASK-1 channels [114].

TASK-3 channels are also involved in both human breast and lung cancers (respectively, 44% and 35% of studied cases). In both cases gene amplification and/or over expression of the channel has been suggested to promote tumor formation and giving the cells survival advantages in serum deprivation and hypoxia conditions, which is observed in poorly oxygenated areas of solid tumors [115]. In its support a recent study showed a monoclonal antibody that specifically targets TASK-3 channels and triggers internalization of them causes inhibition of cancer cell survival, tumor growth and metastasis both in *in vivo* and *in vitro* [110] making TASK-3 channels a potential target for cancer treatment and other K2P channels potential suspects in cancer treatment research.

1.6.2. TALK channels

1.6.2.1. TASK-2 channel

In the pathogenesis of autoimmune diseases like multiple sclerosis and rheumatoid arthritis autoreactive T cells have a critical role [104, 116]. In multiple sclerosis condition CD8+ and to lesser extent CD4+ T cells show an overexpression of TASK-2 channels. Moreover, TASK-2 positive T cells can be found in inflammatory lesions from multiple sclerosis tissue specimens [104]. Likewise in the pathogenesis of rheumatoid arthritis, CD4+ T cells play an important role. It has been shown that TASK-2 expression is increased in CD4+ T cells and expression level is correlated with severity of the disease [116]. Also upregulation of TASK-2 can be observed in cancer pathogenesis. Most primary breast tumors are sensitive to estrogen, which increases cell proliferation. TASK-2 is shown to be involved in estrogen induced proliferation of cancer cells. Estrogen induces an increase in mRNA, protein and TASK-2 current of these cells. While treatment of the cells with TASK-2 siRNA reduces proliferation of cancer cells. It is believed that TASK-2 channels are necessary for normal estrogen-induced proliferation of cancer cells and that TASK-2 plays a role in regulating proliferation of these cells [105].

While upregulation of TASK-2 can cause different diseases, its downregulation can also have pathological consequences. A large decrease in TASK-2 expression is observed in

osteoarthritis chondrocytes. Moreover it is suggested that TASK-2 channels contribute to side effects of local anesthetic drugs like bupivacaine that are widely used following joint surgery. It has been shown that *in vitro* blockage of TASK-2 channels by bupivacaine in addition to membrane depolarization has deleterious effects on human and bovine articular chondrocytes [38]. Also, human proximal renal tubular acidosis syndrome is induced in TASK-2 knockout mice. Therefore it has been suggested that this channel is a potential candidate for this disease and a target for treatment [102].

1.6.2.2. TALK-2 channel

TALK-2 is strongly expressed in Purkinje fibers, atrioventricular node and to a lesser extent in atrium [117]. A mutation of TALK-2 in extracellular cap (G88R) which produces a gain of function channel, is proposed to be involved in some cases of heart arrhythmia by hyperpolarization of the cells and slowing of the conductive system [117].

1.6.3. TWIK-1 channel

Ironically one of the best known physiological roles of TWIK-1 is its role in pathophysiological regulation of the human heart. Hypokalemia in humans can cause heart arrhythmia and sudden death due to heart arrest. As expected from calculation of the Nernst potential in rats and mice, hypokalemia induces strong hyperpolarization of cardiomyocytes. In human, however, hypokalemia induces depolarization of these cells (to around −50 mV). This is known as the paradoxical depolarization. Unlike rats and mice where there is no TWIK-1 expression in the heart, in humans TWIK-1 mRNA is the most abundant K^+ channel mRNA in the atrium, the second most abundant in cardiac Purkinje fibers, and is moderately abundant in the ventricle [18]. It has been proposed that under hypokalemic condition a C-type inactivation intermediate state which is known to be an occluded or short-lived Na^+-permeable state in most K^+ channels, is stabilized in TWIK-1 channels [118]. Using TWIK-1 K274E which is proposed to prevent silencing of TWIK-1 channels by SUMO, it has been shown that a threonine, Thr118, near the SF is responsible for changing selectivity from K^+ permeable to Na^+ permeable TWIK-1 channel. Although mutating Thr118 to a conserved isoleucine existing in other K2P channels abolishes

ion-selectivity shift in TWIK-1 channels, mutation of conserved isoleucine in TASK-3 or THIK-1 channels had much less or no effect [18].

Also it has been suggested that TWIK-1 has a role in cell proliferation in cancer cells by suppressing anchorage-independent growth of cells. The TWIK-1 gene, *KCNK1* has a binding site for p73, a protein which controls pathways limiting tumor aggressiveness and metastasis and its down regulation is observed in glioma, melanoma and ovarian cancer cells. Likewise, down regulation of TWIK-1 is observed in tumor cells from glioma, melanoma and ovarian cancer. However it is yet unclear how TWIK-1 is involved in regulation of cell growth and proliferation in cancer cells [119].

1.7. Pharmacology

Pharmacologically, ion channels are one of targets of pharmaceutical drugs. Among which K2P channels are targets of antidepressants, inhalational anesthetics, neuroprotective agents, and respiratory stimulants [6]. In recent years they have received a lot attention and are studied as potential targets of new medications. In this section I briefly mention major modulators of those K2P channels that were subject of this study, whether they are used as drugs or simply they are ions like Ba^{2+} that change gating of the channels.

1.7.1. TASK channels

TASK-1 channels were found to be relatively insensitive to common blockers of K^+ channels, like tetraethylammonium, 4-aminopyridine, and glibenclamide and sensitive to amiodorone [42]. Sanshool (hydroxy-α-sanshool) also inhibits both TASK-1 and TASK-3 channels. However the inhibitory effect is stronger on TASK-1 than TASK-3, with IC_{50}s of 30 and 450 µM, respectively [120]. TASK-1 is also blocked by methoxamine and Ala293 [93]. Both TASK-1 and TASK-3 channels are also inhibited by PKTHPP, A1899 and doxapram. In TASK-3, amino acids Leu122 on M2 and Gly236, Leu239 and Val242 on M4 have been proposed as a common binding site in the pore for these compounds. Also other residues that in TASK-1 contribute to binding of A1899, are also important in binding of PKTHPP in TASK-3 with exception of Ile118 and Thr121 [121]. However, it should be mentioned that the authors of this study could not exclude binding of these

compounds outside of pore region [121]. Moreover, A1899 is known as the specific blocker of TASK-1 channel. The affinity of the drug for TASK-3 the closest relative of TASK-1 is ten-fold less. Like for TASK-3, A1899 blocks the pore while interacting with lining residues in M2 and M4 and threonines of the SF and the K^+ ion in S4 binding site [122]. ML365 with high aqueous stability is another specific blocker of TASK-1 channels with IC_{50} of 16nM and a 62-fold selectivity over TASK-3 [123]. Compound 23 from Merck with an IC_{50} of 35 nM is introduced as specific blocker for TASK-3 channels. TASK-1 channels are less inhibited by compound 23 (IC_{50} = 303 nM) and other K2P channels are essentially nonresponsive to it. For instance, IC_{50} of TREK-1 is more than 10 µM [124].

In addition TASK-1 and TASK -3 channels are blocked by the endocannabinoid, anandamide and the synthetic cannabinoid agonist WIN55212-2 and 2-AG [53, 54]. Also TASK-1 and TASK-3 are blocked by methanandamide. Six residues (VLRFLT) in the proximal beginning of the C-terminus are responsible for effect of this agent on the channels. It is believed the block is not through binding of methanandamide to VLRFL-motif, but the motif is responsible for transduction of the signal to the gate following binding. [125].

Also TASK-1 and TASK-3 channels are strong candidates for a likely role in anesthesia [71]. Anaesthetics, particularly halogenated volatile anesthetics such as isoflurane and halothane, open various K2P channels [71]. Knockout mouse studies have shown that K2P channels are plausible targets for the actions of these agents. For example TASK-1 and TASK-3 are involved in loss of pain reflex by halothane and isoflurane and knockout mice lose the response to these agents [71]. Indeed, TASK-3 knockout mice have been shown to be significantly less sensitive to the general anesthetic halothane and showed the greatest decrease in sensitivity to an inhalational anesthetic [72]. However it should also be mentioned that K2P channels are not the only targets of anesthetics, as it has been shown that TASK-channel inhibitors do not interfere with anesthesia [71].

It is worth mentioning that the effect of pharmacological compounds can be altered by the channel composition. For instance, isoflurane slightly inhibits TASK-1 channels while activates both TASK-3 and TASK-1/TASK-3 heterodimers. On the other hand ruthenium red inhibits just TASK-3 channels, but not TASK-1 and TASK-1/TASK-3

heterodimers [68]. Likewise both TASK channels are sensitive to Ba^{2+} and Cu^{2+} [3, 42], while TASK-3 homodimers are Zn^{2+}-sensitive and TASK-1 homodimers and TASK-1/TASK-3 heterodimers are Zn^{2+}- insensitive [76].

1.7.2. TALK channels

Extracellular application of tetraethylammonium mildly inhibits both TALK-1 and TALK-2 channels. And Ba^{2+} and quinidine inhibit both TALK-1 and TALK-2 channels. However, quinine inhibits just TALK-1 channels, while it activates TALK-2. Neither 4-aminopyridine nor Cs^{+} affect TALK-1 and TALK-2 currents [22, 35]. TALK-1 and TALK-2 are both inhibited by high concentrations of chloroform and halothane. While TALK-1 is not sensitive to isoflurane, TALK-2 is activated by this anesthetic [22]. Also the local anesthetics bupivacaine and lidocaine weakly inhibit TALK-2 channels [35].

Also the classical K^{+} channels blockers tetraethylammonium and 4-aminopyridine apamin, or charybdotoxin do not inhibit TASK-2 channels [20, 100]. TASK-2 is inhibited by non-selective K^{+} channel inhibitors such as quinidine, lidocaine, and clofilium and is activated by volatile anesthetics [64, 100]. However, Ba^{2+} slightly inhibits TASK-2 currents at 1mM and Cs^{+} shows no inhibition [20].

Nitric oxide and reactive oxygen species activate TASK-2, TALK-1 and TALK-2 [3].

1.7.3. TWIK Channel

TWIK-1 channels are inhibited by quinine, quinidine and Ba^{2+} [37] and are believed to be insensitive to activation by anesthetic compounds although local anesthetics such as bupivacaine have been shown to inhibit the channels [71].

Summary of objectives:

Throughout the previous sections I have discussed that most of K2P channels at the single channel level are inward rectifiers. However upon depolarization even at symmetrical K^{+}

concentrations, the macroscopic currents show outward rectification and time-dependent activation kinetics. Both these effects suggest that depolarization increases the P_O of K2P channels. With the lack of a canonical voltage sensor such as that which exists in classical voltage gated channels, we asked which mechanism do K2P channels use to respond to depolarization, and which part or parts of the channels are responsible for this voltage-dependent gating. In the first part of this work I used electrophysiological methods and mutagenesis to find an answer to these questions. In the second part I investigated the gating properties of TWIK-1 channels and set out to answer; why TWIK-1 channels show very low activity, even if they are manipulated to be overexpressed in the plasma membrane.

In the next chapters I present the results of our experiments and then discuss why and how K2P channels respond to changes in transmembrane voltage. I also present our new findings regarding voltage gating of TWIK-1 and discuss a hypothesis concerning the low activity of TWIK-1 channels at the plasma membrane.

2. Materials and Methods

2.1. Materials

2.1.1. Chemicals

All chemicals were purchased from Sigma. The intracellular solution (K^+_{int}) had the following composition in mM: 120 KCl, 10 HEPES, 2 EGTA and 1 Pyrophosphate, adjusted to the appropriate pH with HCl/KOH. Other intracellular solutions were prepared by replacing K^+ by Cs^+, Na^+, NH_4^+, Rb^+ or Tl^+. Appropriate pH was adjusted with hydroxide of the relevant ion species. Extracellular solution (K^+_{ex}, pipette solution) had the following composition in mM; 120 KCl, 10 HEPES and 3.6 $CaCl_2$. pH was adjusted to 7.4 with HCl/KOH. In other extracellular solutions K^+ was replaced by Cs^+, NH_4^+ or Rb^+ and pH was adjusted with hydroxide of the relevant ion species. Tetrapentylammonium chloride (TPA) were stored as 100 mM stocks at -20°C and prior to use was diluted in the relevant intracellular solution to final concentrations. All solutions were applied to the cytoplasmic side of excised patches for the various ion channels via a gravity driven multi-barrel micropipette.

2.1.2. Biological

Adult female *Xenopus laevis* frogs were purchased from NASCO and maintained in the animal facility according to animal husbandry guide lines. Oocytes were removed surgically by Ms. Ria Neumann and Ms. Michaela Unmack according to proper guidelines and treated with 2mg/ml collagenase type II (Sigma, Taufkirchen, Germany) for one hour at room temperature prior to manual defolliculation.

2.2. Molecular biology

In this study human clones of TASK-1 (GenBank accession number: NM_002246), TASK-2 (NM_003740), TASK-3 (NM_001282534), TALK-1 (NM_032115), TALK-2 (EU978944), TWIK-1 (NM_002245), TREK-2 (NM_021161), and rat TREK-1 (NM_172042) were investigated. All molecular biology was done by Dr. Hariolf Fritzenschaft or Ms. Michaela Unmack. In short; the corresponding cDNA was subcloned into pBF, pFAW, or pSGEM expression vectors for oocyte expression. Site directed mutagenesis was performed using the QuikChangeII system (Stratagene, La Jolla, CA, USA) and verified by DNA sequencing. mRNAs were synthesized *in vitro* by using the SP6 or T7 mMESSAGE mMACHINE kit (Ambion, Austin, TX, USA) and specific linearized cDNA template. The synthesized mRNA stored in stock solutions at -80°C until usage.

2.3. Expression

For expression of the required channel roughly 50 nl of mRNA solution was manually injected into Dumont stage VI oocytes and incubated at 17°C for 1-7 days prior to use.

2.4. Electrophysiology

Giant patch recordings in inside-out configuration under voltage-clamp conditions were made at room temperature. Pipettes were made from thick-walled borosilicate glass, had resistances of 0.3-0.9 MΩ (tip diameter of 5-15 µm) and filled with K^+_{ex} or replaced ions (Cs^+, NH_4^+ or Rb^+). Currents were recorded with an EPC10 amplifier running under Patchmaster software (HEKA electronics, Lamprecht, Germany) and sampled at 10 kHz with analog filter set to 3 kHz (-3 dB) and stored for later analysis.

2.5. Data analysis

The data from the recorded currents were extracted by Fitmaster (HEKA electronics, Lamprecht, Germany) and further analyzed and visualized by Fitmaster, Igor Pro

(WaveMetrics, Inc. USA) and Microsoft Excel. Statistics data are shown in form of mean data with error bars as standard mean error.

Half Inhibition concentrations (IC_{50}) are calculated by fitting data with a Hill Equation:

$$f(C) = A_c + \frac{A - A_c}{1 + \left(\frac{C_{1/2}}{C}\right)^n}$$

Where *A*; the control current in ampere, A_C; inhibited current by concentration *c*, *C*; the concentration of the inhibitor, $C_{1/2}$; the concentration of half-inhibition and *n*; is the Hill coefficient.

Gating charges are calculated by the Boltzmann function:

$$f(v) = \frac{A}{1+e^{-\left(\frac{V-V_{1/2}}{RT/zF}\right)}} + \mathrm{C}$$

Where A is; the measured current in ampere, V; voltage in volt, $V_{1/2}$; voltage of half-activation. R; the universal gas constant, T; absolute temperature in Kelvin, F; the Faraday constant, and z; the gating charge (e_0) and C; the current offset from zero.

3. Results

3.1. Voltage activation is a feature of pH_{ex}-sensitive K2P channels

As mentioned in the first chapter; it has previously been shown that all members of pH_{ex}-sensitive K2P channels, except TWIK-1 (i.e. TASK-1, TASK-2, TASK-3, TALK-1, TALK-2) exhibit slight inward rectification at the single channel level. However, upon depolarization the steady-state macroscopic currents show outward rectification in symmetrical K^+ concentrations. To obtain a comprehensive picture of this voltage-dependent gating I measured currents from various pH_{ex}-sensitive K2P channels in symmetrical K^+ concentrations in response to 300 ms voltage steps (from -100 to +100 mV) from and back to a holding potential of -80 mV in giant patches excised from *Xenopus* oocytes expressing the various channels of interest.

The obtained currents can be dissected into five distinct components (Fig. 3.1); currents at the holding potential which are due to the intrinsic open probability (P_O) of the channels, instant activation currents which are also due to their intrinsic P_O, voltage activated currents that are due to an increase in the P_O due to depolarization, then repolarization and tail currents which are observed as the membrane is repolarized and the P_O of the channels decreases back towards the intrinsic P_O.

Nearly all of these channels exhibit prominent outward rectification as a result of a time- and voltage-dependent activation process. In this thesis I have investigated the voltage-gating and characteristics of each member of the family in the following sections.

Since TASK-3 and TASK-2 channels exhibit the most voltage-dependent activation amongst the pH_{ex}-sensitive K2P channels studied in this thesis, I therefore begin with a description of the TASK-3 channel.

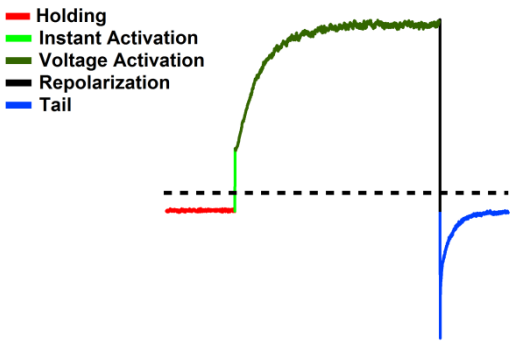

Fig. 3.1. A typical trace from K2P channels, before, during and after voltage activation. The color coding shows the components of the trace as the voltage or the current changes. Note that the voltage for holding, repolarization and tail components are equal. The instantaneous and voltage activations occur during depolarization.

3.1.1 TASK channels

3.1.1.1. TASK-3 channel

TASK-3 channels conducted small inward currents at the holding potential (-80 mV) which can be completely blocked with 1 mM TPA applied from the intracellular side (Fig. 3.2A). These currents are due to the moderate P_O of this channel at this potential.

Upon depolarization from the holding potential to the test potential, the current above the reversal potential (i.e. above 0 mV in symmetrical K^+) shows two distinct components; an instantaneous and a voltage-time dependent component. The latter also shows a gradual increase in current with increasing voltage (Fig. 3.1 and Fig. 3.2C). The voltage-time dependent component is best observed from voltages over 20 mV and has a time course of ≈ 4 ms, which is relatively constant at all voltages (Fig. 3.2C and Fig. 3.3).

The other important feature of these TASK-3 currents is the tail currents (Fig. 3.2D and Fig. 3.1) that appear upon repolarization. Like the outward currents, the tail currents also consist of two components; an instantaneous component which is much larger than the currents at the holding potential, and a time-dependent component, which gradually decreases to reach the currents at the holding potential. Therefore unlike the currents elicited from test pulses the instantaneous and time-dependent components of the tail currents occur in opposite directions, because the tail currents gradually deactivate to reach the level of currents at the holding potential.

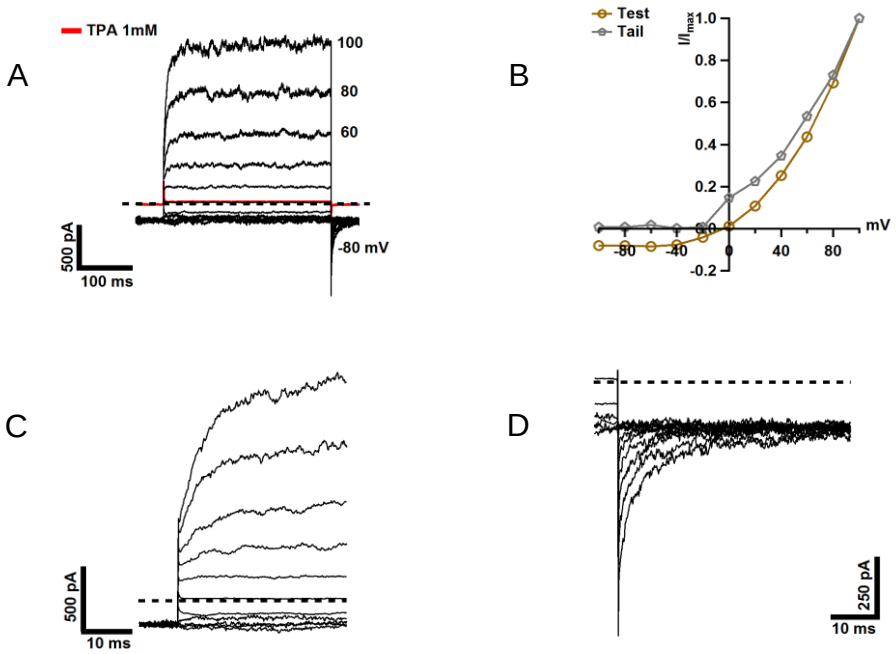

Fig. 3.2. TASK-3 currents. (A); a family of currents elicited by test pulses from -100 to 100 mV from and back to a holding potential of -80 mV in symmetrical K^+ concentrations. 1 mM TPA block indicates that the currents at the holding potential are not leak. (B); normalized IV relationship of test pulses and tail currents. (C); the activation of the currents in (A) are magnified to show the time course of activation. (D); the decaying tail currents from (A) are magnified to show the time course of deactivation.

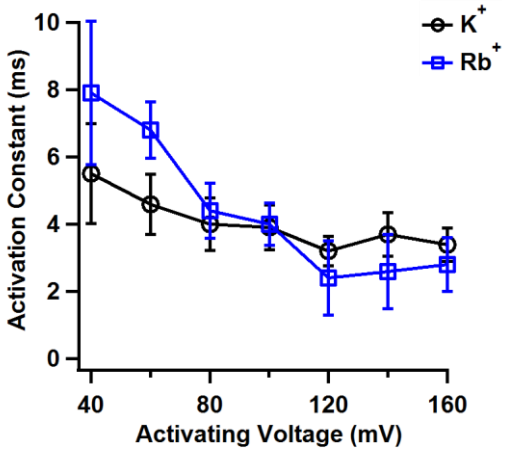

Fig. 3.3. TASK-3 time constant of activation is relatively stable across different voltages. The time constants for activation of K^+ and Rb^+ currents are plotted against the test voltages.

The current-voltage relationship plots from TASK-3 channels show a strong outward rectification, i.e. the currents from the test pulses above the reversal potential (0 mV) are larger than those from below the reversal potential. The absolute values of the tail currents also show a positive rectification and fit well over those of the test pulses (Fig. 3.2B).

3.1.1.2. TASK-2 channel

TASK-2 channels also show voltage-dependent activation of currents at voltages more positive than the reversal potential (Fig. 3.4A and 3.4C). Like TASK-3, TASK-2 channel currents at a holding potential of -80 mV are relatively small and completely blocked by 1 mM TPA which indicates they are not leak currents in the patch. The outward currents are larger and show both instantaneous and voltage-time dependent components. However, the outward currents from TASK-2, in comparison to those of TASK-3, are relatively small. Despite that the corresponding current-voltage relationship clearly shows outward rectification (Fig. 3.4B). However, in contrast to TASK-3, the tail currents from TASK-2 are larger than the outward currents (Fig. 3.4A). The absolute values of the tail currents from TASK-2 channels plotted against voltage also show positive rectification. However unlike those of TASK-3 they do not fit on the plot of currents from the test pulses because TASK-2 channels are relatively open at negative voltages.

Both voltage-time-dependent components of outward currents and tail currents are larger than those of other K2P channels examined. With 22 ms for activation and 8 ms for deactivation, TASK-2 currents activate and deactivate slower than TASK-3 (Fig. 3.2 and Fig. 3.4).

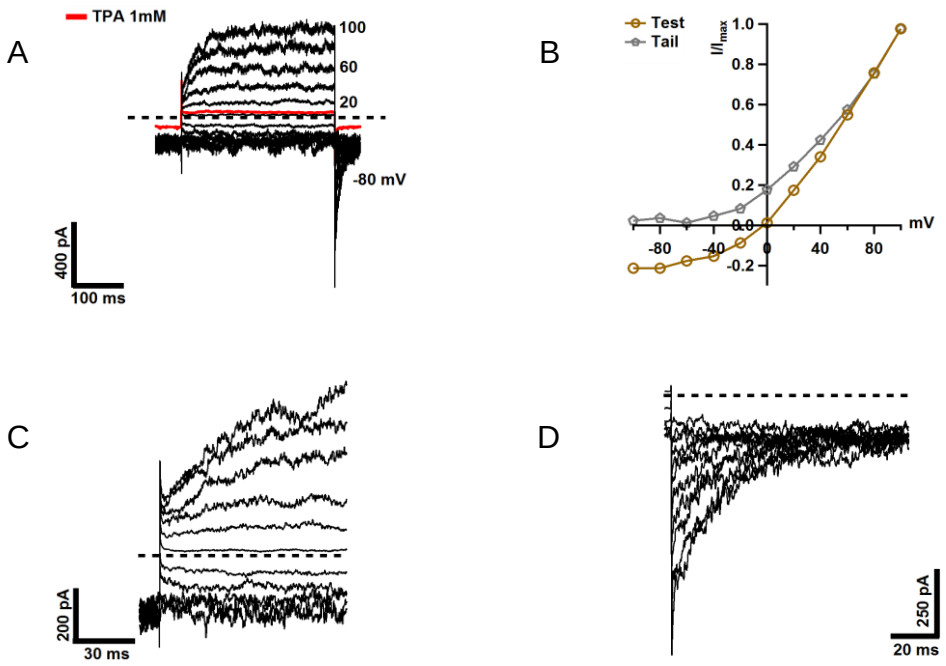

Fig. 3.4. TASK-2 currents. (A); a family of currents elicited by test pulses from -100 to 100 mV from and back to holding potential of -80 mV in symmetrical K^+ concentrations. 1 mM TPA block indicates that the currents at holding potential are not leak from the patch. (B); normalized IV relationship of test pulses and tail currents in (A). (C); the activation of the currents in (A) are magnified to show the time course of activation. (D); the decaying tail currents in (A) are magnified to show the time course of deactivation.

3.1.1.3. TASK-1 channel

Unlike TASK-3 and TASK-2, TASK-1 channels conduct relatively larger currents at voltages negative to the reversal potential. These can be completely blocked by 1mM TPA, indicating relatively higher intrinsic P_O. As a result the current-voltage relationship of these channels with only minor outward rectification is almost like a classic open rectifier (Fig. 3.5B). Nevertheless after repolarizing the membrane to the holding potential, clear and indistinguishable deactivating tail currents develop (Fig. 3.5A).

Although the channels are relatively open at all voltages, with a time constant of 4ms, the voltage-time-dependent component of the outward currents is easily resolved (Fig. 3.5C). With a time constant of 3 ms, the tail currents show clear deactivation to the level of currents at the holding potential (Fig. 3.5D). Interestingly both of these values are very similar to those of TASK-3 which is the most homologous K2P channel to TASK-1.

Also indistinguishable from TASK-3, the absolute values of the tail currents plotted against voltage show a positive rectification that indicates the tail currents also increase with voltage. However unlike TASK-3 it does not fit over that of test pulses (Fig. 3.5B).

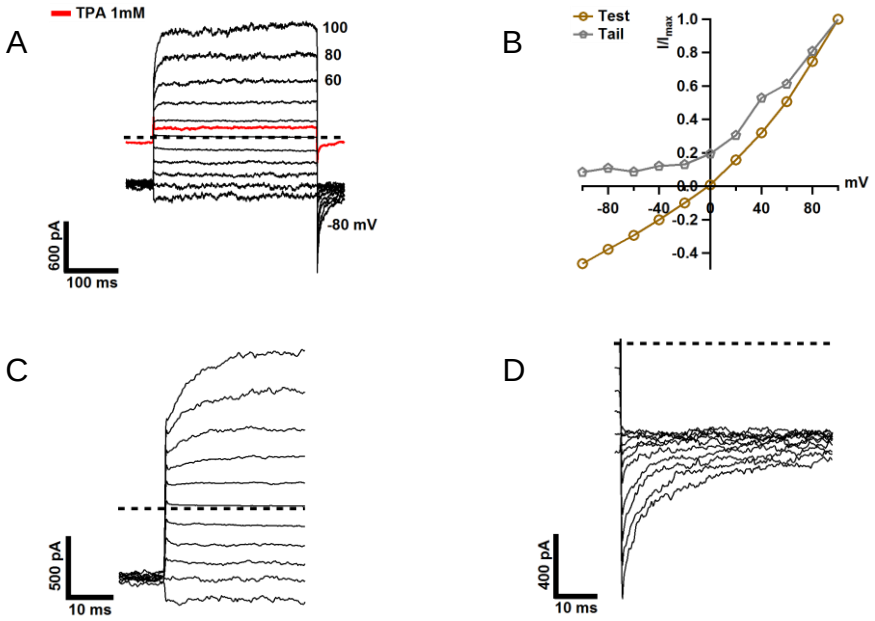

Fig. 3.5. TASK-1 currents. (A); a family of currents elicited by test pulses from -100 to 100 mV from and back to holding potential of -80 mV in symmetrical K^+. 1 mM TPA block indicates that the currents are not leak. (B); normalized IV relationship of test pulses and tail currents in (A). (C); the activation of the currents in (A) are magnified to show the time course of activation. (D); the decaying tail currents in (A) are magnified to show the time course of deactivation.

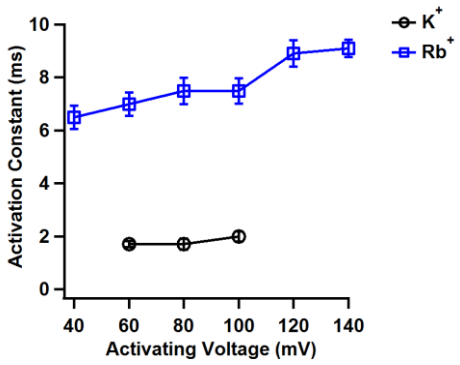

Fig 3.6. Time constant of activation for TALK-2 is constant across different voltages. The time constants for activation of K^+ and Rb^+ currents are plotted against depolarizing voltages.

3.1.2. TALK channels

3.1.2.1. TALK-2 channel

TALK-2 channels, similar to TASK-1, have a relatively high P_O at voltages negative to the reversal potential. As a result the current-voltage relationship and rectification of these channels is similar to that of TASK-1 (Fig. 3.7B). However, steady state outward currents from TALK-2 channels show slight deactivation at voltages above 40 mV which increases with voltage (Fig. 3.7A).

Like other K2P channels we studied, activation with test pulses show the instantaneous and voltage-time dependent components, with the time constant of 2 ms for the latter (Fig. 3.6). Likewise, deactivating tail currents develop after the test pulses and upon repolarization to the holding potential of -80 which increase with increase of test pulses and with a time constant of 1 ms for the deactivation are the fastest resolvable tail currents in terms of deactivation (Fig. 3.7A).

3.1.2.2. TALK-1 channel

In our hands, TALK-1 channels did not produce any reliable K^+ currents. However we could measure these channels using ions rather than K^+ that I show in the next section.

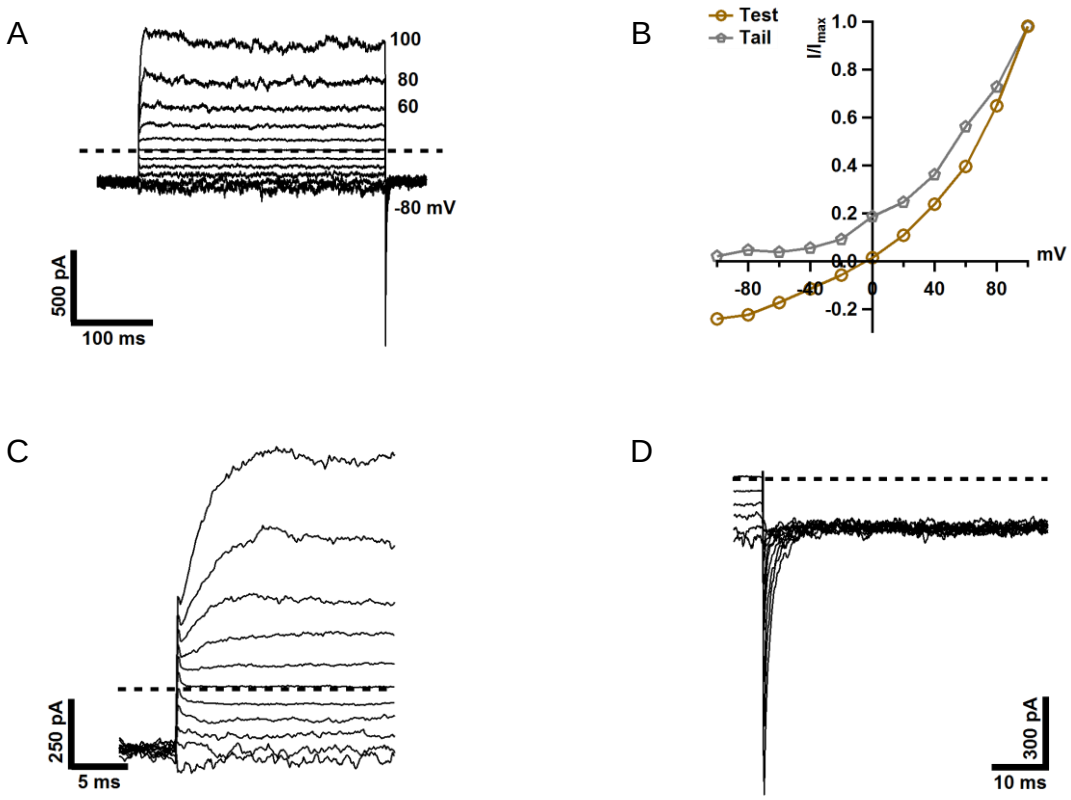

Fig. 3.7. TALK-2 currents. (A); a family of currents elicited by test pulses from -100 to 100 mV from and back to holding potential of -80 mV in symmetrical K^+ concentrations. (B); normalized IV relationship of test pulses and tail currents in (A). (C); the activation of the currents in (A) are magnified to show the time course of activation. (D); the decaying tail currents in (A) are magnified to show the time course of deactivation.

3.2. Gating by non-physiological ions.

We have observed that at all voltages positive to the reversal potential, intracellular NH_4^+ and Rb^+ ions increase the outward and tail currents of K2P channels like TREK and TRAAK [126]. Cs^+ ions on the other hand are not permeable through K2P channels, or are only poorly permeable at supra-physiological voltages. However, they also evoke large tail currents at potentials positive to the reversal potential. I therefore set out to find out how these non-physiological ions activate pH_{ex}-sensitive K2P channels.

K^+ is the most potent ion in activating TASK-1 channels. Both Rb^+ and NH_4^+ elicit outward currents which are half or smaller in size than those of K^+ ions (1.28 nA, 0.62 nA and 0.57 nA, respectively for K^+, Rb^+ and NH_4^+ at 100 mV in the representative patch in Fig. 3.8). As expected, Cs^+ does not permeate through TASK-1 channels.

Likewise, tail currents elicited by these monovalent ions are either comparable to, or smaller than, those carried by K^+, (-1.4 nA, -0.98 nA, -1.7 nA and -0.67 nA respectively for K^+, NH_4^+, Rb^+ and Cs^+, in the representative patches shown in Fig. 3.8). The time course of activation is similar for all outward currents evoked by these monovalent ions (τ = 3 ms, 3 ms and 4 ms respectively for K^+, NH_4^+ and Rb^+ at 100 mV,). This is also the case for deactivation of the tail currents, with a time course of about 2 ms.

TASK-3 channels also seem to be less or equally activated by monovalent ions in comparison to K^+. Interestingly however, the tail currents evoked by these ions, including non-permeable Cs^+, are significantly larger than those elicited by intracellular K^+ (Fig. 3.9A and 3.9D).

However the time constants for activation were different for these ions, in Fig. 3.9, as a representative measurement, the time constants for activations are; 14, 7 and 4 ms respectively for K^+, Rb^+ and NH_4^+. Time constants of tail current deactivation are more similar, still for K^+ deactivation is slower, with constant of; 8, 4, 5 and 3 ms for K^+, Cs^+ Rb^+ and NH_4^+, respectively.

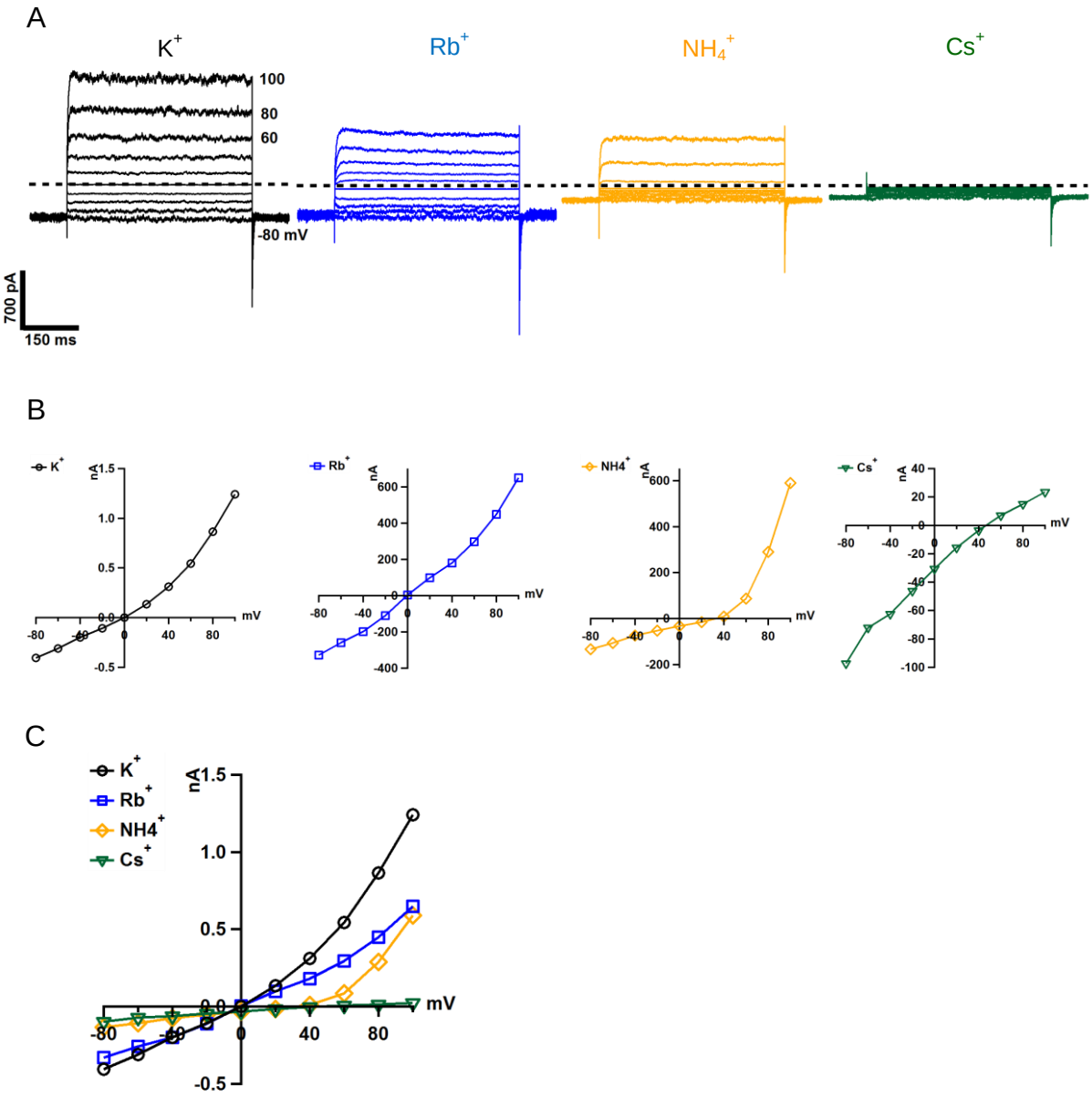

Fig. 3.8. Activation of TASK-1 channels by different intracellular ions. (A); families of currents elicited by test pulses from -100 to 100 mV from and back to holding potential of -80 mV with extracellular K^+ and indicated intracellular ions. The families are sorted by potency of activation from higher to lower. (B); IV relationships from measurements in (A) individually shown to indicate the rectification of currents by each ion. (C); superposition of IVs in (B) for comparing activation of TASK-1 by different ions.

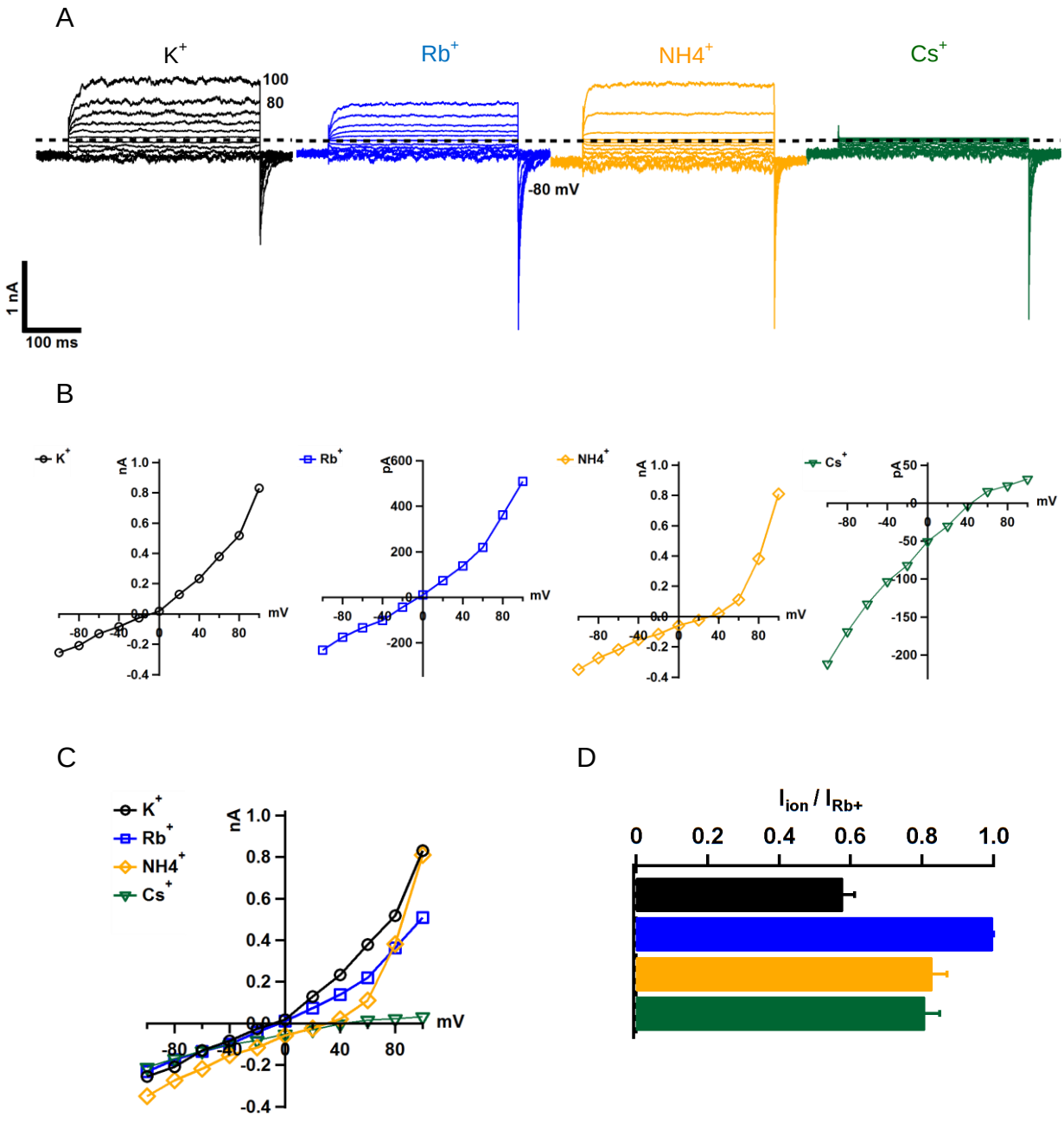

Fig. 3.9. Activation of TASK-3 channels by different ions. (A); families of currents elicited by test pulses from -100 to 100 mV from and back to holding potential of -80 mV with extracellular K^+ and indicated intracellular ions. Note that Cs^+ is not permeable however it activates the TASK-3 channels similar to Rb^+ and large K^+ tail currents develop upon repolarization. (B); IV relationships from measurements in (A) individually shown to indicate the rectification of currents by each ion. (C); superposition of IVs in (B) for comparing activation of TASK-3 by different ions. (D); tail currents amplification by different ions. The tail currents are normalized to that of Rb^+ activated tail currents.

Among pH_{ex}-sensitive K2P channels, TALK-2 channels stand out regarding their activation by non-physiological monovalent ions. For instance in the representative experiment while outward K^+ currents at the end of the 100 mv test pulse are about 0.8 nA, those of NH_4^+ and Rb^+ are; 2 and 14.5 nA, respectively (Fig. 3.10A). Tail currents evoked by intracellular application of these ions are also proportionally larger than those of K^+. While tail currents from K^+ are -1.3 nA those of NH_4^+ and Rb^+ are -2.3 and -17.3, respectively (Fig 3.10A). Interestingly tail currents from intracellular application of non-permeable Cs^+ ions are very similar to Rb^+ with an amplitude of 15 nA. This was true for all TALK-2 channel measurements (Fig 3.10D).

Another interesting observation is that for all three ions that carry outward currents, the instantaneous components are almost equal, 0.53, 0.54, 0.67 nA for K^+, Rb^+ and NH_4^+, respectively. However as is mentioned above, Rb^+ ions carry a large 14.5 nA current that mostly consist of the voltage-time dependent component. Also the Rb^+ outward currents from TALK-2 channels reach the steady state almost at the end of 300 ms pulse. Therefore, it seems that despite the fact that Rb^+-induced voltage activation of TALK-2 channels is very prominent, it is also very slow.

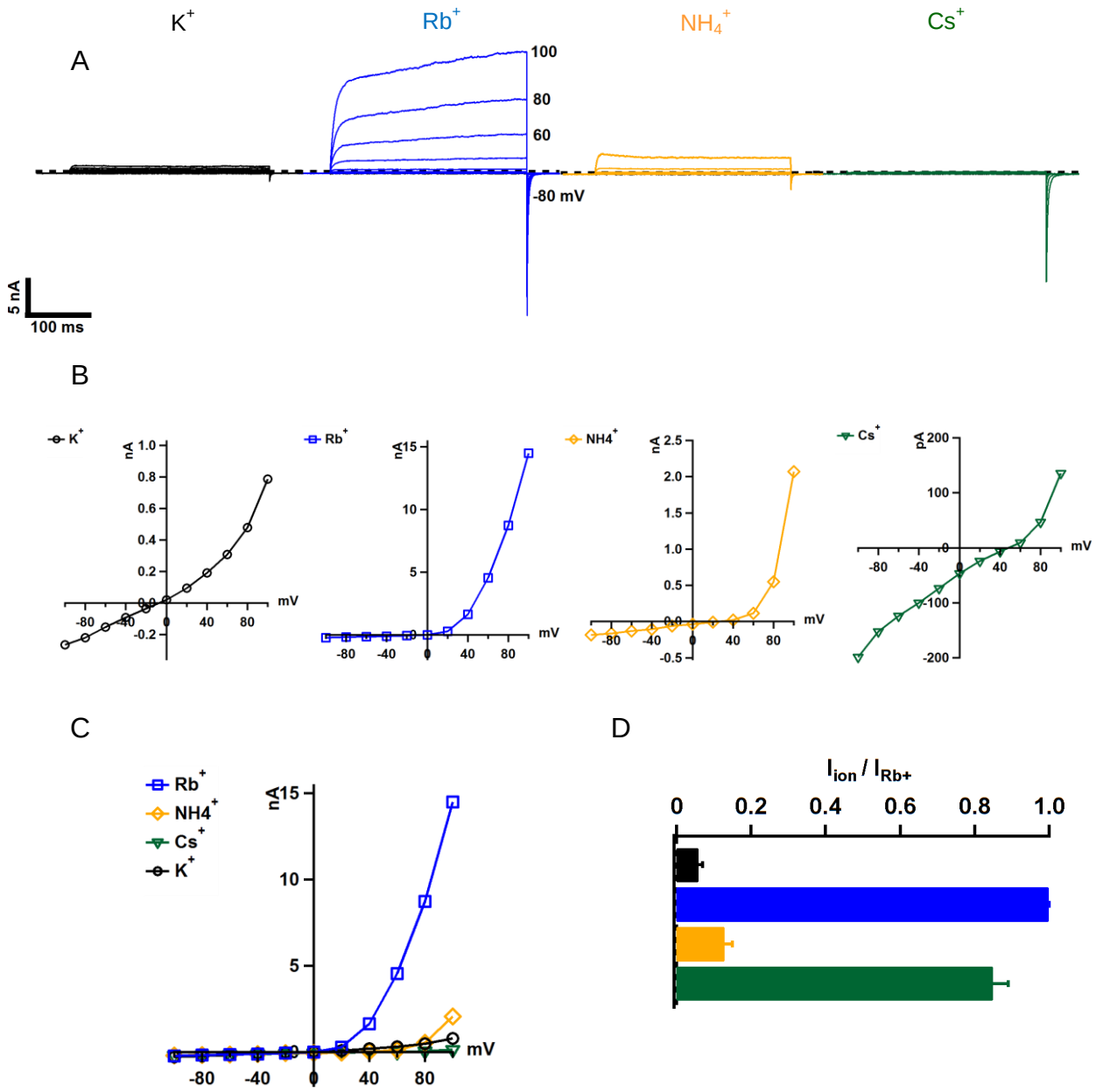

Fig. 3.10. Activation of TALK-2 channels by different ions. (A); families of currents elicited by test pulses from -100 to 100 mV from and back to holding potential of -80 mV with extracellular K^+ and indicated intracellular ions. Note that Cs^+ is not permeable however it activates the TAlK-2 channels very similar to Rb^+ and large K^+ tail currents develop upon repolarization. (B); IV relationships from measurements in (A) individually shown to indicate the rectification of currents by each ion. (C); superposition of IVs in (B) for comparing activation of TALK-2 by different ions. (D); tail currents amplification by different ions. The tail currents are normalized to that of Rb^+ activated tail currents.

As mentioned before, TALK-1 channels did not produce any reliable K^+ currents. However they can be activated and characterized by intracellular Rb^+ ions (Fig. 3.11). Activation of outward currents carried by intracellular Rb^+ and deactivation of tail currents carried by extracellular K^+ ions are both slow, 22 ms and 14 ms, respectively, and the tail currents are smaller than the corresponding outward currents.

I did not investigate the effect of other monovalent ions on voltage activation of TALK-1 channels.

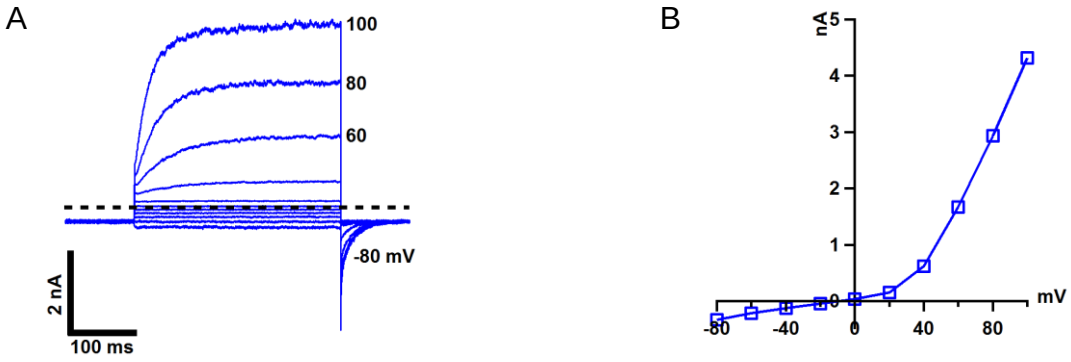

Fig. 3.11. Activation of TALK-1 channels by Rb^+. (A); a family of currents from -100 to 100 mV from and back to holding potential of -80 mV with intracellular Rb^+ and extracellular K^+ ions. (B); IV relationship from traces in (A).

3.3. Identifying the voltage-dependent gate

In the previous sections I showed that depolarization activates pH_{ex}-sensitive K2P channels and some channels like TASK-3, TALK-1 and TALK-2 show strong voltage activation in response to intracellular non-physiological ions such as Cs^+ and Rb^+. Next we set out to locate the voltage sensor and the gate. As mentioned in the introduction, most studies show that gating of K2P channels occurs either within, or close to, the selectivity filter (SF). We have also shown that in TREK-1 the channel is open at the intracellular side and blockers and modifiers have access to the pore even if the channel is functionally closed [126]. Therefore I focused on the SF to find out if voltage activation takes place at the SF. In the signature sequence, TIGY/FG within P1 or P2 from TASK-1, TASK-2 and TASK-3 the threonines were mutated to cysteines. All mutant channels; TASK-1 T199C, TASK-2 T98C, TASK-2 T203C, TASK-3 T93C and TASK-3 T199C, expressed well and with injection of higher concentration of mRNA, produced currents almost similar in amplitude to that of the corresponding WT channels. However all mutants were different from the WT channels in terms of gating and voltage activation.

Firstly, in contrast to the WT channels all the mutant channels were open rectifiers, producing linear current-voltage relationship indicating that the channels are open at all

voltages (Fig. 3.12). Secondly, the voltage-time dependent component of activation which is observed in all WT channels at the beginning of the depolarizing pulses are absent from the mutants and they just show an instantaneous response to the voltage pulses (Fig. 3.12). Thirdly, in contrast to the WT, all the mutated channels lack tail currents which are an indicator of channel activation beyond the initial P_O in response to depolarization.

Together these observations suggest that the SF and its integrity are the key elements in the voltage gating of the pH_{ex}-sensitive K2P channels.

Fig. 3.12. Mutation in the SF abolishes voltage gating of pH_{ex}-sensitive K2P channels. (A); a family of currents elicited by test pulses from -100 to 100 mV from and back to holding potential of -80 mV in symmetrical K^+ for WT TASK-3, T93C and T199C channels, respectively. The T199C mutant has an individual scaling at right. (B); same as in (A), but for WT TASK-2, T98C and T203C, respectively. (C); same as in (A), but for WT TASK-1, T199C, respectively. (D); superimposed IV relationships from the WT and the mutant channels in (A), (B) and (C). Note that in all cases unlike the WT channels the SF mutants are open rectifiers. Also all the WT channels develop deactivating tail currents that are absent in the mutant channels.

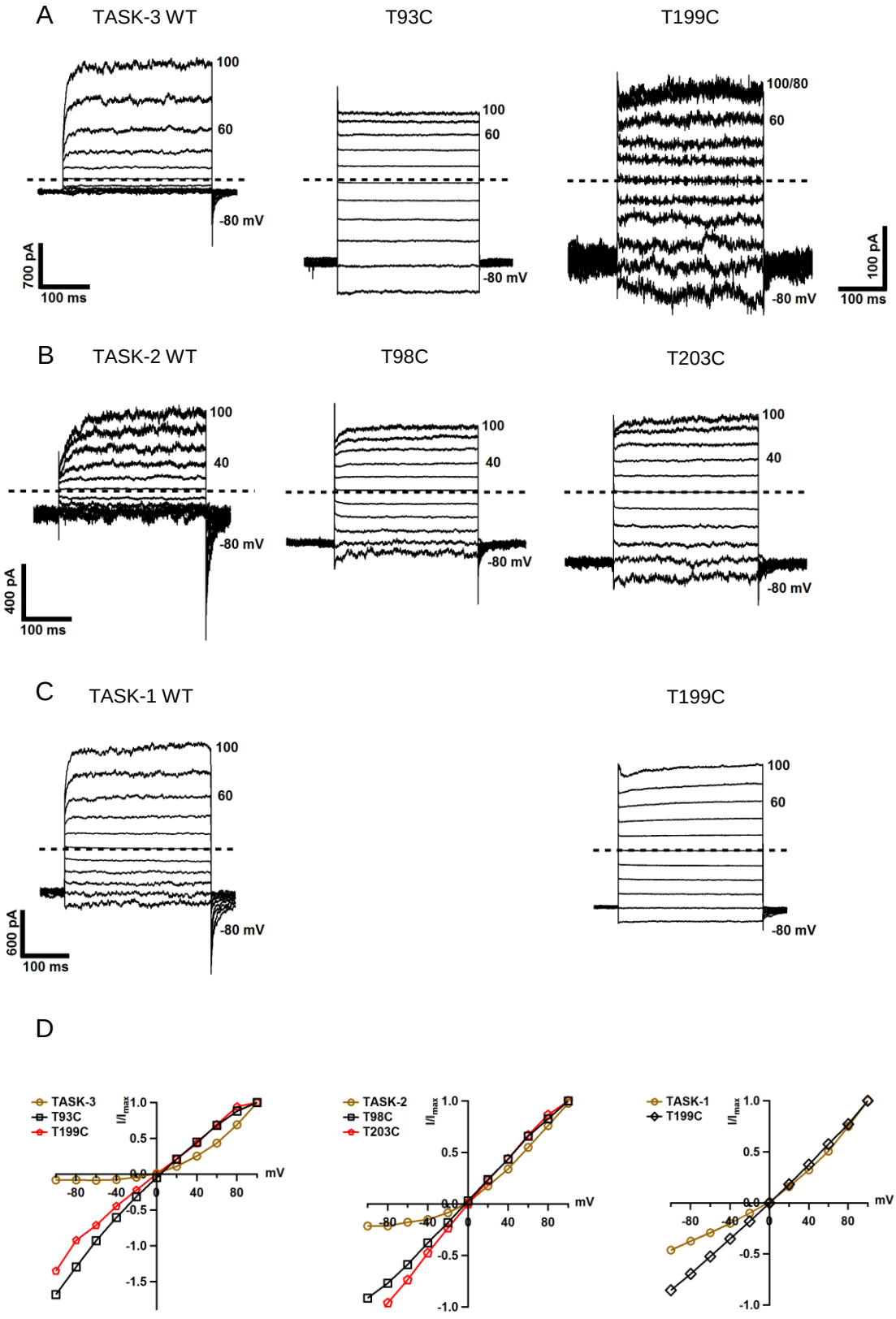
A
TASK-3 WT
T93C
T199C
100
60
-80 mV
700 pA
100 ms
100
60
-80 mV
100/80
60
-80 mV
100 pA
100 ms
B
TASK-2 WT
T98C
T203C
100
40
-80 mV
400 pA
100 ms
100
40
-80 mV
100
40
-80 mV
C
TASK-1 WT
T199C
100
60
-80 mV
600 pA
100 ms
100
60
-80 mV
D
TASK-3
T93C
T199C
I/I max
mV
TASK-2
T98C
T203C
I/I max
mV
TASK-1
T199C
I/I max
mV

3.4. The gating charge

K2P channels do not possess a conventional S4-like transmembrane voltage sensor similar to that found in classical voltage-gated potassium channels. However, as shown in the previous sections, even in symmetrical ion concentrations they respond to depolarization by conducting larger currents at positive voltages to the reversal potential than at negative voltages. That implies that depolarization increases the P_O of the channels. We therefore asked, in the absence of such a sensor, what is the equivalent gating charge required to translocate across the electric field in order for the channels to open?

Measuring a gating charge is relatively simple and can be achieved by plotting the conductance of the channels against the voltage change and fitting the plot with a Boltzmann function. The slope of the fit then represents the equivalent gating charge which moves through the entire electric field of the membrane. At any given voltage the conductance correlates with the current (V = IR and S = 1/R → S = IV), thus at a constant voltage, we can use currents as a measure of conductance. However, steady-state currents evoked by test pulses are not suitable for this purpose because both the voltage and driving forces change during each pulse. However, tail currents are perfectly suited as the membrane is repolarized to a constant voltage of -80 mV which also keeps the driving force constant. Therefore, the amplitude of the tail currents directly correlates with conductance of the membrane, and hence the P_O of channels during the relevant test pulses.

The Boltzmann function measures the distribution of P_O with the change of voltage, and therefore the P_O should have both an upper and lower limit. The lower limit is obviously the P_O before activation whilst the upper limit would be the maximum P_O that the channels can achieve under particular experimental condition, where further depolarization does not increase the P_O. Hence the tail currents need to saturate, i.e. the amplitudes of tail currents need to reach a maximum and then remain constant with further increases in voltage.

None of K2P channels we studied demonstrated tail current saturation using intracellular K^+ ions in the tested voltage range. However, most of the pH_{ex}-sensitive K2P channels examined including; TALK-1 and TALK-2 showed tail current saturation using intracellular Cs^+ or Rb^+ application (Fig. 3.13).

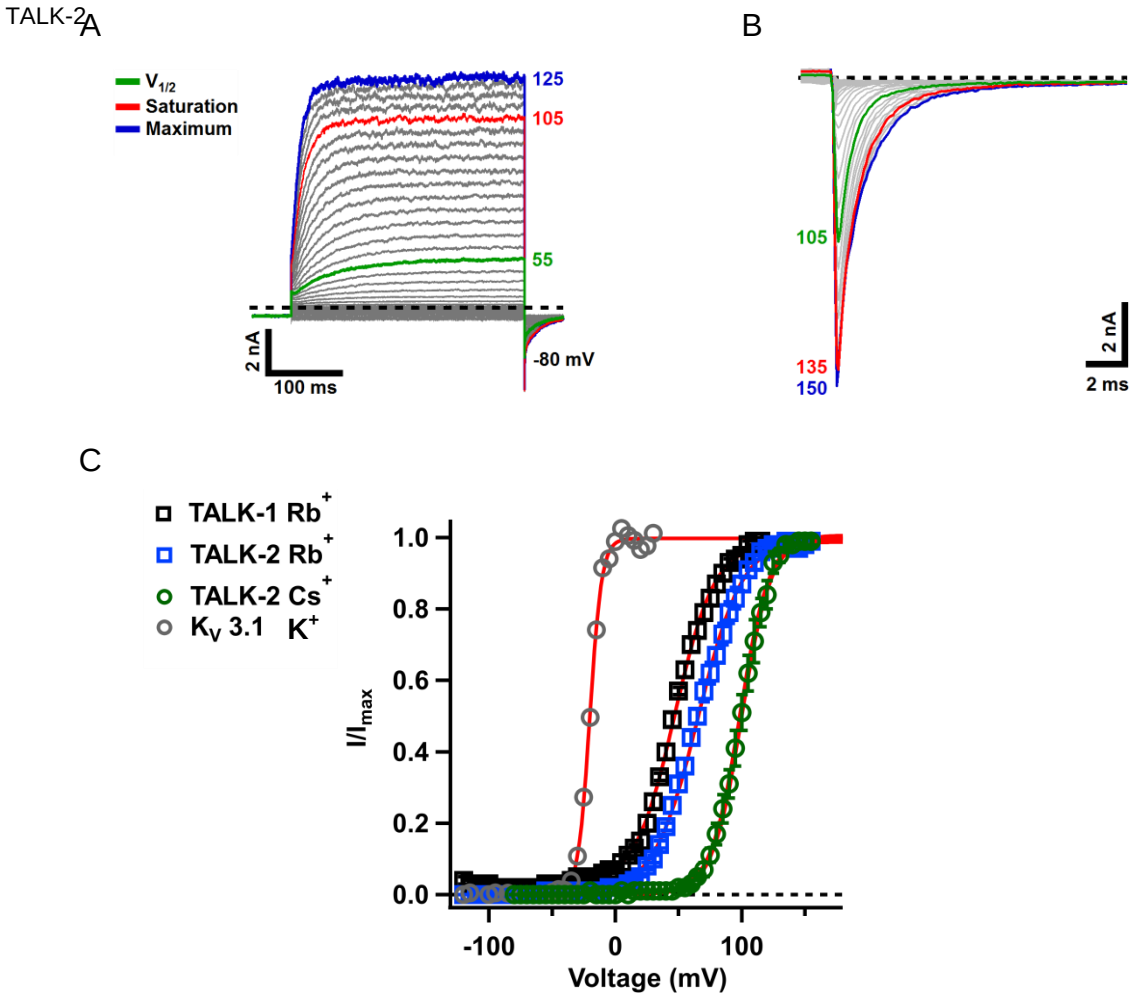

Fig. 3.13. Measuring the gating charge for pH_{ex}-sensitive K2P channels, TALK-1 and TALK-2. (A); TALK-1, a family of currents elicited by test pulses from -125 to 155 mV from and back to holding potential of -80 mV with intracellular Rb^+ and extracellular K^+. With increasing voltage of the test pulses, tail currents increase to become constant. (B); tail currents from TALK-2 measured as in (A) with intracellular Cs^+ and up to 150 mV. (C); absolute normalized tail currents from measurements same as in (A) for TALK-1, TALK-2 and $K_V3.1$ channels against test pulse voltages. Note that TALK-2 channels are measured with intracellular Rb^+ as well. Also at 55 mV where the tail current is half of the maximum tail current at 125 mV the outward current is about 22% of the steady state outward current.

Fitting these tail current-voltage plots (G-V) with a Boltzmann function revealed an equivalent gating charge of 1.8 e_0 and 2.2 e_0 for TALK-1 and TALK-2, respectively (Fig. 3.13). We have previously calculated the average gating charge for different K2P channels to be about 2.2 e_0 [126].

3.5. Voltage of half-activation

The Boltzmann distribution also predicts the voltage of half-activation ($V_{1/2}$) for K2P channels. It is the voltage at which the P_O reaches the half maximal point and is represented by the point at which the macroscopic tail currents reach their half maximal point upon repolarization. The $V_{1/2}$ for TALK-1, measured with intracellular Rb^+, was 48 ± 2 mV. TALK-2 tail currents do not saturate with intracellular Rb^+. However they do saturate with intracellular Cs^+. The $V_{1/2}$ of TALK-2 is 100 ± 3 mV (Fig. 3.13).

TASK channels are not activated by Rb^+ or Cs^+ any more than they are by K^+. Therefore the tail currents never appear to saturate within the measured voltage range. This means that the Boltzmann equation cannot be used to estimate the equivalent gating charge and $V_{1/2}$ for these channels. However, since the action potential in most organism has an upper limit of e.g. approx. 100-130 mV, one can define the $V_{1/2}$ experimentally by setting an upper limit to the depolarizing voltage pulses. This then results in a $V_{1/2}$ of ≈ 80 mV for TASK-3 in symmetrical K^+ condition and 0 mV in physiological K^+ concentrations.

In the next section I use the empirically measured $V_{1/2}$ for further validation of our model regarding the voltage gating of K2P channels, especially in TASK channels.

3.6. Voltage activation is tightly coupled to the electrochemical gradient

For several different K2P channels including; TRAAK, TREK-1 and TREK-2 which exhibit saturation of tail currents by either intracellular Rb^+ or Cs^+, we found that irrespective of whether the intracellular or extracellular ion concentration was changed, the $V_{1/2}$ for voltage activation shifted in parallel with the reversal potential [126]. In the same way the experimentally defined $V_{1/2}$ for TASK-3 channels shifts with the reversal potential, i.e. under physiological conditions TASK-3 channels reach both half and maximal activation at much lower voltages in comparison to symmetrical ionic concentrations (Fig. 3.14). These results clearly demonstrate that it is not the transmembrane voltage *per se* which drives K2P channel gating, but the electrochemical

driving force, i.e. the difference (Δμ) between the actual membrane voltage (V_m) and the reversal potential (E_{rev}.) (Δμ = V_m – E_{rev}).

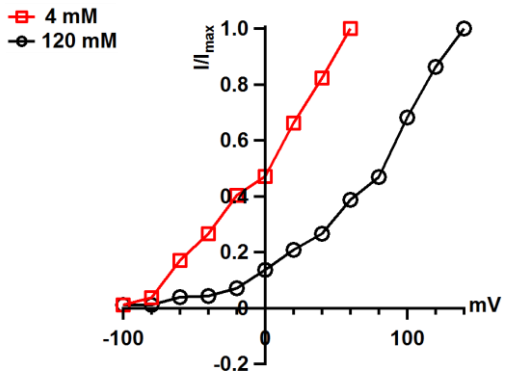

Fig. 3.14. Activation of TASK-3 channels depends on ion concentrations. Absolute normalized tail currents are plotted against test pulse voltages. The TASK-3 channels are measured in symmetrical K^+ concentrations of 120 mM, or the extracellular concentration is reduced to 4 mM. The decrease in extracellular K^+ concentration causes the TASK-3 channels to be activated at lower voltages and as a result the plot of tail currents against voltage shifts to the left in comparison to measurements in symmetrical K^+.

3.7 TWIK-1 channel

3.7.1. Intracellular pH regulation of TWIK-1

In the first chapter I have mentioned that TWIK-1 channels are known to be regulated by extracellular pH. However, I found that change in intracellular pH also regulates the activity of TWIK-1 channels. However, unlike TREK channels, pH regulation of TWIK-1 channels can just be assessed after voltage activation by Rb^+. ^{M}TWIK-1 channels (TWIK-1 II293-294AA) exhibit maximum activation at pH 8.5 and are inhibited by H^+. Therefore I did all the experiments with ^{M}TWIK-1 channels at pH 8 to be as close as possible to a physiologically relevant pH (Fig. 3.15). It should be noted that at very low pH (<6.0) TWIK-1 currents appear to show some biphasic activation, however this effect is probably an artifact due to activation of endogenous currents in oocytes; these currents are variable from patch to patch and can be smaller or larger than the leak currents that remain after block of TWIK-1 channels by 1 mM TPA. I calculated an IC_{50} of pH 7.8 for ^{M}TWIK-1 channels (Fig. 3.15).

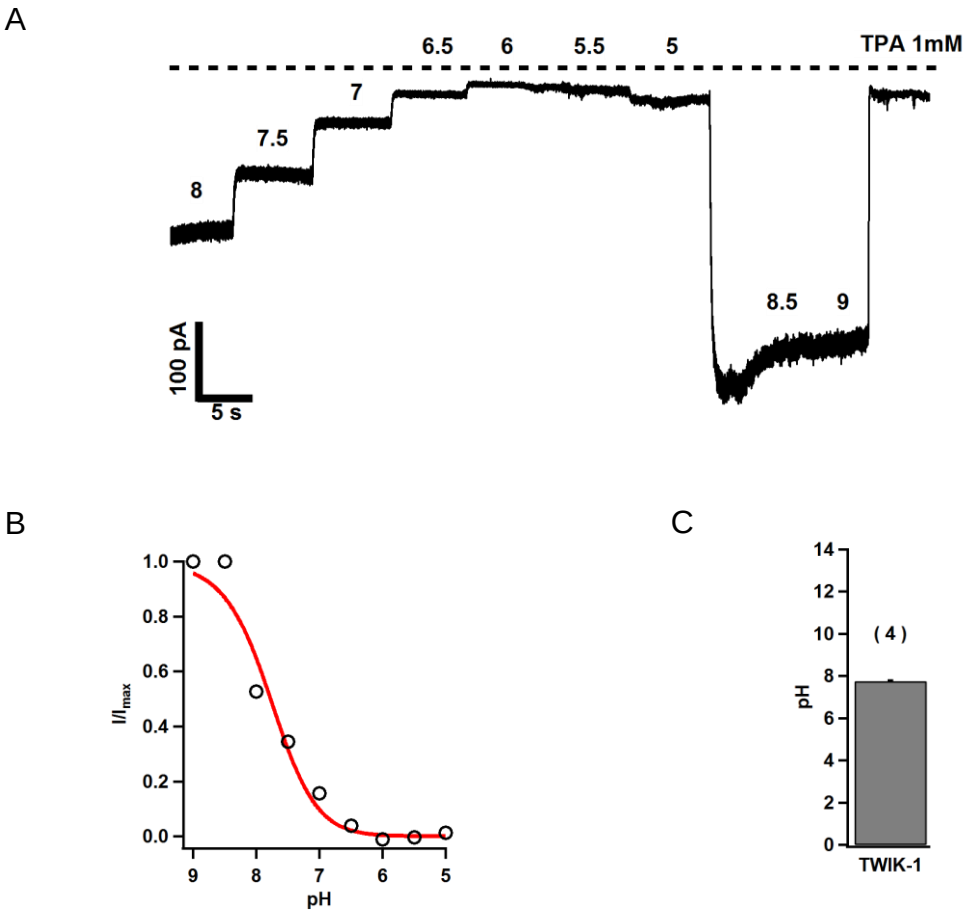

Fig. 3.15. pH gating of TWIK-1 channels. (A); acidic pH inhibits TWIK-1 channels. ^{M}TWIK-1 currents are elicited by a continuous pulse at -80mV with extracellular Rb^+ and intracellular K^+ of different pH as are labeled on the trace. Note that the slight increase of current at pH lower than pH 6 is due to activation of oocyte endogenous currents. (B); a representative Hill fit from measurements as in (A). (C); statistics representation of four fits as in (B).

3.7.2. Monovalent Ion-voltage gating

Amongst the pH_{ex}-sensitive K2P channels, TWIK-1 is in many ways very different (see introduction for a detailed description). In brief; TWIK-1 channels have a SF which is different from other K2P channels, and they exhibit very low levels of functional activity even when clearly present in the plasma membrane. Therefore, I now describe my studies on TWIK-1 channels separately from those of other K2P channels.

Previously it has been shown that WT TWIK-1 expressed in CHO cells can conduct very large NH_4^+ and Rb^+ currents in the whole cell configuration [59]. However, in our hands WT TWIK-1 measured in giant patches from *Xenopus* oocytes did not conduct any currents different from the endogenous currents (Fig. 3.16), irrespective of the ion

composition. This suggests perhaps the density of TWIK-1 channel within the membrane is not high enough to produce measurable currents and is certainly consistent with previous reports regarding the surface expression of TWIK-1.

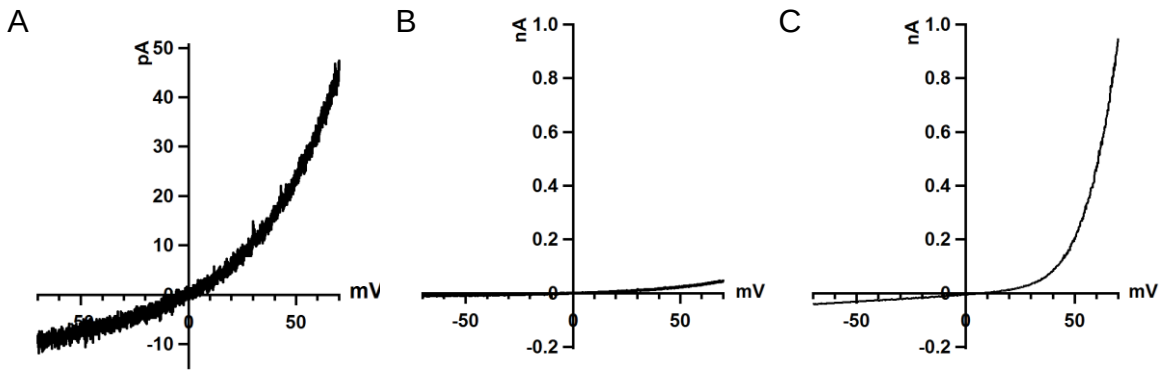

Fig. 3.16. WT TWIK-1 and II293-294AA mutant (^{M}TWIK-1) currents elicited by ramps from -70 to 70 mV. (A); WT TWIK-1, currents with intracellular Rb^+ and extracellular K^+. (B); the same measurements as in (A) scaled up to be compared with (C). (C); ^{M}TWIK-1 currents with intracellular Rb^+ and extracellular K^+. While the WT channels conduct currents that are not distinguishable from the endogenous currents, the density of the mutant ^{M}TWIK-1 is high enough to conduct relatively large macroscopic currents.

The II293-294AA mutation is known to inactivate a retention motif from the C-terminus thereby increasing the density of TWIK-1 channels in the plasma membrane (Fig. 3.16). Since only the retention motif of the channel is changed and the rest of the channel is intact, it is well-suited for studying biophysical and pharmacological studies of the channel. Therefore I used this mutant (^{M}TWIK-1) for further investigation.

Although ^{M}TWIK-1 is not internalized and should be abundant in the membrane, when measured in giant patches from *Xenopus* oocytes, it still does not appear to conduct currents that are distinguishable from the endogenous currents. However, we have previously shown that both Cs^+ and Rb^+ are much more potent than K^+ to trigger voltage activation of most of K2P channels [126]. Therefore I investigated the voltage activation of TWIK-1 channels triggered by intracellular application of non-physiological monovalent ions such as Cs^+ NH_4^+ and Rb^+ (Fig. 3.17).

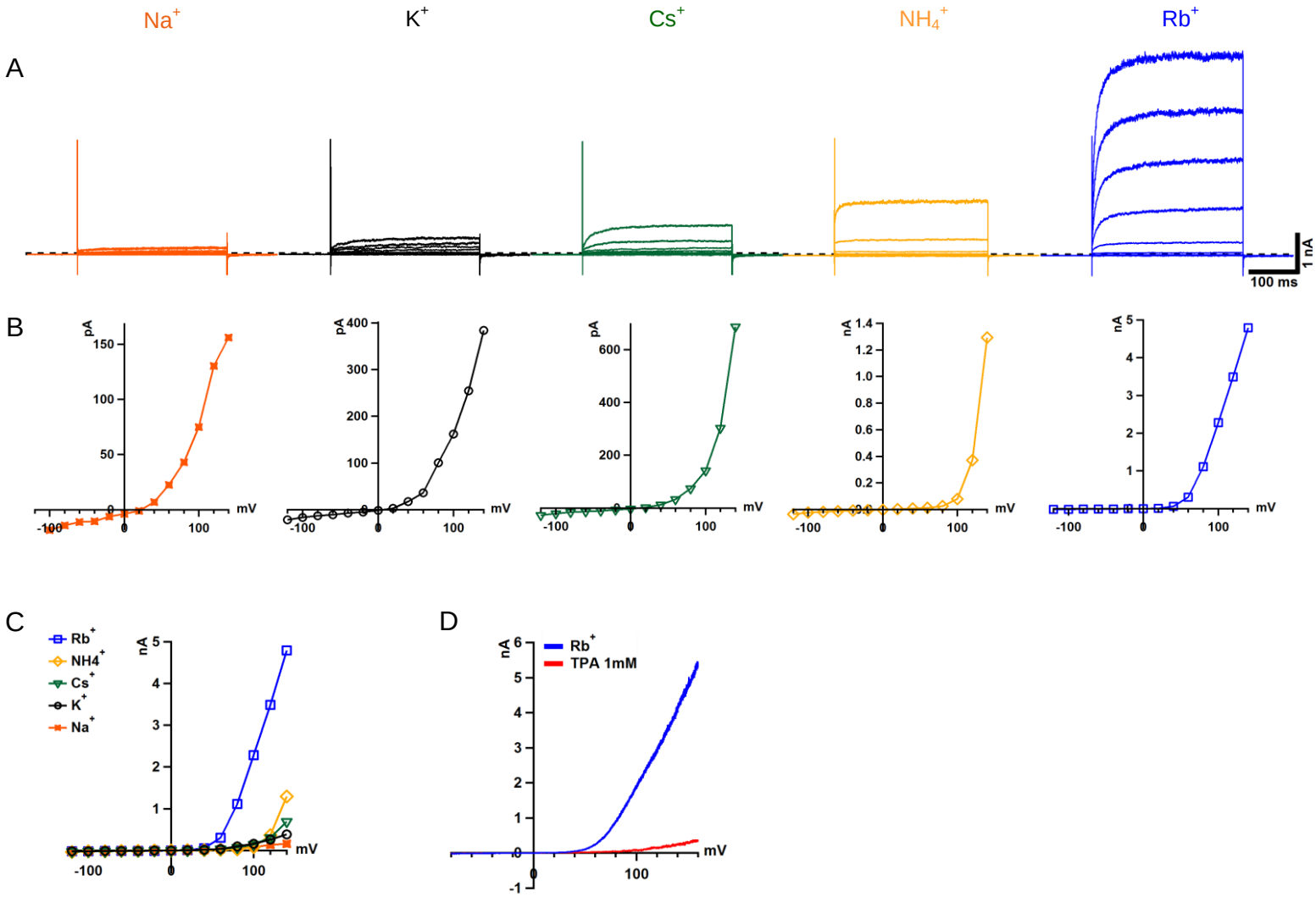

Fig. 3.17. TWIK-1 gating by non-physiological ions. (A); families of currents elicited by test pulses from -120 to 140 mV from and back to holding potential of -80 mV in one single inside-out patch. The traces are ordered based on activation potency of the ions. (B); IV relationships from traces in (A) individually shown to indicate the rectification of currents by each ion. (C); superposition of IVs in (B) for comparing activation of ^{M}TWIK-1 by different ions. (D); TPA block of the Rb^{+} currents from the same patch.

As expected in the voltage range between -100 to 100 mV, K^+, Cs^+ and Na^+ did not produce any large currents. However, currents carried by K^+ and Cs^+ ions were more or less identical and about twice the size of the Na^+ currents (Fig. 3.18). NH_4^+ currents were not larger (than Na^+) within this voltage range. However, Rb^+ currents were very large and could reach several nA at +100 mV (Fig. 3.17). Strangely in contrast to other K2P channels like TRAAK, TREK-1 [126], TALK-2 or TASK-3, I did not observed any tail currents from ^{M}TWIK-1 channels upon repolarization.

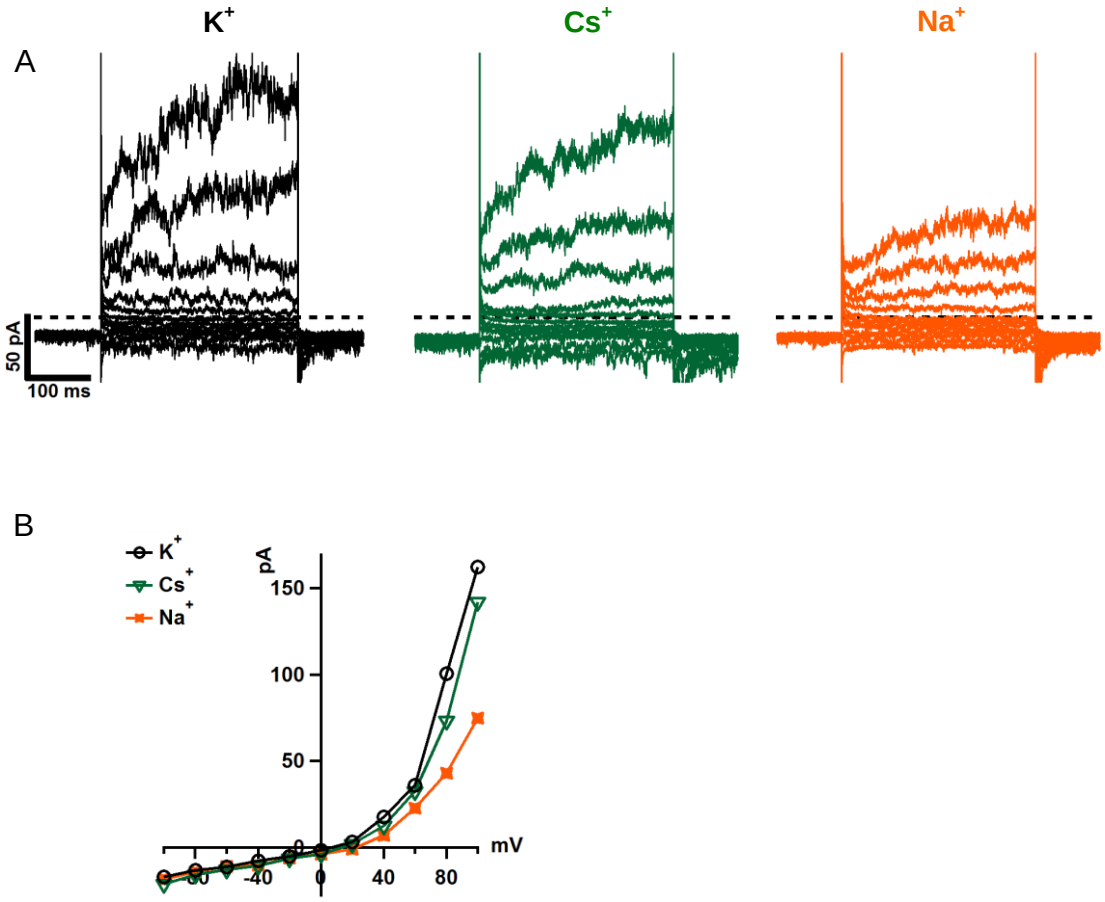

Fig. 3.18. (A); current traces from measurements in Fig. 3.17. for K^+, Cs^+ and Na^+ for voltages from -100 to 100 mV. (B); the superimposed IVs from (A). Note that Cs^+ and K^+ currents are very similar in amplitude and larger than those of Na^+.

Previously it has been shown that TWIK-1 channels conduct large inward Rb^+ and NH_4^+ currents [59]. We have recently shown that in K2P channels voltage-dependent gating is a one way phenomenon, i.e. only relevant intracellular ions can gate K2P channels open in a voltage-dependent manner [126]. We named this mechanism **check-valve ion-flux gating**. To find out if ion-flux gating is also true for TWIK-1 channels, I tested extracellular

application of Rb^+ and NH_4^+ ions on voltage-gating of ^{M}TWIK-1. As was reported before [59], both Rb^+ and NH_4^+ carried large inward currents. However, surprisingly, the Rb^+ and NH_4^+ currents had most of the characteristics of voltage activation of other K2P channels, including; instantaneous and voltage-time dependent components of activation (Fig. 3.19).

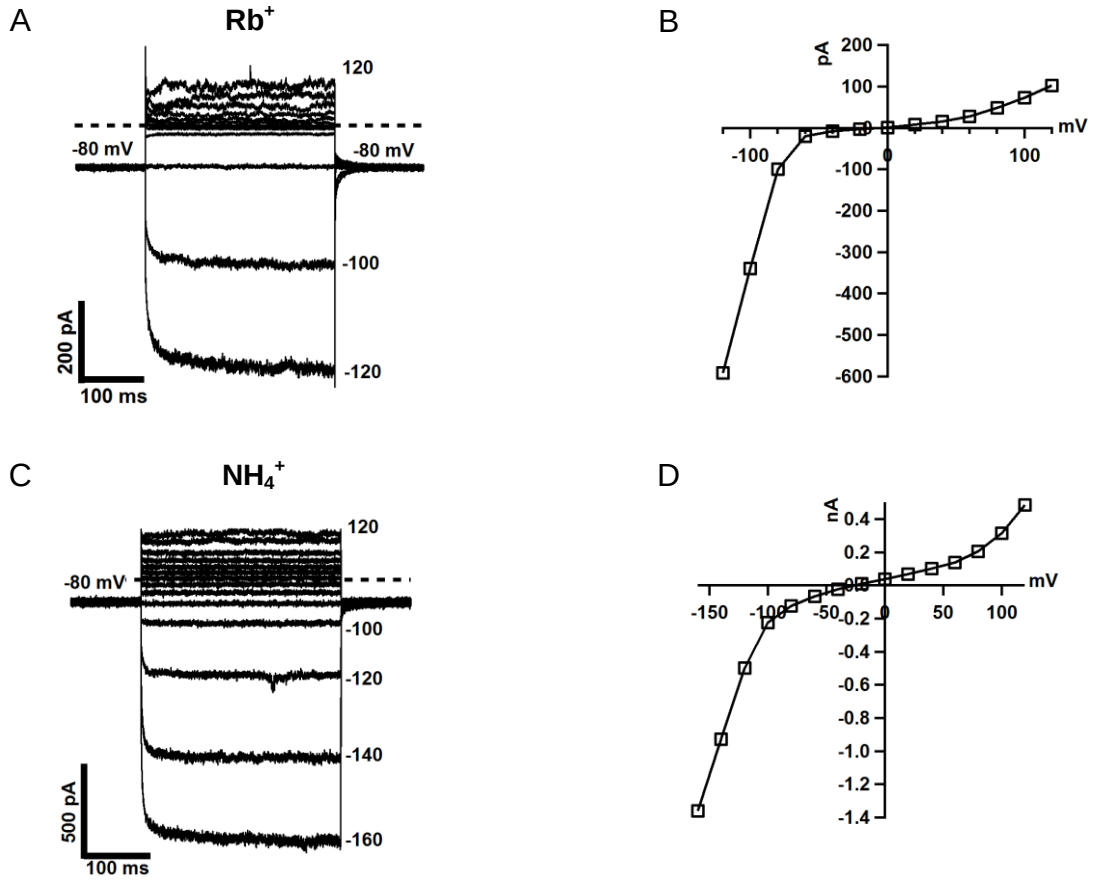

Fig. 3.19. Voltage activation of ^{M}TWIK-1 by extracellular ions. (A); a family of currents elicited by test pulses from -120 to 120 mV from and back to holding potential of -80 mV with extracellular Rb^+ and intracellular K^+. (B); IV relationship for the traces in (A). (C); same as in (A), but with extracellular NH_4^+. The pulses begin from -160 mV, since NH^+ is less potent than Rb^+ (Fig. 3.17) and hence the voltage activation is less obvious at less hyperpolarized voltages. (D); IV relationship for the traces in (C).

We have shown that the ion-flux gating is valid for symmetrical concentration of non-physiological ions, like Rb^+ that strongly potentiates the P_O [126]. For instance under this condition, Rb^+ activates TREK-1 channels only from the intracellular side and not from the extracellular side. Therefore, I tested gating of TWIK-1 channels under symmetrical Rb^+ or NH_4^+ concentrations to see if this concept also applies or whether

TWIK-1 channels are different from other K2P channels. Under both symmetrical Rb^+ and NH_4^+ concentrations TWIK-1 channels turned into open rectifiers, i.e. leak channels with little or no rectification (Fig. 3.20). More surprisingly, under symmetrical Cs^+ concentrations, I observed relatively large currents at higher depolarizing voltages with instantaneous and voltage-time dependent components and strong outward rectification (Fig. 3.19). In other words under symmetrical Cs^+ concentrations, ^{M}TWIK-1 channels did indeed exhibit ion-flux gating.

Cs^+ ions are a known K^+ channel blocker and are routinely used to block endogenous K^+ channels if other channels like Na^+ or Ca^{2+} channels are studied. Therefore I did not expect to observe relatively large currents carried by Cs^+ ions. So I examined whether Cs^+ conduction by ^{M}TWIK-1 channels was due to the absence of K^+ from both sides of ^{M}TWIK-1 channels. I repeated the experiments with K^+ on the intracellular and Cs^+ on the extracellular side. The channels did not conduct any currents beyond the endogenous currents with test pulses from -160 to 120 mV (Fig. 3.21). However, with intracellular Cs^+ and extracellular K^+ ion-flux gating was observed. In those cases where the patches were stable enough to resist very high voltages then I was able to record the voltage activation by intracellular Cs^+, as well (Fig. 3.21).

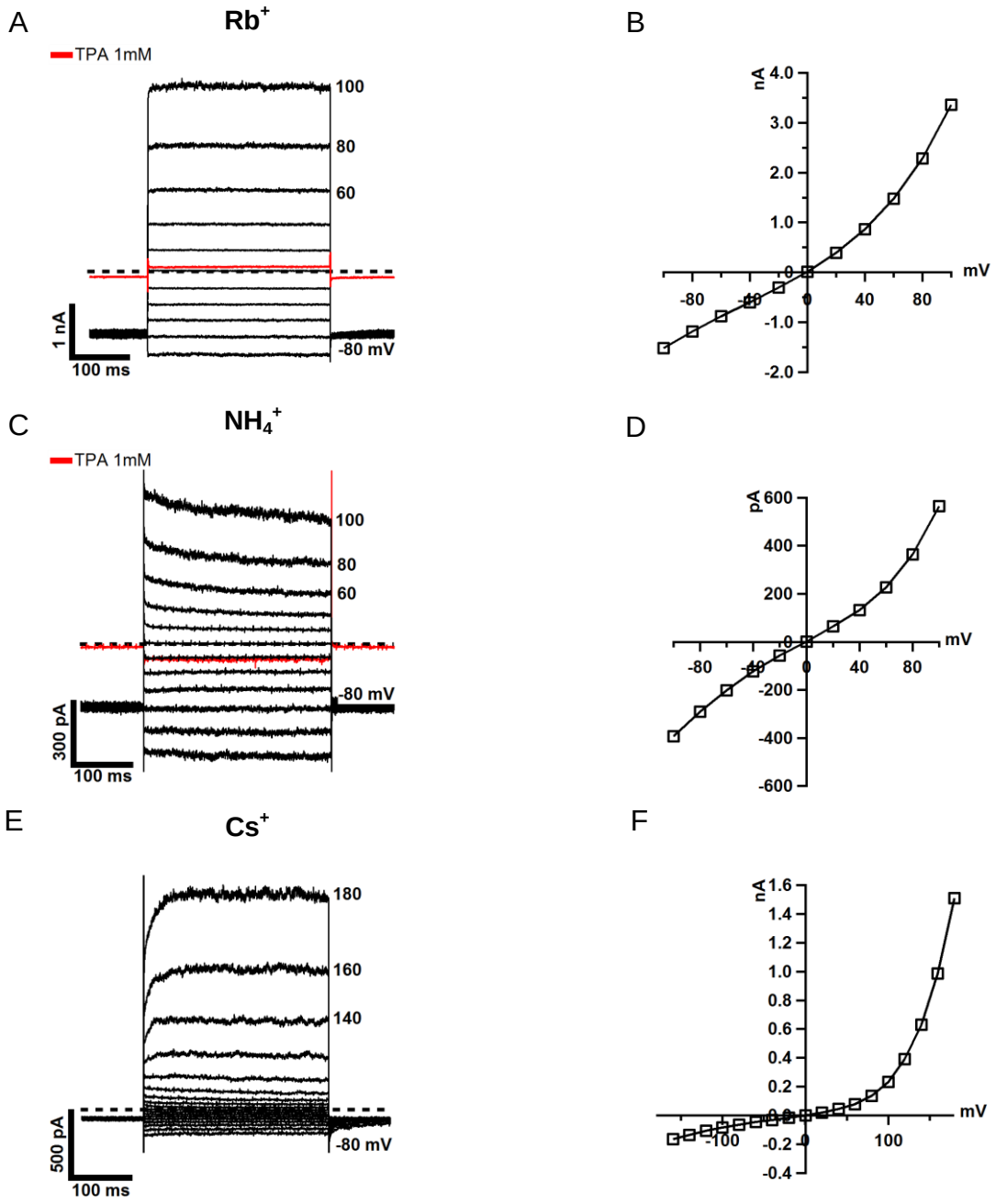

Fig. 3.20. TWIK-1 gating by symmetrical non-physiological ions. (A); a family of currents elicited by test pulses from -100 to 100 mV from and back to holding potential of -80 mV in symmetrical Rb^+ concentrations. The TPA test pulse is 100 mV. (B); IV relationship for traces in (A). (C); same as in (A), but in symmetrical NH_4^+. The TPA test pulse is -160 mV. (D); IV relationship for traces in (C). (E); same as in (A), but test pulses are from -160 to 180 mV in symmetrical Cs^+. (F); IV relationship for traces in (E).

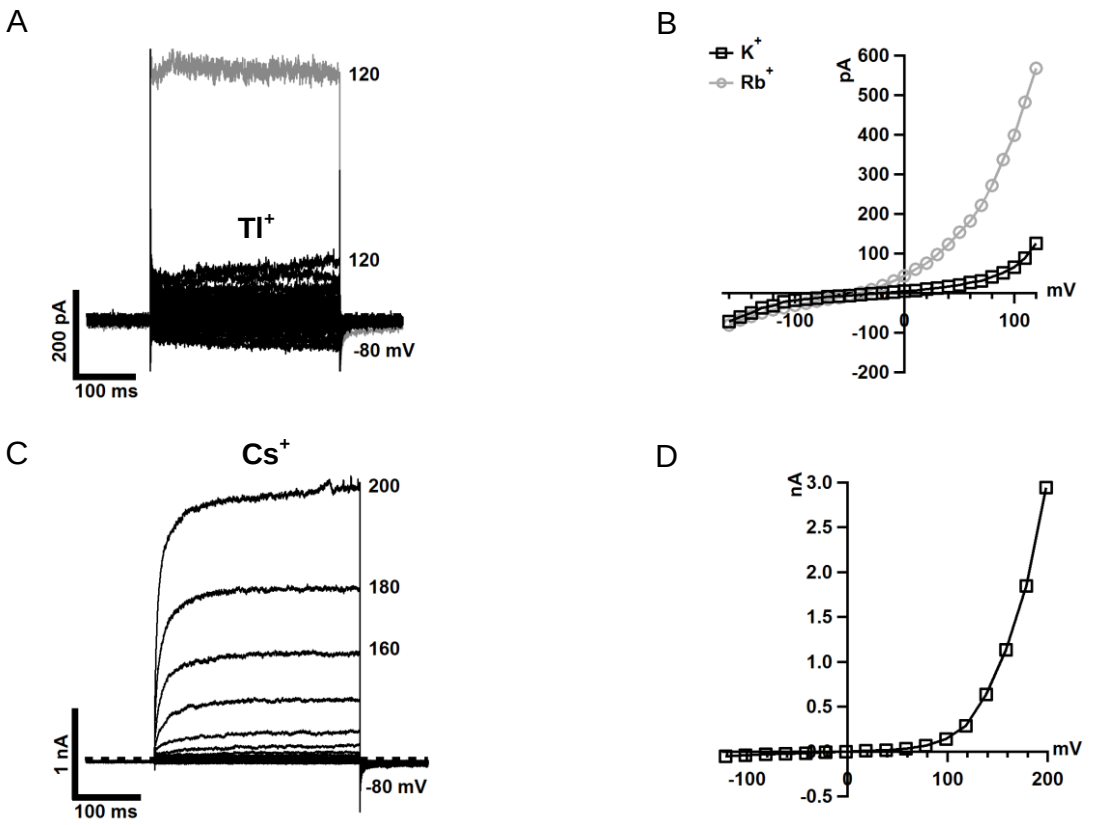

Fig. 3.21. Gating of ^{M}TWIK-1 channels by extracellular or intracellular Cs^+. (A); a family of currents elicited by test pulses from -160 to 120 mV from and back to holding potential of -80 mV with intracellular K^+ and extracellular Cs^+. For comparison the Rb^+ currents from the same patch at 120 mV are superimposed in gray. (B); IV relationship for the traces from (A). That of Rb^+ currents from the same patch is superimposed in gray. (C); a family of currents elicited by test pulses from -120 to 200 mV from and back to holding potential of -80 mV with intracellular Cs^+ and extracellular K^+. (D); IV relationship from traces in (C). Note the time-dependent activation is observed in all traces above 100 mV.

I also looked into the gating of TWIK-1 channels in symmetrical Tl^+ and Na^+ concentrations. ^{M}TWIK-1 channels under Tl^+ and pulses up to 200 mV conducted no reliable currents, although patching the same oocyte at the same place where the Tl^+ patch was excised gave large Rb^+ currents (Fig. 3.22.), indicating that channels are at the plasma membrane but are not activated by Tl^+. However ^{M}TWIK-1 channels under symmetrical Na^+ concentrations showed small but reliable currents that possessed the properties of ion-flux gating; outward rectification and voltage-time dependent component upon voltage activation (Fig. 3.23). As with gating by Cs^+, ^{M}TWIK-1 channels also showed ion-flux gating under intracellular Na^+ and extracellular K^+ conditions. However in comparison to Rb^+ currents from the same patch, the currents were much smaller and again no tail currents were observed (Fig. 3.23).

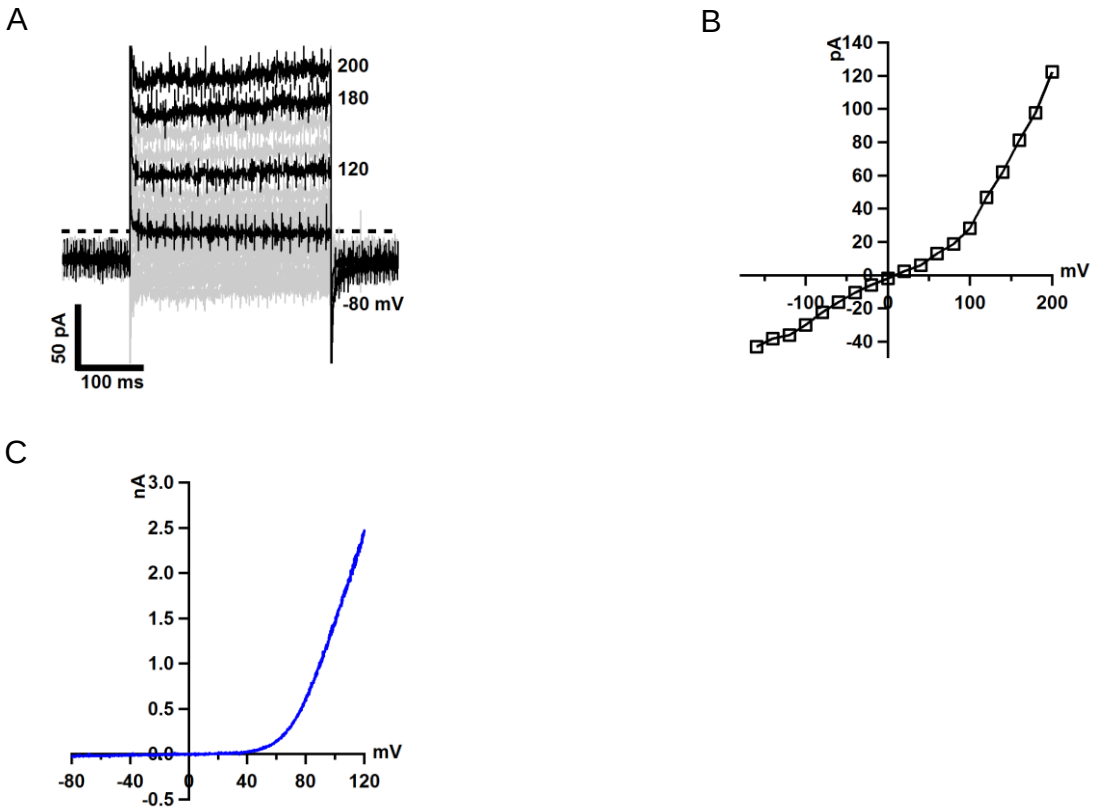

Fig. 3.22. Gating of ^{M}TWIK-1 channels in symmetrical Tl^+ concentrations. (A); a family of currents elicited by test pulses from -160 to 200 mV from and back to holding potential of -80 mV. For clarity some of the traces are shown in gray. (B); IV relationship for traces in (A). (C); Rb^+ currents from a ramp measurement of a new patch from the same place where the Tl^+ patch was excised to confirm the expression of TWIK-1 channels.

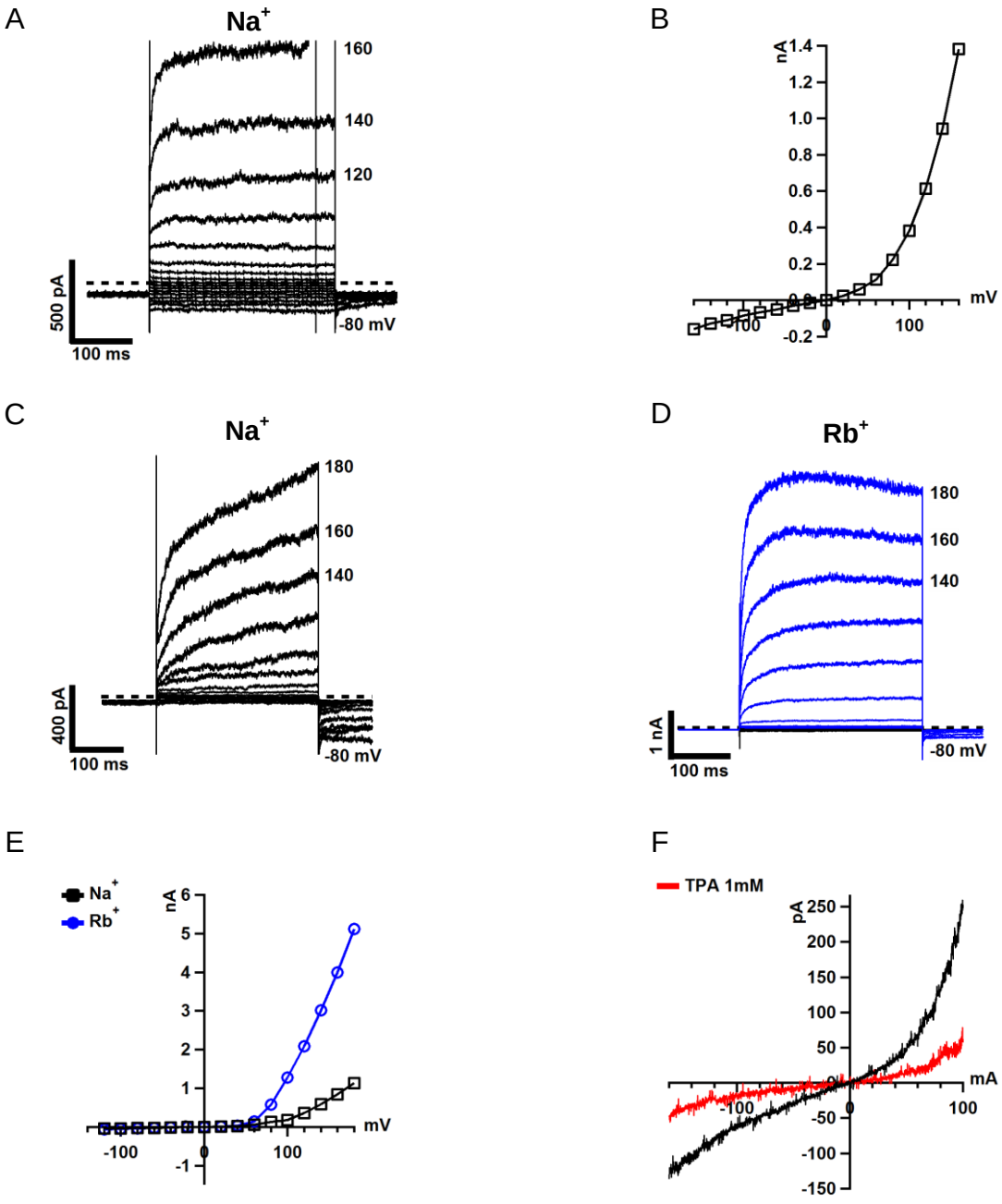

Fig. 3.23. Gating of ^{M}TWIK-1 channels by Na^+ ions. (A); a family of currents elicited by test pulses from -160 to 160 mV from and back to holding potential of -80 mV in symmetrical Na^+ concentrations. (B); IV relationship for traces in (A). (C); gating of ^{M}TWIK-1 with intracellular Na^+ and extracellular K^+ by test pulses from -120 to 180 mV from and back to holding potential of -80 mV. (D); the same patch as in (C) but with intracellular Rb^+. (E); IV relationships for Na^+ and Rb^+ in (C) and (D) are superimposed. (F); Na^+ currents from a ramp measurement of the same patch as in (A) and TPA block of the Na^+ currents.

Based on these observations, I used higher voltages for symmetrical K^+ concentrations as well. Like most of the monovalent ions tested, K^+ ions were also found to be capable of

inducing voltage-gating in ^{M}TWIK-1 channels. However, this voltage gating only occurred at voltages above 100 mV (Fig. 3.24). When these K^+ currents were compared with Cs^+ currents from the same patch, I noticed that at voltages above 100 mV, the Cs^+ currents are always larger than K^+ currents (Fig. 3.17). This is in contrast to the expected behavior of K^+ channels, which are normally blocked by Cs^+.

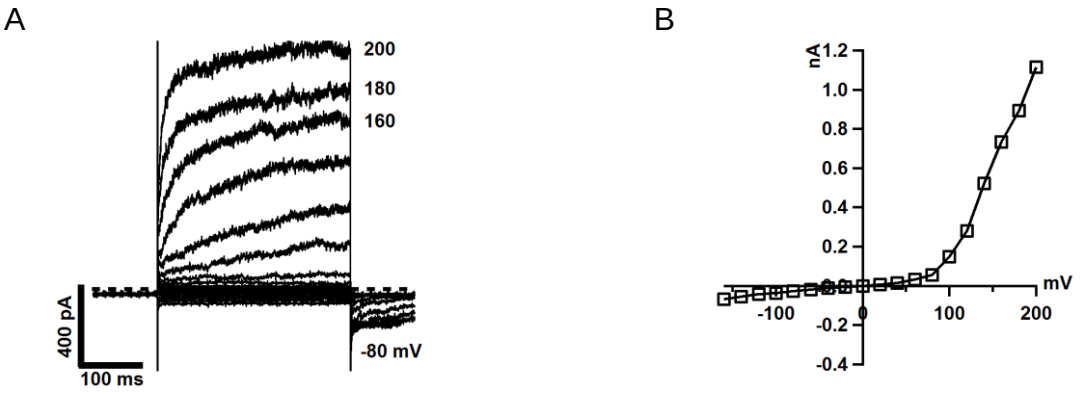

Fig. 3.24. Gating of ^{M}TWIK-1 channels in symmetrical K^+ concentrations. (A); a family of currents elicited by test pulses from -160 to 200 mV from and back to holding potential of -80 mV. (B); IV relationship for traces in (A). Note that activation and increase of the currents occurs mostly above 100 mV.

At higher voltages, ^{M}TWIK-1 channels can also conduct very large Rb^+ currents. These currents have both instantaneous and voltage-time dependent components, however show no tail currents. The currents also do not saturate even up to 280 mV. However, rather small deactivation of currents is observed at these voltages (Fig. 3.25).

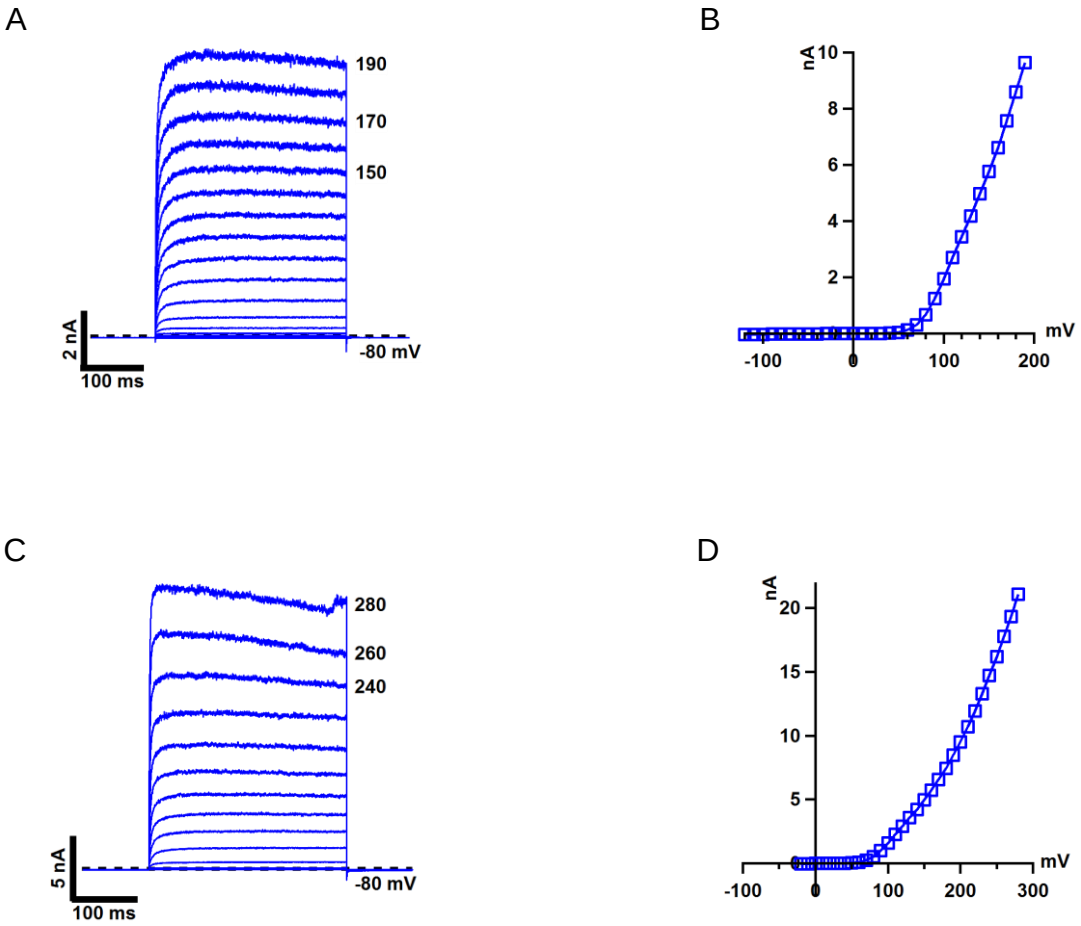

Fig. 3.25. Gating of ^{M}TWIK-1 channels at high voltages. (A); a family of currents elicited by test pulses from -120 to 190 mV in 10 mV increments from and back to holding potential of -80 mV with intracellular Rb^+ and extracellular K^+. (B); IV relationship for traces in (A). (C); the same patch from -20 to 280 mV with increments of 20 mV. Note that from 240 mV some deactivation of the currents begins. (D); IV relationship for traces in (C).

3.7.3. TWIK-1 channels are inhibited by K^+ ions

Based on the gating behavior of TWIK-1 by different ions, presented above, I hypothesized that TWIK-1 may be inhibited by K^+ ions. To test this idea I developed an experimental protocol whereby stable, reliable large ^{M}TWIK-1 currents could be evoked and the inhibitory effect of different ions could then be tested. To do this, voltage-activated Rb^+ currents were used as control. By keeping the Rb^+ concentration constant I added 10 mM of different ions to the test solutions. While all ions show some inhibition of Rb^+ currents, the inhibition by K^+ was the highest (81%). 1 mM TPA could block the control

currents further to near zero. In contrast to K^+, an equal concentration of Cs^+ (10 mM) inhibited only 42% of Rb^+ currents. Therefore these experiments indicate that K^+ ions have a greater inhibitory effect on TWIK-1 channels than even Cs^+ ions (Fig. 3.26).

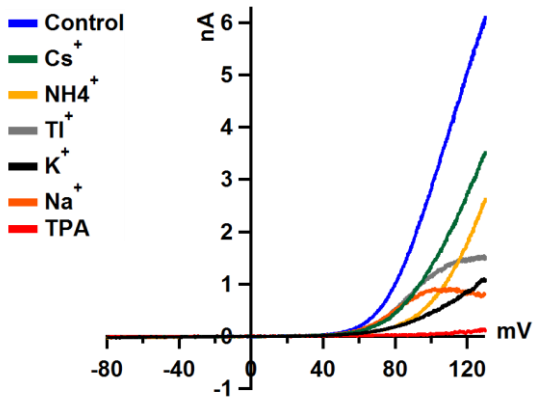

Fig. 3.26. Inhibitory effect of different ions on ^{M}TWIK-1 Rb^+ currents. 10 mM of each ion was added to 120 mM of Rb^+ solution. The currents were elicited by ramps from -80 to 130 mV. Note that K^+ has the highest inhibitory effect. TPA concentration is 1 mM in Rb^+ solution.

To gain a better understanding of this inhibitory effect of K^+ ions on TWIK-1 I measured the dose response inhibition for K^+ on ^{M}TWIK-1 currents. To do this the concentration of Rb^+ ions was kept constant and increasing concentrations of K^+ were added to the solution. As expected with an increase of K^+, the inhibition of Rb^+ currents increased (Fig. 3.27). An IC_{50} of 2.8 mM for inhibition of TWIK-1 channels by K^+ ions was calculated from this data.

Similar to voltage activation of TWIK-1, we have shown Rb^+ ions are highly potent in activating most of K2P channels upon depolarization [126]. Therefore I asked if K^+ has the same inhibitory effect on Rb^+ currents from other K2P channels, or if their effect is different (Fig. 3.27). In contrast to the potent inhibitory effect on TWIK-1, only a weak inhibitory effect was observed for TREK-1 (IC_{50} = 68 mM) whilst concentrations of K^+ up to 120 mM increased the apparent Rb^+ currents from TREK-2.

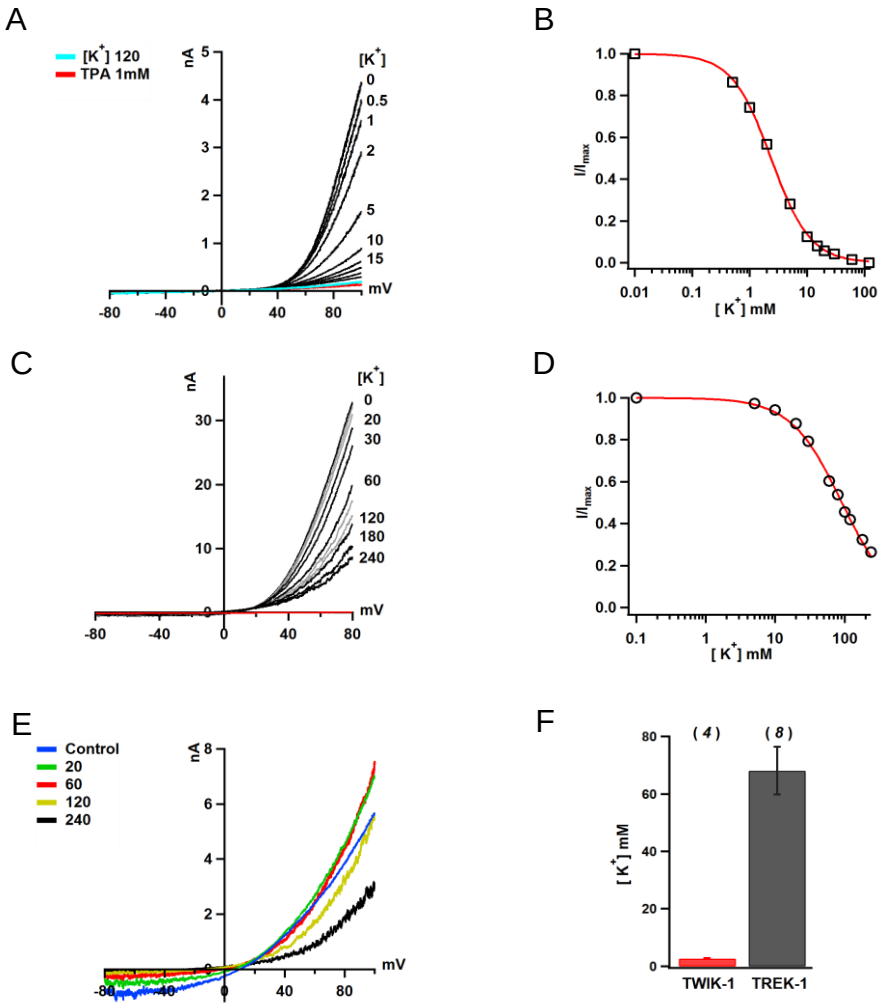

Fig. 3.27. Inhibition of Rb^+ currents by K^+ ions for different K2P channels. Rb^+ concentration was kept at 120 mM and increasing concentration of K^+ was added. Currents were elicited by ramps of the indicated voltages. (A); ^{M}TWIK-1 Rb^+ currents inhibited by K^+ ions. The inhibitory effect of 120 mM K^+ is similar to that of 1mM TPA. (B); normalized currents plotted against K^+ concentrations and fitted by Hill equation. (C); same as in (A), but for TREK-1. For clarity the labeled traces with K^+ concentration are shown in black. Other concentrations' traces are shown in gray. In comparison to TWIK-1, even 240 mM K^+ does not fully block the Rb^+ currents. (D); same as in (B), but for TREK-1. (E); same as in (C), but for TREK-2. Note that 20 and 60 mM K^+ enhance the apparent Rb^+ currents, while 120 mM weakly blocks the currents. (F); summary of Hill fits from measurements same as in (A) and (C) for TWIK-1 and TREK-1 channels.

3.7.4. Do TWIK-1 channels deactivate too fast?

With the K2P channels examined so far (i.e. TREK-1, TREK-2 and ^{M}TWIK-1), it seems K^+ ions have a specific inhibitory effect on TWIK-1. As mentioned above, both TREK-1 and TREK-2 channels show large deactivating tail currents upon repolarization to the

holding potential. However, despite activation by Rb^+ such tail currents are absent in ^{M}TWIK-1 currents.

One possible reason for this could be very fast deactivation of the channels upon repolarization. It has been shown that at positive voltages, hERG channels deactivate much faster than they are activated [127]. Hence very small currents are evoked up on depolarization. So, does TWIK-1 (in presence of K^+) also deactivate faster than it can be activated? In other words, does inhibition of Rb^+ currents by K^+ correlate with fast deactivation of these channels?

To address this question conditions were needed in which the channels deactivate very slowly. However, no such experimental conditions or mutants which can slow down the rate of deactivation of TWIK-1 channels were obviously available. However in our repertoire of TREK mutants, I identified a few that make deactivation of the channels much faster than that of WTs. One such mutant is a version of the TREK-2 channel in which both the N- and C-termini are truncated. This construct is developed for expression and crystallization of TREK-2 channels and its pharmacological profile is similar to that of the WT TREK-2 [11]. For simplicity, from now on this channel is referred to as ^{T}TREK-2.

I observed that, in contrast to the WT TREK-2, these truncated channels produce very small tail currents although the outward currents upon depolarization are very large and similar to those of the WT (Fig. 3.28). I therefore hypothesized that fast deactivation of the channel might be the reason behind its observed phenotype. To test this I cooled down the patch clamp system to about 3°C which, amongst other things, should reduce thermal fluctuations and slow structural transitions within the proteins. Intriguingly, at these low temperatures ^{T}TREK-2 channels produced tail currents similar to those of the WT TREK-2 at room temperature (Fig. 3.29). However, these low temperatures had no obvious effect on TWIK-1 channels tail currents although the activation seems to be much slower in comparison to similar measurements at room temperature (Fig. 3.30).

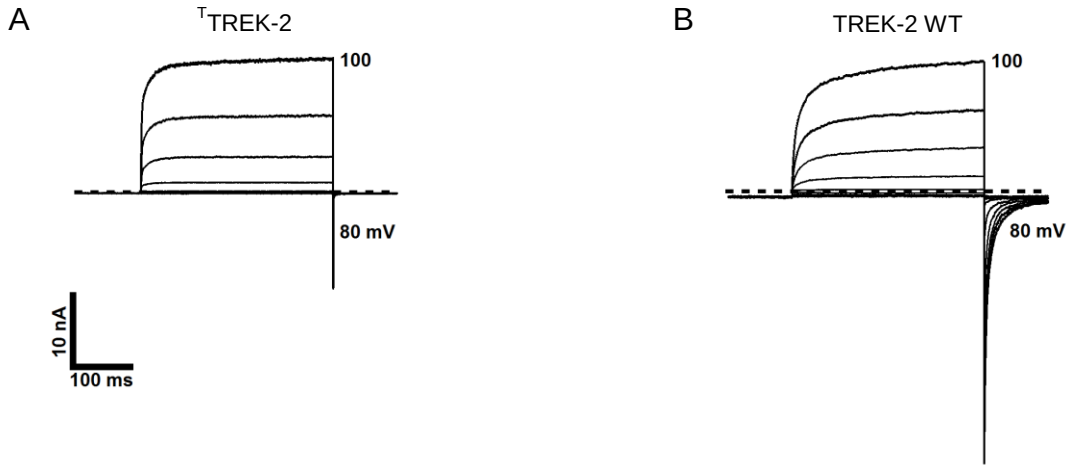

Fig. 3.28. Gating properties of ^{T}TREK-2 and the WT at room temperature. Rb^{+} currents are elicited by test pulses from -100 to 100 mV with 20 mV increments from and back to holding potential of -80 mV. (A); ^{T}TREK-2, (B); the WT. Note despite that the amplitude of the activating currents are almost identical, the ^{T}TREK-2 activates faster and deactivating tail currents are much smaller than those of the WT.

To further investigate the correlation of fast deactivation and inhibition by K^{+} ions, I tested the inhibitory effect of K^{+} ions on Rb^{+} currents from ^{T}TREK-2. Both 20 and 60 mM K^{+} concentrations have already been shown to potentiate Rb^{+} currents from WT TREK-2 and in conditions where the K^{+} and Rb^{+} concentrations are equal, I found that the test currents were roughly similar to the control (Fig. 3.31). Surprisingly, all concentrations of K^{+}, including 20 and 60 mM strongly inhibited Rb^{+} currents from ^{T}TREK-2 (Fig. 3.31).

Another fast deactivating mutant examined was the ^{100}TREK-1 channel from which the last 100 residues of C-terminus were truncated (as opposed to both the N and C-termini in the ^{T}TREK-2 construct). This mutant is especially interesting, since in many ways appears to exhibit a phenotype similar to TWIK-1. But, despite expressing very well, this mutant channel is not activated by K^{+} ions. Instead, the K^{+} currents from this channel are very small and are not distinguishable from those endogenous to oocytes. However just like ^{M}TWIK-1 the currents are strongly activated by Rb^{+} and do not exhibit any tail currents (Fig. 3.32).

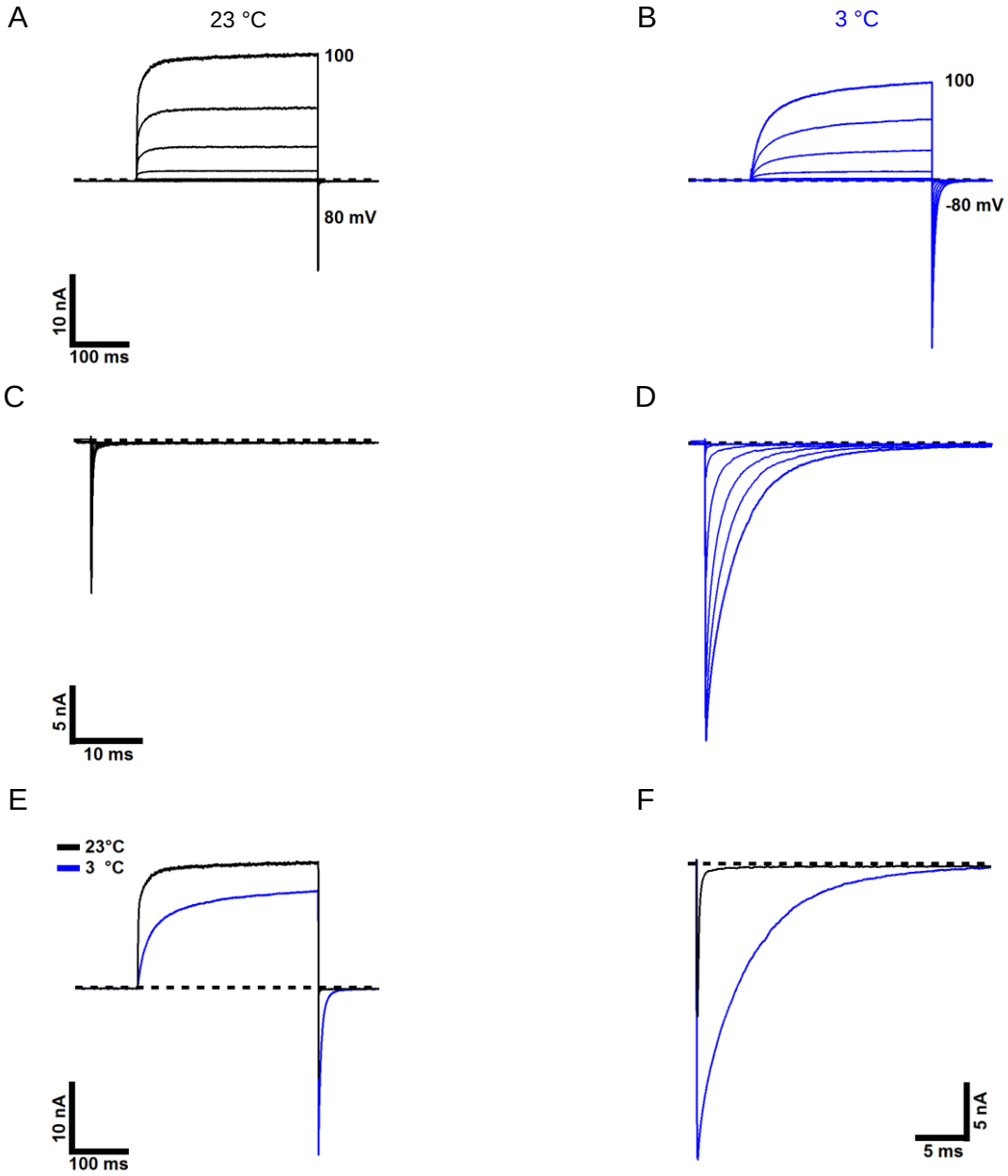

Fig. 3.29. Gating properties of ^{T}TREK-2 in room and low temperatures. (A); Rb^{+} currents elicited by test pulses from -100 to 100 mV with 20 mV increments from and back to holding potential of -80 mV at room temperature. (B); same as in (A), but at 3°C. (C) and (D); tail currents from traces in (A) and(B), respectively, are magnified to compare and emphasize on the kinetics of the tail currents at room temperate (C) and low temperature (D). (E); from (A) and (B) traces elicited by 100 mV test pulse are superimposed for comparison. (F); tail currents from (E) are magnified for better comparison. Note that although the amplitude of the outward currents at 3°C is smaller, the tail current is much larger and also deactivates slower.

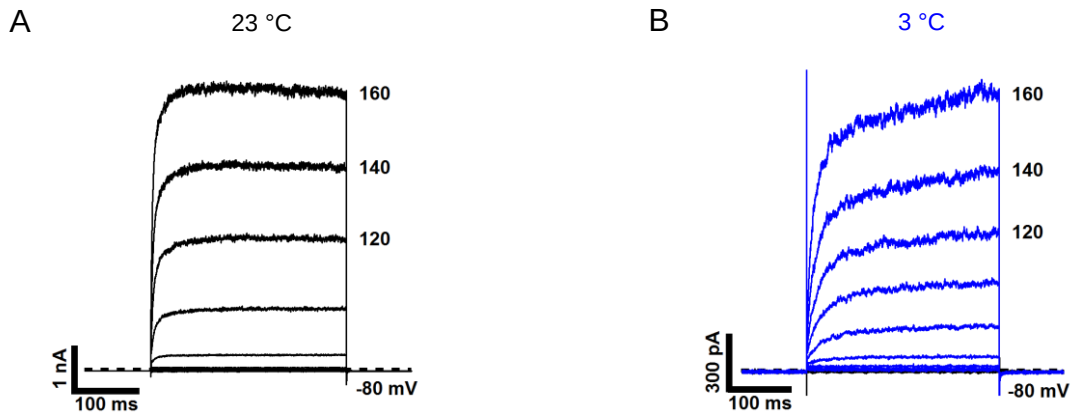

Fig. 3.30. Effect of temperature on gating of TWIK-1. Rb^+ currents elicited by test pulses from -100 to 160 mV with 20 mV increments from and back to holding potential of -80 mV. (A); 23°C. (B); 3°C. Despite the slower activation and steady-state currents at the end of pulse, there are no obvious tail currents.

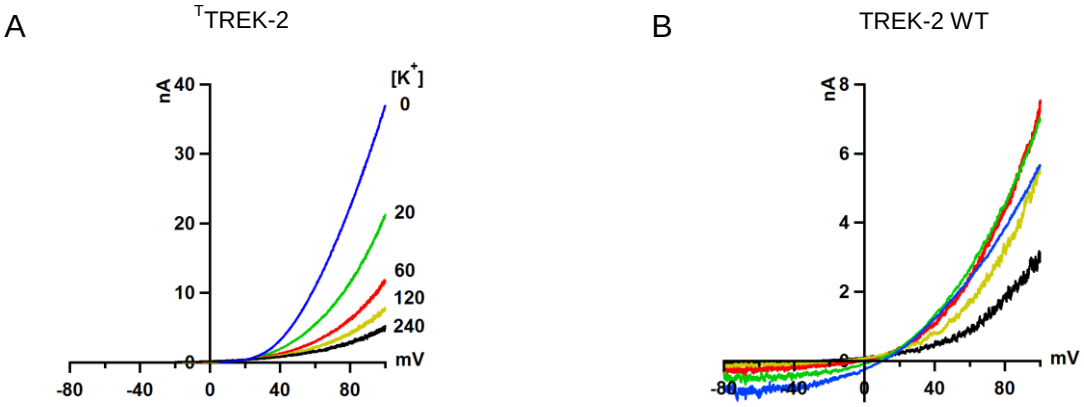

Fig. 3.31. Inhibitory effect of K^+ on Rb^+ currents from TTREK-2 and the WT. Currents are elicited by voltage ramps from -80 to 100 mV. (A); TTREK-2. (B); the WT. While TTREK-2 is strongly inhibited by 20 and 60 mM K^+ the currents from the WT are potentiated at these concentrations. The colors identify the equal K^+ concentrations.

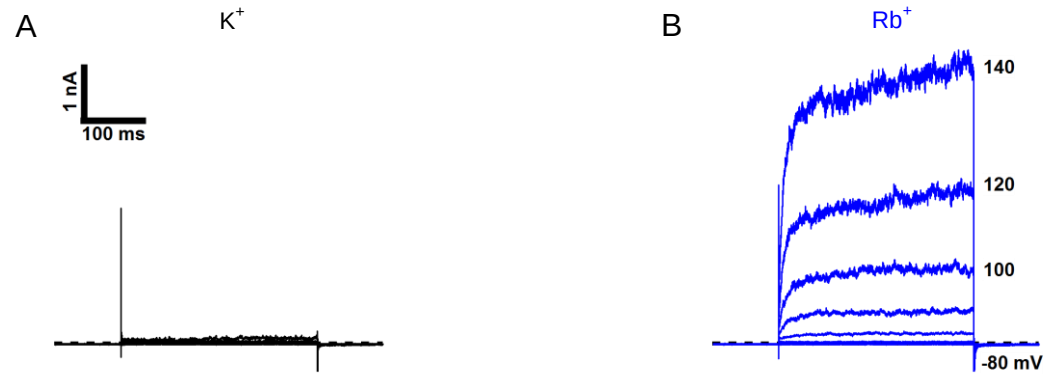

Fig. 3.32. Activation of C-terminus truncated TREK-1 channel is similar to that of ^{M}TWIK-1. (A); K^+ currents are elicited by test pulses from -120 to 140 mV with 20 mV increments from and back to holding potential of -80 mV in symmetrical K^+ concentrations. (B); the same patch with intracellular Rb^+. Note that despite relatively large Rb^+ currents, no tail currents develop.

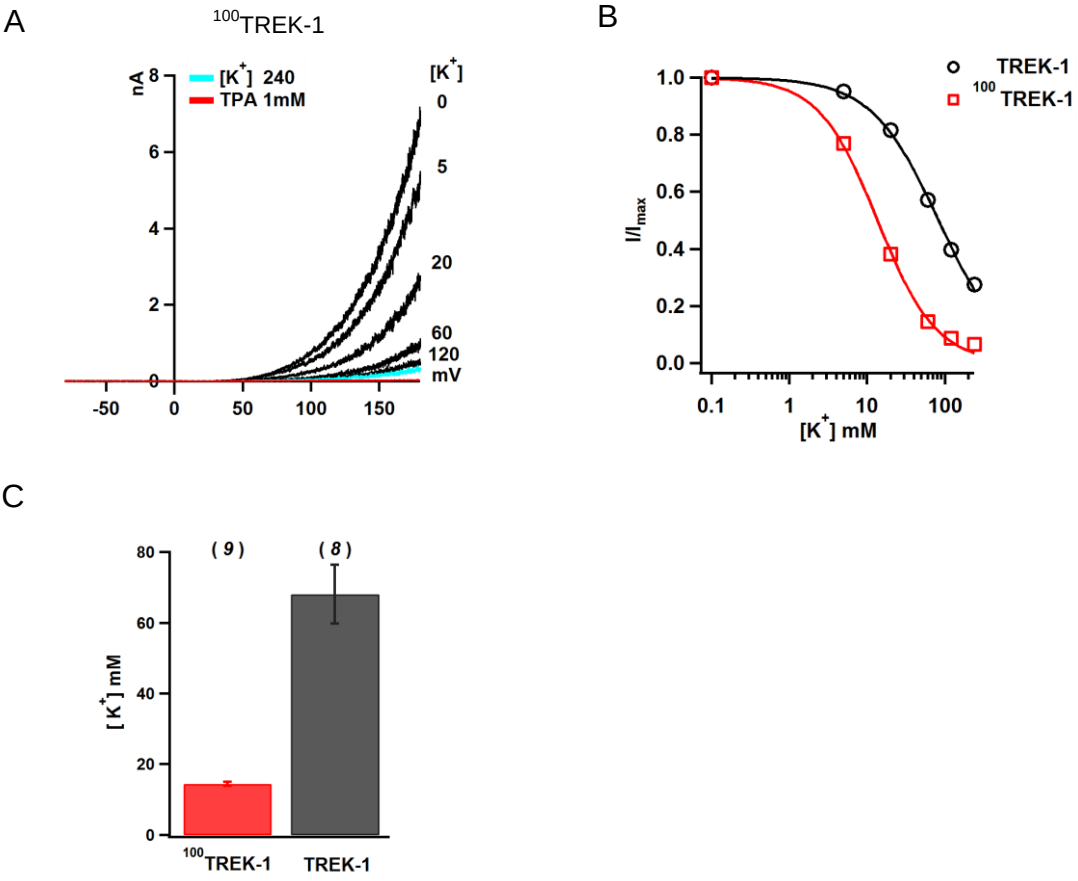

Fig. 3.33. Inhibitory effect of K^+ on Rb^+ currents from ^{100}TREK-1. (A); currents elicited by ramps from -80 to 180 mV, in extracellular K^+ and intracellular Rb^+. Increasing concentrations of K^+ is added to the Rb^+ solution as labeled next to each trace. (B); corresponding normalized currents in comparison to that of WT TREK-1 are plotted against K^+ concentrations and fitted by Hill equation. (C); summary of Hill fits as in (B) shows the IC_{50} for inhibition of each channel by K^+ ions.

I did not examine whether low temperatures could slow down ^{100}TREK-1 channels to evoke tail currents similar to those observed for ^{T}TREK-2. However, very similar to ^{M}TWIK-1, K^+ ions inhibited the Rb^+ currents from ^{100}TREK-1 with an IC_{50} of 14 mM (Fig. 3.33).

Another piece of evidence which indicates that fast deactivation and inhibition by K^+ ions may be correlated comes from single mutations of TREK-1 channels that conduct very small tail currents. One of these mutations is L304C in the M4 helix. TREK-1 L304C currents exhibit small and rapidly deactivating tail currents. Similar to the other fast deactivating mutants of TREK, Rb^+ currents from TREK-1 L304C were more susceptible to K^+ inhibition (IC_{50} of 30 mM) than the WT (Fig. 3.34). This suggests that there may indeed be a correlation between fast deactivation of K2P channels and the inhibitory effect of K^+ ions on channel activity.

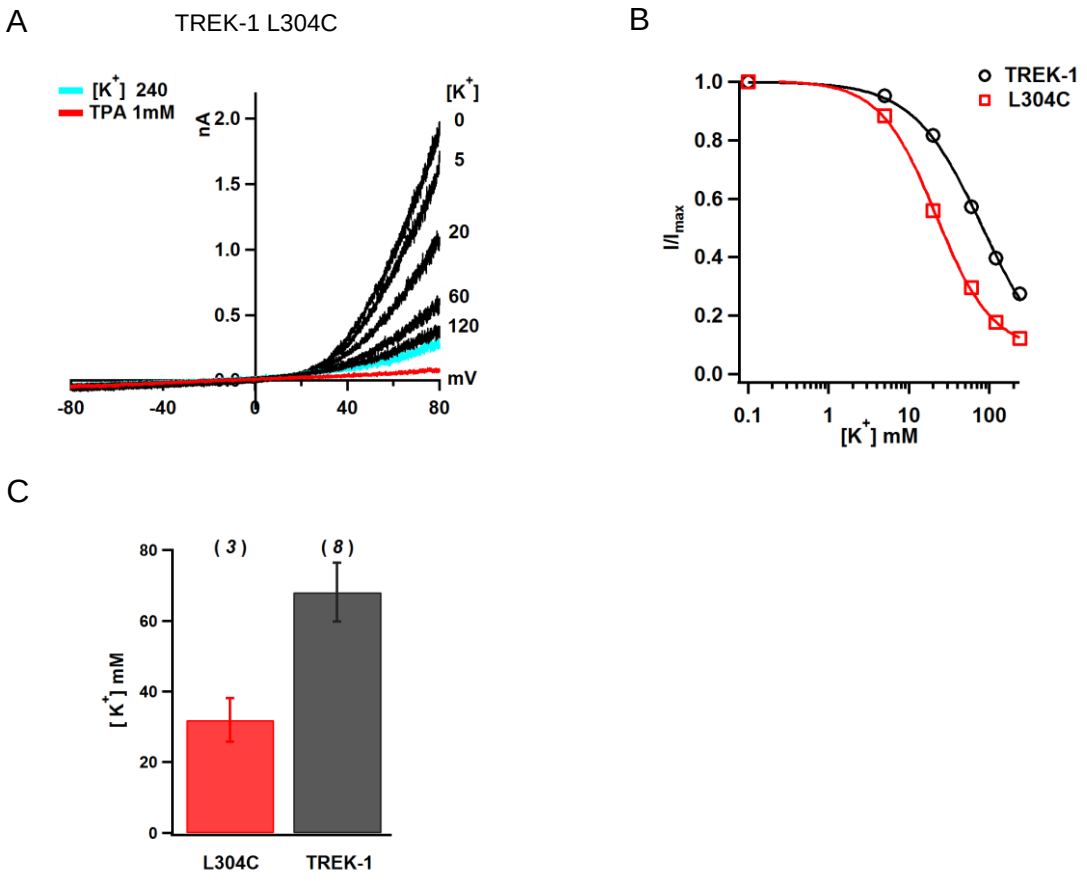

Fig. 3.34. Inhibitory effect of K^+ on Rb^+ currents from TREK-1 L304C. (A); currents elicited by ramps from -80 to 80 mV, in extracellular K^+ and intracellular Rb^+. Increasing concentrations of K^+ is added to the Rb^+ solution as labeled next to each trace. (B); corresponding normalized currents in comparison to that of WT TREK-1 are plotted against K^+ concentrations and fitted by Hill equation. (C); summary of Hill fits as in (B) shows the IC_{50} for inhibition of each channel by K^+ ions.

3.7.5. TWIK-1 is blocked by QA blockers

Although QA ions hardly affect K2P channel activity when applied from the extracellular side, they are highly potent in inhibition when applied intracellularly. I therefore examined intracellular TPA inhibition of TWIK-1 channels conducting Rb^+ currents. With an IC_{50} of 3.36 µM, TPA was found to be a potent blocker of TWIK-1 channels (Fig. 3.35).

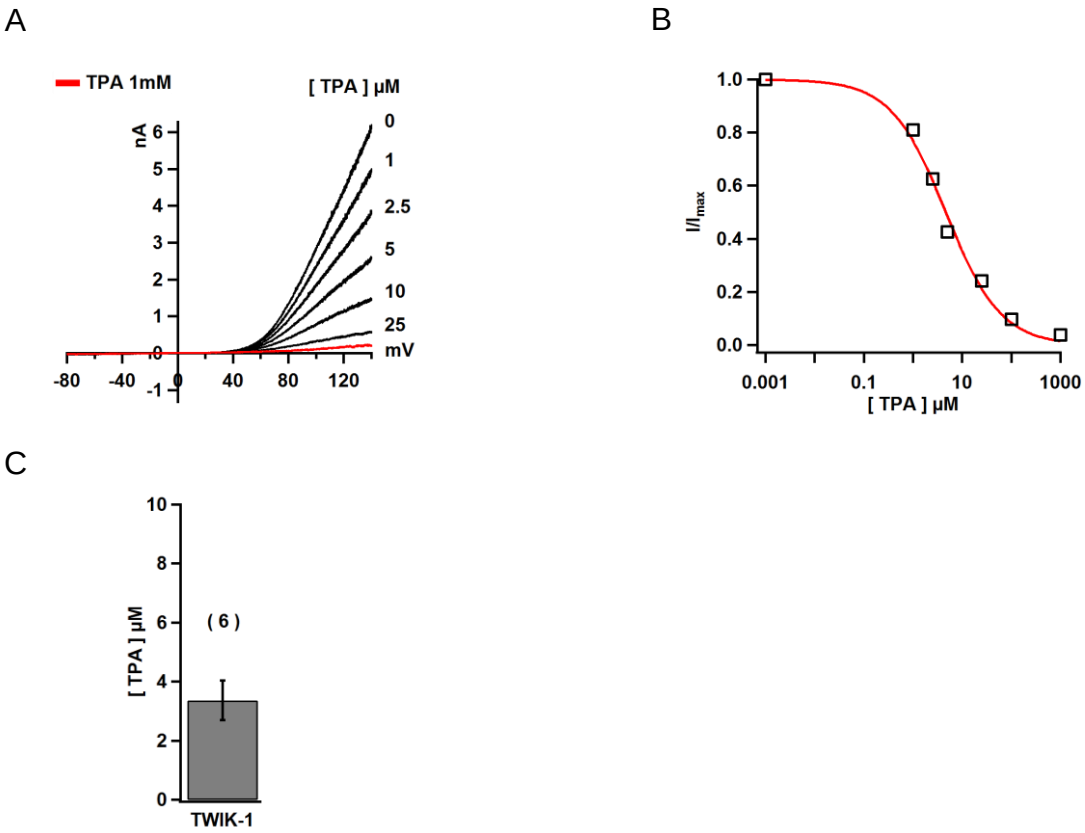

Fig. 3.35. TPA inhibition of TWIK-1. (A); currents elicited by ramps from -80 to 140 mV in extracellular K^+ and intracellular Rb^+ concentrations. The corresponding TPA concentrations are marked next to the traces. (B); the corresponding normalized currents from (A) are plotted against TPA concentrations and fitted by Hill equation. (C); summary of Hill fits as in (B) shows the IC_{50} for inhibition of TWIK-1 by TPA.

In the following chapter I will discuss the results and explain the mechanisms that govern gating of the pH_{ex}-sensitive and other K2P channels.

4. Discussion

4.1. K2P channels are not open leak channels

Potassium currents that develop without delay in response to voltage steps and pass current across the physiological voltage-range are called leak, background, or resting conductances [15]. However none of the K2P channels completely fit this description. It is well known that they do not act simply as open pores that facilitate movement of K^+ ion across the membrane. If these channels were just open at all voltages they would cause the cell to be clamped at resting membrane potential. Comparing TRAAK activity in physiological ($120_{in}/4_{ex}$ mM) and reverse physiological K^+ concentrations ($4_{in}/120_{ex}$ mM) we have shown that these channels are highly activated by voltages positive to the reverse potential but in contrast show no sign of conductance by voltages below the reversal potential [126], proving that K2P channels are not open across all voltages. Therefore voltage activation of K2P channels facilitates repolarization and the ability to retain firing. Thus, not only are these channels regulated tightly by different physiological signals from the cell but also single channel recordings show that in physiological conditions K2P channels gate continually with varying degrees of openness depending on the channel type and membrane potential. For instance TWIK-1 channel, the first mammalian K2P channel to be discovered is considered as weak inwardly rectifying K^+ channel. However single channel measurements from the original work [37] show that with increase of voltage the open probability (P_O) of the channel substantially increases (0.3 and 1.9 ms at -80 and +80 mV, respectively), indicating voltage activation of TWIK-1 channels due to depolarization. Therefore voltage gating of K2P channels can be a mechanism that increases the P_O of these channels to facilitate the repolarization of the membrane after depolarization. In chapter 1 we learned that K2P channels can be highly activated from a low P_O by different signals including; pH, PIP2, inhalational general anesthetics, nitric oxide and even reactive oxygen species. Such high degrees of activation by different signals indicate that the channels are functioning at low P_O but can be activated by a wide range of different signals. One of these signals as I showed in chapter 3 is a change in membrane potential.

Also physiological signals that increase the activity of K2P channels do not necessarily shift them to the leak mode. For instance, activation of TASK-2 by extracellular alkalization does not modify the kinetic of the channel gating [20], i.e. it does not shift the channel to the leak mode, but facilitates voltage activation. This also indicates that K2P channels are not simply leak channels and also suggests that voltage activation of TASK-2 channels could have a significant role in this process. Furthermore, activation of TALK-1 and TALK-2 by nitric oxide or reactive oxygen species dose not significantly alter current kinetics of the channels and they still show voltage activation, although their rate of activation increases [58]. This is more interesting in the case of TALK-2 since under physiological conditions these K2P channels are relatively silent and need alkalization of the extracellular medium to be activated. However upon activation by physiological nitric oxide TALK channels conduct K^+ currents that are similar to Rb^+ activated currents in our experiments. Therefore I propose that in contrast to activation of TRAAK and TREK channels by arachidonic acid, PIP2 or intracellular pH, activation of K2P channels does not necessarily require switching of the channel from the voltage activated mode to the leak mode. It also suggests that Rb^+ activation of K2P channels (which we have simply used as a biophysical tool in our experiments), is not far from the physiologically relevant activation of these channels by K^+. But more importantly, it indicates that the voltage activation of K2P channels may be relevant in the physiological regulation of the cells.

Although, we have shown that arrangements of K^+ and Rb^+ ions in the selectivity filter (SF) differ from each other [126] and the mechanism of activation of the channels by nitric oxide is not yet known. I therefore propose that activation by nitric oxide may induce structural changes in the SF which affects the interaction with K^+, allowing the K^+ ions to behave like Rb^+ and trigger voltage activation. It is possible that this may also share some similarity with the activation of TRPC channels by S-nitrosylation of two cysteines which are located on the N-terminal side of pore forming region [128]. In TALK channels, there are cysteine residues on transmembrane helices that are close to the pore domain and can be modified from extracellular side where TALK channels are modified by nitric oxide. Therefore one possibility to investigate this proposal would be to see if nitric oxide activated TALK channels can be further voltage activated by Rb^+ ions or not and if mutation of the cysteines have any effect on the activation.

4.2. Voltage activation is a feature of pH_{ex}-sensitive K2P channels

Interestingly, most K2P channels, except for TWIK-1, show single channel inward rectification. However we in this study and others before have seen that macroscopic currents in symmetrical ion conditions are always outward rectifying. This observation might also be explained by voltage activation which is the increase of the P_O upon activation, as is mentioned above for TWIK-1 [37].

Voltage activation of canonical voltage-dependent channels is due to outward movement of transmembrane helices that bear positively charged residues. Despite the lack of such voltage sensors, the voltage activation of K2P channels has been recognized from an early stage. For example, TREK-1 channels expressed in *Xenopus* oocytes and COS cells, both in physiological and symmetrical K^+ concentrations showed outward rectification and time dependent increase of currents in response to voltages positive to the reversal potential. Moreover, it has been emphasized that TREK-1 does not behave as a pure open rectifier as predicted by the Goldman–Hodgkin–Katz (GHK) theory [129]. Although, the voltage-dependency of K2P channels was first characterized in TASK-3. The currents from these channels were not well fit by the GHK relationship and there was a time-dependent portion of currents observed upon depolarization that could be fitted with exponential function. Therefore it was concluded that TASK-3 channels possessed a form of voltage-dependent gating [33]. The same characteristics were also observed for TRAAK, TALK-2, TASK-1, but the mechanism of voltage gating remained elusive.

Since these channels do not possess any S4-like voltage sensor the voltage-dependent behavior was attributed to an unknown, but intrinsic mechanism within the channel [130]. Moreover in symmetrical K^+ concentration TREK-1 channels have been shown to develop tail currents [129]. As I have shown in chapter 3 and discussed below, tail currents are an indication of activation of channels beyond basal P_O and their deactivation suggests they switch to a deactivated mode after repolarization of the membrane. With this information, I therefore set out to systematically characterize the voltage activation of pH_{ex}-sensitive K2P channels, as shown in chapter 3.

We can now dissect current traces elicited from K2P channels into a few distinct components (Fig. 3.1). The instantaneous component is due to the initial intrinsic P_O of the channels at resting potential (-80 mV). However, the developing component shows a time dependency and gradual increase of current (Figs. 3.2C, 3.4C, 3.5C & 3.7C). This voltage and time dependent component is due to further increase of P_O upon an increase in voltage which increases with time. In other words, as the voltage increases the channels stay open for a longer period, which results in an increase of the voltage-time dependent component. However the shift in P_O is gradual and increases with time.

Tail currents are the best indication for voltage activation of the channels. Tail currents after test pulses above the reversal potential are always larger than currents at the holding potential, despite the fact that both are elicited at equal voltage (-80 mV). This proves that channels are activated beyond their initial P_O. Moreover their amplitudes increase with the increase in test pulse voltage. Likewise, the decay of tail currents to the amplitude of currents at holding potentials demonstrates deactivation and is also an indication of voltage activation of K2P channels.

4.3. The biophysical role of voltage gating of K2P channels

The levels of expression of K2P channels in the cell membrane are generally quite low, also they are not constantly open and have a very low P_O. This allows them to contribute to the resting membrane potential. However, the voltage gating of K2P channels, by increasing the P_O of these channels during membrane depolarization potentiates the hyperpolarizing effect of the channels, makes them not only capable of contributing to hyperpolarization of the cell membrane after depolarization, but also setting an upper limit to membrane depolarization and controlling excitability and rate of firing.

K_V channels are involved in repolarization of the membrane shortly after depolarization whereas K_{ir} channels stabilize the resting membrane potential by conducting outward K^+ currents at resting membrane potential, but are strongly blocked during depolarization. At physiological concentrations the Nernst reversal potential for K^+ is typically

around -95mV. However, the resting membrane potential for most of the cells is between -80 to -55 mV. Therefore K2P channels are constantly subject to depolarization and in contrast to the both K_V and K_{ir} channels, K2P channels can therefore contribute to the resting membrane potential at rest and during depolarization.

The contribution of K2P channels to repolarization, by increasing the membrane conductance will decrease the membrane time constant which in turn helps faster recovery of Na^+ channels and will facilitate the fast firing ability of some neurons. For example, in TASK-3 knockout neurons, not only was the amplitude of action potentials decreased, but also action potential failure occurred during fast firing [90], thus indicating the unavailability of Na^+ channels due to incomplete recovery from deactivation. Non-linear leak currents, on the other hand, in comparison to linear leak currents are more potent in maintaining the action potential and successive firing of cells, while causing briefer action potential pulses with higher amplitudes [131]. Thus by an increase in the P_O at positive potentials, as I showed in chapter 3, the voltage dependence of K2P channels can ensure the non-linear increase of membrane conductance and hence reduce the time constant of the membrane.

4.4. Voltage activation by non-physiological ions

I observed that for TASK-1, TASK-3 and TALK-2 channels in Rb^+_{in}/K^+_{ex} configuration, K^+ tail currents are larger than the preceding Rb^+ outward currents. We have also shown before that in symmetrical Rb^+_{in} /Rb^+_{ex} configuration, Rb^+ tail currents are much smaller than K^+ tail currents from Rb^+_{in} /K^+_{ex} configuration [126] Although outward currents were similar and comparable between the two ion configurations. These observations suggest that permeation of Rb^+ ions in the SF of K2P channels is less in comparison to that of K^+ ions, therefore the channels conduct smaller Rb^+ outward or tail currents. Indeed, single channel conductance in Rb^+ is less than that of K^+, e.g. 64 pS vs. 85 pS for TREK-1 channels, respectively [132]. Therefore we can conclude that for channels, like TALK-2 and most other K2P channels large Rb^+ outward currents are due to the large increase in channel P_O in comparison to symmetrical K^+ concentrations.

This phenomenon can only be possible if the binding of Rb^+ ions to the SF is the critical step in voltage gating and not the permeation of ions *per se*. Experiments with Cs^+ are the best indication for this idea. Cs^+ is poorly permeable in K2P channels. However it evokes large K^+ tail currents upon repolarization to the holding potential. This is another indication that it is not the permeation of the ions *per se*, but binding to the SF that is responsible for voltage activation of K2P channels. Interestingly, in TRAAK the ion occupancy of both Rb^+ and Cs^+ is markedly different to that of K^+, with much stronger binding to S1 binding site [126].

As a consequence, this may also explain why for both TASK-1 and TASK-3 channels NH_4^+ and Rb^+ outward currents are very similar, or even smaller, than those of outward K^+ currents (Fig. 3.8 & Fig. 3.9). The behavior of K2P channels toward these potent activators also relies on the intrinsic P_O of the channels as well. We saw that TASK-1 has an almost linear IV, indicating a high intrinsic Po. Therefore for non-physiological ions despite their ability to act as potent activators, there is not much channel activity left to activate. Hence they evoke tail currents similar to those by K^+. In contrast TASK-3 channels show a strong outward rectification by K^+ ions, which suggests that the channels have a low P_O that can be increased further. As a result the TASK-3 tail currents evoked by non-physiological ions are significantly larger than those by K^+.

In contrast to other K2P channels K^+ currents from TALK-2 show some deactivation during depolarization, which can account for the relatively weak outward rectification of these channels and also their relatively small and fast deactivating tail currents. Rb^+ currents, in contrast to K^+ reach the steady state near the end of depolarization pulse, showing no sign of deactivation, which means the P_O constantly increases. Hence they carry huge outward current and evoke even larger tail currents. Similar to K^+, slight deactivation of NH_4^+ currents and small K^+ tail currents upon repolarization supports this idea.

In the next section I explore the mechanism of K2P voltage activation in more details.

4.5. A check-valve ion-flux governs K2P channels activation

The results in chapter 3 show that absolute value of tail currents form all pH_{ex}-sensitive K2P channels are positive rectifying and matching on that of outward currents, i.e., the tail currents becoming larger with increase of depolarization from -100 to 100 mV, which indicate voltage activation of the channels. Likewise substitution of intracellular K^+ with Rb^+ increased the tail currents for all the pH_{ex}-sensitive K2P channels. Moreover we noticed that activation of the tail currents from TASK-3 (Fig. 3.14) shifts with ion gradient, i.e. it follows the reversal potential and therefore is dependent on electrochemical driving force (sum of both the reversal potential and voltage, $\Delta\mu = V - E_{rev}$). More extensive experiments on mechanosensitive K2P channels (TREK-1 & TRAAK) showed the same results [126] and that sensing the electrochemical driving force was independent from how the reversal potential changed i.e. change in either extra- or intracellular ion concentrations had the same effect. More than that in contrast to intracellular Rb^+, extracellular Rb^+ had no effect on activation of the channels. These observations together suggest that the SF can sense the direction of ion flow and adopt the proper structure accordingly. At positive electrochemical driving force ions are pushed from intracellular side of the filter to extracellular side and the SF is opened. At negative electrochemical driving force ions follow the opposite direction and the SF adopts the closed state. We named this special gating mechanism **check-valve ion-flux gating**, to emphasize that voltage activation of K2P channels is a one way process. As an analogy one can consider the heart and the aortic valve which allows one direction flow of the blood. In this context the ventricle contraction represents the positive driving force which opens the valve and the aortic blood pressure which causes closure of the valve is the negative driving force.

To explain this model we have assumed that inactive filter can be ion-depleted or fully ion-occupied at negative and positive driving forces, respectively. Then the ion-occupied filter transforms to the open state due to direct coulombic interactions between ions which powers the opening. Then upon reversion of the current the filter becomes unstable probably due to change of ion occupancy within the filter with reduction of S1 and S4 similar to the MD simulations of non-inactivating TRAAK threonine mutants [126]. In the following I propose a hypothesis to explain the possible structural mechanism that

underlines the check-valve ion-flux gating and provide evidence from our work and the literature that support it.

4.5.1. A possible mechanism of check-valve ion-flux

So how does the check-valve ion-flux mechanism work? The SF is an important part of the K2P channel gating mechanism. Therefore, it must be structurally dynamic and MD simulations of various K^+ channels have indicated that this may be the case. Indeed, these experiments show that in both TASK-1 and hERG channels, the aromatic residues of GFG/GYG motif function as the gate and hence closing and opening the channel due to mobility of the peptide bond between the phenylalanine/tyrosine and the second glycine, which can rapidly rotate the carbonyl oxygen away from the conduction axis causing deactivation of the channel at the SF [45]. The flexibility of the peptide bond have been also confirmed in MD simulation of TWIK-1 channel where rotation of the leucine residue in the filter consensus sequence, TIGLG causes deactivation of the channel [133]. Probably the existence of the one-residue gap between S1 and S0, makes these structural rearrangement possible as S1 is ion depleted.

In K^+ channels as K^+ ions diffuse from intracellular to extracellular side of the filter they are thought to be fully dehydrated and interacting with carbonyl groups of the filter which make S4 to S0 binding sites. As they reach to the S0 site the K^+ ions first are becoming partially rehydrated, weaken their interaction with the S0 site and repulsion with the ion from S1 site makes them free to escape into the extracellular mouth of the channel where they fully rehydrate. I therefore propose a model in which movement from S2 to S1 to S0 is fast enough to prevent turning of the upper carbonyl groups at S1 site (Aromatic carbonyls) away from the SF and close the channel.

However, if the voltage changes direction and pushes the ions from extracellular toward intracellular side of the SF (i.e. from S0 toward S4), then ions will arrive at S0 partially hydrated but must be fully dehydrated to enter the filter and progress to the S1 site. Moreover, there is no significant repulsion on the ion from those in the bulk as it would be

from the well aligned ion in the S1 binding site (i.e. repulsion from S1 to S0). These two together can slow down ion transition from S0 to S1 which may give the SF backbone enough time to turn the oxygen carbonyl groups away from the ion pathway and close the channel. In other words, the ion in S1 is pushed to the next binding site (S2) before the ion in S0 can be fully dehydrated and move to S1 which can reduce ion occupancy at this site without effecting dwell time and ion flow rate. I call this model "Pause-and-Turn". This hypothesis may also explain the temperature dependency of deactivation, i.e., the decaying tail currents (Fig. 3.29F) because at lower temperature, thermal motions will decrease which may reduce the probability of structural rearrangement within the SF.

There is much existing evidence to support this proposed mechanism. The closure of TASK-1 channels and the increase in decay of tail currents are both correlated with extracellular K^+ concentration and are more prominent at low K^+ concentrations [42, 134] i.e. when there is a lower probability that K^+ ions will bind to S0 site or become fully dehydrated and move to S1. In contrast with increase of extracellular K^+ concentration this probability increases and hence stabilizes the open filter. The other piece of evidence is that the pH-sensitivity of TASK-1 channels depends on the extracellular K^+ concentration i.e. with an increase of extracellular K^+, the pH-sensitivity of the channel decreases. As we learned in chapter 1, the pH-inhibition of TASK channels is thought to be due to destabilization of the S0 and S1 binding sites due to repulsion of K^+ ions by an adjacent protonated histidine residue. In this context excess K^+ ions binding to S0 can overcome the repulsion of the positive charge next to the SF and stabilize the binding sites and prevent turning of oxygen carbonyl group away at S1-S0 and closure of the channels. Likewise, when the proton concentration is reduced, this will decrease the fraction of the decaying tail currents [42] which means fewer channels deactivate upon repolarization and the channels stay open.

For the same reason an increase of extracellular K^+ concentration will increase the outward currents [42], even though the driving force decreases. This is because in higher K^+ concentrations, due to higher occupancy of S0 the probability that S1 becomes empty decreases. Consequently this will reduce the probability of the SF closing and will increase the overall voltage-activated current.

However the most compelling evidence lies in our own experiments. I have shown in chapter 3 that both Cs^+ and Rb^+ strongly activate pH_{ex}-sensitive K2P channels. This, indeed, is a general feature of all K2P channels [126]. Interestingly, in comparison to K^+ both ions show strong increase of ion occupancy in S1 [126], which in turn can prevent rotation of the aromatic carbonyl group away from the ion pathway and hence closure of the SF. This evidence becomes more convincing if one takes into account that Cs^+ strongly activates K2P channel. The simple explanation is that despite impermeability, during depolarization Cs^+ ions eventually reach the S1, and due to strong binding prevent the SF from deactivation. The large K^+ tail currents upon repolarization of the membrane indicate that the SF has been in the open state during depolarization.

It is possible that this proposed hypothesis might be tested by MD simulation via measuring the time difference in hydration and dehydration of K^+ ions at S0 binding site and whether an ion pushed by voltage can jump out of S1 (to S2) before that in S0 becomes dehydrated, in other words to see if the ion occupancy of S1 is dependent on and changing with direction of ion flow and driving force. However, the interpretation of ion permeation events in MD simulations remains highly controversial.

The above mechanism also explains both instantaneous and time-dependent components of the activating currents. As voltage pushes ions from intracellular to extracellular side of the channels depending on orientation of the aromatic carbonyl groups in the SF the channels can be either in open or closed states. If they are in the open state flow of the ions to extracellular side keeps the channels open as explained above. This represents the instantaneous currents that are always seen upon depolarization. The opening of the rest of channels is a matter of time and thermal motion of the entire SF. As Fig. 3.28E shows, low temperatures slow down the voltage time-dependent activation of the channels where channels reach hardly to steady state at the end of voltage pulse, in contrast to room temperature where steady state is achieved at very beginning of the voltage pulse.

4.5.2. Importance of the check-valve mechanism

At the resting membrane potential K2P channels allow the efflux of K^+ ions out of the cell. However before the K^+ ions diffuse into the bulk medium they will make a concentrated cloud in the extracellular microenvironment (enhanced by the presence of the cap domain) which will favors inward diffusion back towards the filter and into the cell. The check-valve mechanism may prevent this happening. Also K2P channels do not possess a fast N-type inactivation as K_V channels do, however they also contribute to membrane repolarize after an action potential. The check-valve mechanism would therefore enables K2P channels to overcome a lack of fast inactivation mechanisms and control the flow of K^+ ions to suit the requirements of cell in terms of repolarization.

Therefore the check-valve mechanism guarantees that at voltages above the K^+ reversal potential, (i.e. resting membrane potential and during depolarization) the K2P channels are activated and conduct K^+ out of the cell. While upon repolarization it will prevent return of K^+ ions into the cell.

4.5.3. Inactivation of tail currents

The proposed model for deactivation of K2P channels involves the rearrangement of the SF backbone between S1 and S0 binding sites as the membrane potential falls below the K^+ reversal potential. This structural change will destabilize the rest of binding sites and the ions in S1 to S4 will therefore leave the SF due to the applied voltage, or simply diffusion toward the only possible exit, therefore the filter will eventually become empty. On the other hand upon depolarization, ions will move one by one from S5 to S4 and S3 etc. Since four carbonyl oxygen atoms of one binding site are shared with that of binding site immediately next to it, occupation of each site will trigger the correct and most favorable arrangement of the upper binding site for ion occupancy and stabilizes it in that correct arrangement. In contrast, as an ion leaves a binding site it will make occupancy of the next site less favorable and pushes it toward destabilization. Therefore during repolarization, as S1 becomes empty the probability that the ion bound to S2 will leave

increases. In the same manner, if S2 is occupied the probability of S1 being occupied increases. This means that binding of ions to one binding site is influenced by the binding of ions to the adjacent site. Then what would happen, will depend on the direction of voltage, concentration of ions at two sides and thermal fluctuations. Therefore the decay of tail currents does not happen immediately and is a gradual procedure that can be fitted with an exponential function similar to that used to describe random decay. Thus when the temperature is low as in Fig.3.29F, the tail currents will deactivate slower, as well. In section 4.7.2 I come back to this model and use it to explain the K2P channels voltage activation due to ion occupancy of the filter.

4.5.4. Activation of K2P channels by Rb^+ and Cs^+

An interesting question is why Rb^+ and Cs^+ are much more potent than K^+ in activating K2P channels. As mentioned before, the gating at the SF is probably due to flexibility of the peptide bond between F/YG in the TXGF/YG consensus sequence, where is also the S1 binding site.

A closer look at outward macroscopic K^+ and Rb^+ currents show that, the K^+ currents are rough and flickering while Rb^+ currents are larger and smoother. This is reminiscent of the KCNK1 channel gating in Rb^+ where at negative voltages large and smooth Rb^+ tail currents are observed while the corresponding K^+ currents are of smaller amplitude and more flickery [140]. Pusch *et.al.*, have attributed it to modulation of fast gating process by the binding of K^+ or Rb^+ to the gating structure and ability of Rb^+ to reduce the "flicker-blocked state" (i.e. closed state) in KCNK1. For K2P channels the differences may be due to a differential occupancy of the S1 site by Rb^+ vs. K^+. Despite the ability of the K^+ to activate channels, at any instant some in the large population deactivate which causes the relative smaller K^+ currents and flickering. While slightly larger Rb^+ ions are better coordinated in the S1 (i.e. higher ion occupancy) and hence stabilize the filter much better than K^+ in the open state which results larger and smoother Rb^+ currents.

In the same manner, Cs^+ ions despite being impermeable can increase the P_O of the K2P channel (i.e. tail currents). This should not be a surprising since Cs^+ is even slightly larger than Rb^+ and in our MD simulations shows higher ion occupancy in the S1, indicating that it may be even better coordinated in S1 than Rb^+ ions.

4.5.5. Impermeability of Cs^+

In chapter 3 I showed that Cs^+ is almost impermeable in pH_{ex}-sensitive K2P channels, which was also true for other K2P channels [126]. This behavior of the channels toward different ions can easily be explained by a mechanism of ion diffusion in the SF of K^+ channels and a careful examination of ion distribution in SF of K2P channels.

Köpfer *et.al*. [28] have shown that ion permeation in K^+ channels is due to coulombic repulsion (knock-on) between ions in S3 and S2 with in coming of an ion into the S4 site. We have shown that in the TRAAK SF, K^+ distribution is relatively even; all binding sites are occupied, with higher occupancy of S2 and S3. In comparison Rb^+ shows higher occupancy in S1 and S4 and that of S2 is decreased and shifted toward S3. In comparison, Cs^+ ions show the most distortion of ion occupancy. That of S1 and S3 is highly increased. The S2 site is practically disappeared and that of S4 is slightly lower than occupancy of K^+. I propose that lack of binding to S2 prevents the required coulombic repulsion (knock-on) between ions for diffusion. In other words it creates an energy barrier against ion flow in the SF (between S3 and S1). The observation that at very high potentials Cs^+ ions permeate in K2P channels favors the existence of such energy barrier and supports this hypothesis. Therefore these unique arrangements may cause inhibition of the SF by Cs^+ ions while simultaneously producing a high P_O.

4.5.6. Na^+ does not activate K2P channels and is impermeable

We have shown that the Na^+ conductance of K2P channels is very low and cannot activate the channels like other monovalent ions [126]. In comparison to other monovalent ions, the dehydration energy of Na^+ ions is very high (105 and 85 kcal/mol for Na^+ and K^+

respectively). To overcome this Na^+-selective channels employ a short and wide SF with negative charges inside, which allows partially hydrated Na^+ ions to pass through [1]. In contrast K^+ channel filters do not bear any charged residues, and are long and narrow. As a result, hydrated Na^+ ions do not easily permeate and interact (unlike Cs^+) and are therefore incapable of voltage activating K2P channels.

4.6. Roll of structural components of K2P channels in voltage gating

4.6.1. C- and N-termini influence the voltage gating

Independent from phosphorylation of C-terminal site, truncating the C-terminus impaired both voltage and stretch activation of TREK-1 channels, while replacing it with that of TASK-1 restored voltage activation to some extent but did not rescued outward rectification of the channels [129]. Based on these it has been proposed that voltage activation of stretch-sensitive TREK-1 channels is due to change in the membrane curvature and stretch due to depolarization [129]. As I showed in chapter 3 however TREK-1 channels with a truncated C-terminus showed very strong voltage activation by intracellular Rb^+ ions while conducting no tail currents (Fig. 3.32). Likewise, TREK-2 channels lacking both C- and N-termini show relatively small and very fast deactivating tail currents that can be fully developed in low temperatures. Together these suggest that although voltage gating happens primarily at the SF, it can be modulated by the intracellular domains and therefore be influenced by a variety of intracellular signaling pathways which operate via these domains.

4.6.2. The selectivity filter is the main gate

In the absence of crystallographic data from K2P channels, based on K_VAP structure, Ashmole *et.al.* [135], developed a kinetic model which assumes in addition to the SF and independent from that, TASK-3 channel gating happens at helix bundle crossing by movement of M2 and M4 around hinge glycines [135]. In contrast to that report, by

mutating threonine residues in consensus sequence of the SF (TIGY/FG) of pH_{ex}-sensitive K2P channels in chapter 3 I have demonstrated that the mutated channels turn to open rectifiers that neither activate nor deactivate and are voltage insensitive (Fig. 3.12). Likewise corresponding mutations in either P1 or P2 of the stretch-sensitive K2P channels (TREK-1 & TRAAK) were voltage insensitive and constantly open [126]. These results indicate that the conserved threonine residues have a significant role in the voltage gating of all K2P channels and K2P channels do not gate at intracellular moth of the channel.

Moreover we noticed that in comparison to the WT channels, overall currents of these threonine mutant channels are reduced. We could compensate for lower activity of these channels by increase of mRNA injected into oocytes. Although we cannot rule out decrease in membrane expression, but MD simulation on the TRAAK T103C mutant shows 94% reduction of total permeation events [126] which fits well to the electrophysiology experiments. Also the MD simulation indicates that the ion occupancy of S1 and S4 in these mutant channels is lost. In contrast ion occupancy of both S2 and S3 highly increases. Interestingly S4 is the only binding site which is solely consisted of one residue i.e. side chains and carbonyl groups of four threonines (T103 in TRAAK). Further analysis of the WT and mutant channels by MD simulations showed that the WT threonine side chains are stable and pointing towards the ion pathway during the experiment. In contrast in the mutant channels, the cysteine side chains, in both subunits are turned away. This observation perfectly explains the loss of S4 binding site (Fig 4.1). The other binding sites are assembled from 8 carbonyl groups of two adjacent residues in each P domain and replacing them cannot affect the SF as much as replacing a side chain that is directly involved in selectivity of the channel. For instance, Yuill *et.al*. have shown replacing the first glycine in GFG motif within P1 with alanine or aspartate, by increasing the voltage time-dependent current component, makes the voltage gating more prominent [9]. Comparing this with our results implies that different regions of the filter have different effects on coordination of the ions which causes different behavior of the mutant channels in response to the voltage. Loss of voltage sensitivity of the threonine mutants in parallel to loss of S1 binding site in MD simulation is another strong evidence that S1 represents the principal gate in the SF.

It seems in the mutant SF, rotation of the cysteine side chain away from the ionic pathway triggers structural changes in the filter that lock the S1 at a rigid configuration that cannot close the filter off and coordinate K^+ ions either, which can explain why these channels are constantly open. On the other hand significant reduction of number of ions in the SF (to two ions in the S2 and S3), accounts very well for reduction of permeation events in the MD simulation and K^+ currents in the electrophysiology experiments, due to decrease of ions knock-on in the SF.

For these observations to be true, the SF should have some degree of structural plasticity and flexibility at different modes. Interestingly experimental data support this idea. For instance while the instantaneous currents from TOK-1 are sensitive to Ba^{2+} block (IC_{50} 20 µM) the voltage-time dependent component of the currents is rather insensitive to the divalent ion (IC_{50} 3 mM). But both components are equally sensitive to TEA (IC_{50} 5.5 mM) [136] which blocks the channels by binding to a site beyond the SF. K2P channels block by Ba^{2+} is due to binding to S4 binding site deep in the SF [137]. This requires that the SF structure to be different in these two modes, those that are in the leak mode pass Ba^{2+} ions down to S4, while those channels that are in the voltage gating mode, even after being open, will prevent Ba^{2+} from reaching and binding to S4.

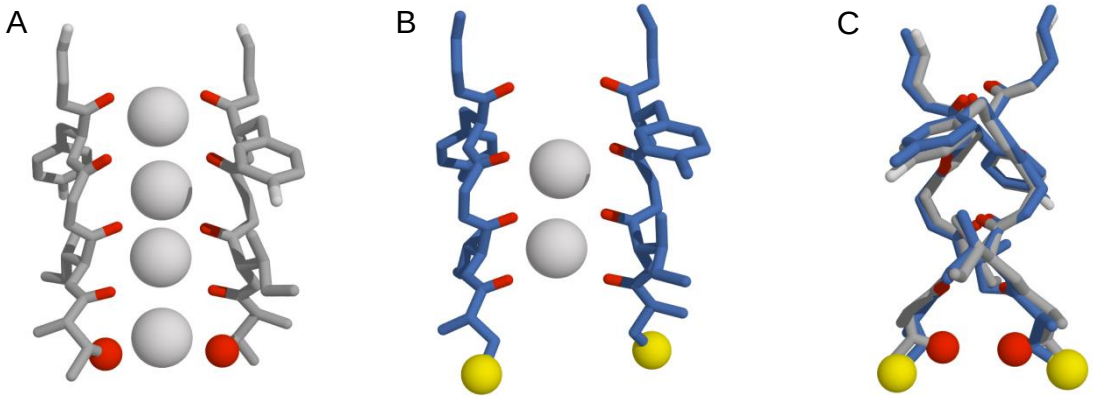

Fig.4.1. SF comparison between WT TRAAK and the T103C mutant. The MD simulations show that the cysteine residues side chains turn away from the ion pathway. (A); WT channel. (B); T103C mutant channel. (C); (A) and (B) superimposed and turned 90° to emphasize on the position of threonine and cysteine side chains in the WT and the mutant channels. Oxygen atoms are depicted in red, sulfur in yellow and K^+ in gray. Note that the mutant channel coordinates just two K^+ due to loss of S4 binding site.

4.7. Voltage gating of K2P channels

4.7.1. The gating charge

The gating charge for a channel represents the lower limit of charges that should be moved in response to the voltage steps required for the channel to open. Therefore they are important in studying the kinetics of voltage gating. Voltage activation of K_V channels is accompanied by a gating current that is experimentally measurable as the movement of positively charged residues in the electrical field. However, this gating current is independent from the ionic currents that go through the pore and can be measured in closed, blocked or nonconductive channels to assess the gating charge.

However K2P channels lack such a classical voltage sensor and measuring the gating currents in absence of ionic currents would be impossible. Despite this, if K2P channels are voltage-dependent then voltage activation should still have an associated charge movement which moves in the electrical field in response to voltage steps and which can be experimentally measured (albeit in the presence of the permeant ionic currents). Using the Boltzmann function, from steepness of the voltage dependence of gating a lower limit for magnitude of the gating charges per channel can be calculated [1]. This approach revealed an equivalent gating charge of 1.8 and 2.2 for TALK-1 and TALK-2, respectively, in comparison to an average of 2.2 for the K2P channels superfamily. This is also in good agreement with previously measured gating charges of 2.5 for TREK-1 calculated using the P_O of single channels [132]. To achieve this we should make two assumptions. First, the voltage drop along the SF accounts for about 80% of the drop across the entire thickness of the membrane [138, 139]. Then the inactive filter is completely ion depleted. Upon depolarization, translocation of an ion from the S5 cavity site to the S1 would contribute 0.8 e_0, translocation of a second ion to S2 would contribute three-fourths of 0.8; 0.6 e_0, translocation of another ion to S3, about half of 0.8; 0.4 e_0 and finally translocation of the fourth ion would contribute 0.2 e_0. Sum of contribution of all ions is 2.0 e_0 which is very close to our experimental measurements. Therefore our electrophysiological

experiments support a previous MD simulation that suggest four ions can simultaneously occupy the SF [28].

In chapter 3 I showed that activation of TASK-3 tail currents shifts with change in ion gradient. We have also shown [126] that for both TRAAK and TREK-2 channels saturation of the tail currents are also dependent on ion gradient. The ion sensitivity of this process and dependence upon the reversal potential makes the K^+ ions the only candidate to represent the gating charges and the SF must therefore represent the voltage sensor.

4.7.2. Ion occupancy of the filter in different voltages and its role in gating

In our recent publication we have proposed that the filter is not entirely ion depleted as K2P channels are in an inactive state which simply conducts ions at a very low rate [126]. This ion occupancy of the SF fits perfectly to a condition in which the driving force is zero where the channels are apparently inactive. Because the electrochemical driving force is zero, i.e. the net flow of ions to both sides is zero, the filter cannot be empty. Since the ion occupancy of ion binding sites inside the filter is a matter of thermal fluctuations and the filter can be either conductive or nonconductive, this explains how the channel can harbor ions at the inactivated state. But how is the ion occupancy of the SF at negative electrochemical driving force and hyperpolarized voltages? In this state the SF should become depleted very fast. Since after closure of the channel no additional ions enter the S1 site and those below it are forced out.

In contrast, upon depolarization even if the SF is totally ion depleted, binding of the first ion into the S4, shifts S3 to the favorable arrangement for being occupied. Then as S3 becomes occupied the S2 rearranges and so up to S1. This model also predicts the time dependency of activation. Otherwise a fully occupied SF should open instantaneously and a partial occupied one should open faster than a depleted one. The important point here is that every binding site is connected to the lower and the upper binding sites next to it and binding of an ion to one binding site changes arrangement of the adjacent empty one and facilitates the binding of incoming ion. In the same way an empty binding site makes it

easier for an ion to leave the next binding site and not to become occupied again (makes the binding less favorable). Therefore this new model predicts that there is reason for the SF first to become fully ion occupied and then afterwards ion permeable. It also predicts that as each binding site becomes occupied the channel will gradually adopts the open configuration, until the S1 site being occupied by which time the channel will already be in the open state as soon as all four S1 aromatic carbonyl groups are in the ion pathway (Fig 4.2). For an analogy one can think of the SF as a three dimensional zipper where K^+ ions represent multiple sliders. Therefore I name it Ion-Zipper Model.

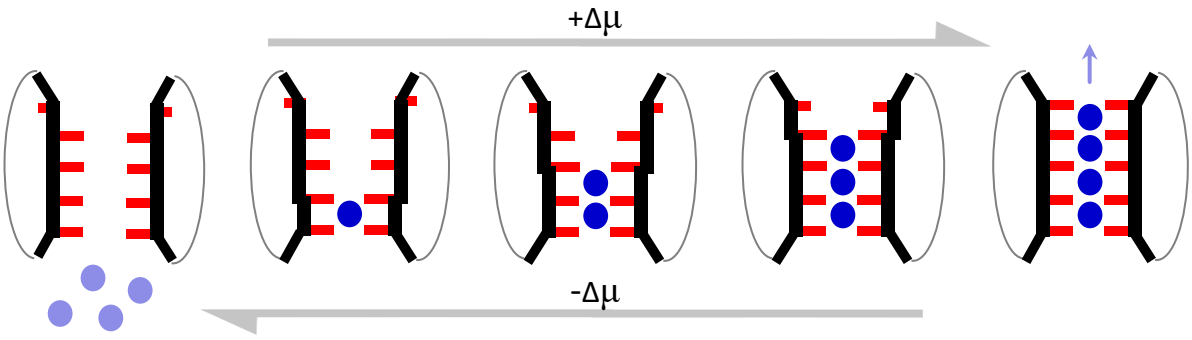

Fig.4.2. The Ion-Zipper model for K2P channels voltage activation. From left, positive electrochemical driving force, +Δμ, pushes K^+ ions into the filter. Occupation of each site will trigger the correct and most favorable arrangement of the upper binding site for ion occupancy and stabilizes it in that correct arrangement, till S1 being occupied when the channel is already open.−Δμ will do the reverse and deactivates the filter. Note that carbonyl groups of the aromatic residues (S1-S0) are turned away from the ion pathway axis, before S1 being occupied. Oxygen atoms are depicted in red, filter backbone in black and K^+ ions as blue circles.

4.8. Open rectification versus voltage activation

The voltage gating of ion channels and rectification should not be confused and correlated with each other. Even classical voltage-gated channels can have an ohmic IV relationship. For instance, in symmetrical K^+ concentration, voltage-gated delayed rectifier K^+ channels, including $K_V2.1$ have a linear IV relationship [17]. The misunderstanding that voltage activation of K2P channels and outward rectification are intertwined probably arises from observation that C-terminus phosphorylation of TREK-1 produces channels that are strongly voltage dependent and outward rectifying [132].

Therefore in the literature K2P channels are mostly described as leak channels insensitive to voltage. However some K2P channels like TASK-3 and TREK-1 are not only activated by voltage, but even in symmetrical K^+ concentration show outward rectification. Others like TASK-1 show a linear IV relationship in symmetrical K^+ concentration (Fig. 3.5B). However this linear IV relationship is also due to their voltage activation. Under this condition the elicited currents show time-dependent development at positive voltages to reversal potential, and the deactivating tail currents upon repolarization to the holding potential provide strong evidence that this voltage activation lies beyond their initial P_O. Therefore the linear IV relationship of a K2P channel like TASK-1 is the direct result of voltage activation of the channels.

4.9. Physiological significance of voltage gating of K2P channels.

4.9.1. TASK channels

In cerebellar granule neurons, TASK-1 channels contribute to the back ground current and their inhibition depolarizes the resting membrane potential [89]. In contrast in atrial myocytes inhibition of TASK-1 currents with the specific blocker, A293 has no effect on resting membrane potential. However it increases the action potential duration [112]. This indicates that in contrast to its role in neurons, in atrial myocytes TASK-1channels are not acting as leak channels and are silent at the resting membrane potential. However, during action potentials they are voltage activated and contribute to repolarization of the cell membrane and hence regulate action potential duration. Therefore these channels appear to be regulated differently in different tissues. Although it remains to be confirmed if regulation of K2P channels by other proteins and signals can shift the channels between leak and voltage gating.

Voltage activation of K2P channels may also not be just restricted to excitable cells. In proximal tubules of nephrons, the regulatory volume decrease in which TASK-2 channels have a crucial role is preceded by an outflow of anions (Cl^- and HCO_3^-) from the cytoplasm to alkalinize the tubular fluid [101]. However this efflux of anions also depolarizes the

plasma membrane. Therefore in tissues like kidney where TASK-2 channels are the major player in volume regulation, voltage activation of these channels by depolarization of the membrane due to cell swelling may have a significant role in cell volume regulation.

4.9.2. TALK channels

Secretion of hormones from pancreatic cells is also highly dependent on their membrane potential. As the cell membrane become depolarized hormones such as insulin are secreted. It has been suggested that TALK-1 may regulate hormone secretion by repolarization of cell membrane after the depolarization increase [34]. In this context voltage activation of TALK-1 might also facilitate repolarization.

Also, TALK-2 channel is expressed in heart in Purkinje fibers and atrioventricular node. Overexpression of TALK-2 in HL-1 cells, which are spontaneously beating sinoatrial node like cardiomyocytes, whilst it did not significantly change the action potential threshold, it did reduce the action potential overshoot and slowed the upstroke velocity [117]. Such a change in the action potential might also be explained by voltage activation of TALK-2 channels.

4.10. The unusual TWIK-1 channel

TWIK-1 inward Rb^+ and NH_4^+ conductances have been observed in whole cell patch clamp from CHO cells [59]. I was interested to see if I can use these and other monovalent ions to observe voltage activation of the channel as well. In contrast to that report, in inside out giant patches I could not evoke TWIK-1 Rb^+ currents recognizable from endogenous currents. However large Rb^+ and NH_4^+ currents could be elicited from ^{M}TWIK-1 mutant. This indicates that the density of WT TWIK-1 in giant patches is too low to deliver any measurable current. However for the ^{M}TWIK-1 mutant, the density of the channels is increased to a measurable quantity by alterations in trafficking.

The low conductivity of TWIK-1 for K^+ and its high conductivity for NH_4^+, have led to ideas that TWIK-1 is essentially a regulatory channel for NH_4^+ uptake in hippocampal astrocytes [67]. My data confirm both low K^+ conductivity and high NH_4^+ conductivity of TWIK-1. But in my experiments NH_4^+ conductance was not due to loss of selectivity due to constant recycle between internal compartments and the cell membrane. ^{M}TWIK-1 mutant is stationary at the cell surface. Therefore the precise physiological role of these channels in astrocytes, and most other tissues, remains to be determined.

4.10.1. Gating of TWIK-1 channel

4.10.1.1. Voltage gating

Voltage gating of TWIK-1 is very different from most other K2P channels. K^+ ions, in comparison to other monovalent ions, except for Na^+ and Tl^+ are weakly permeable (Fig.3.17) and voltage activation by K^+ in symmetrical concentrations is only observed at very high voltages beyond the physiological range. However these currents show the characteristics of check-valve ion-flux gating. Also similar is the behavior of Cs^+ and Na^+ ions as the permeant ions, with difference that Cs^+ is more permeable than K^+ (Fig.3.17). This is despite the fact that Cs^+ strongly blocks most K^+ channels including K_V and K_{ir} channels [1]. In contrast to K^+, Cs^+ and Na^+, both Rb^+ and NH_4^+ carry large inward and outward currents. However unlike most other K2P channels significant currents are observed at much higher voltages (Fig. 3.17). Also in symmetrical concentrations of both Rb^+ and NH_4^+ the check-valve ion-flux disappears and TWIK-1 behaves as an open rectifier with no voltage activation (Fig. 3.20).

Interestingly this behavior is identical to the gating in the other K2P channels where the threonines in the consensus sequence of the SF are mutated because it abolishes both the voltage gating and the check-valve ion-flux. MD simulations [126] suggest that this mutation might change the ion occupancy of the SF. Therefore it would be to future investigations to see if in absence of K^+ from both extra- and intracellular side of the channel, Rb^+ and NH_4^+ ion occupancy would be similar to that of the threonine mutants.

With the above explanation one may consider that the voltage activation of TWIK-1 is an artifact and the observed time-dependent activation is simply due to release of channels from block. However for this to happen the ions need to be able to access the SF. In inward voltage activation, where Rb^+ and NH_4^+ are at extracellular side of the channels (Fig. 3.19), between voltage pulses the membrane is kept for 3-5 second at -80 mV, which is long enough to exclude any blockage by K^+ ions. Moreover, small inward Rb^+ or NH_4^+ currents should prevent K^+ ions from reaching the filter. Therefore similar to other K2P channels, TWIK-1 has the check-valve ion-flux gating mechanism, although a modified version of it.

4.10.1.2. The hydrophobic inner pore of TWIK-1

A recent study has hypothesized that a hydrophobic barrier exists within the inner pore of TWIK-1 which contributes to the low functional activity of TWIK-1 channels [61]. Consistent with the notion of a hydrophobic barrier the authors showed that mutation of the key residues to polar or charged residues produced channels that were highly conductive and this was supported by a computational studies which demonstrated dewetting of the inner pore [61]. However, the authors also pointed out that these mutations may indirectly influence gating within the filter, and mutation or chemical modification of a similar residue in TM2 of TREK-1 (G186) is known to modify channel gating within the filter. My results are therefore consistent with the existence of a complex gating mechanism within the SF of TWIK-1. However despite the hydrophobic barrier, we have observed strong activation of TWIK-1 by both Rb^+ and NH_4^+. Therefore although a hydrophobic barrier could have significant effect on the low activity of TWIK-1, it cannot be the only and major reason for it. In the following section I discuss the main reason for this notion.

4.10.2. Inhibition of TWIK-1 by K^+ ions

Early work on TWIK-1 has shown that at depolarized potentials, the channel is rapidly inactivated producing the apparent weak inward rectification of the channel [37]. I also noticed that despite activation by Rb^+, TWIK-1 conducts no tail currents, though it is not the only K2P channel without tail currents. Because TOK-1 channels also do not show any

tail currents which has been associated with a very fast deactivation of the currents upon repolarization [136]. I was therefore interested to find out if fast deactivation prevents TWIK-1 channel from conducting tail currents as a similar mechanism observed in hERG channels upon depolarization.

To probe this I undertook the temperature experiments which cooled down the membrane. Interestingly, under these conditions ^{M}TWIK-1 channels exhibited slower activation at lower temperature, but still no tail currents. However, the control channel, ^{T}TREK-2, showed both slow activation and large slow deactivating tail currents at low temperatures. This was despite the fact that it has small fast deactivating tail current at room temperature.

Therefore the fast deactivation of TWIK-1 channels, if exists, cannot be the only reason for its low activity and hence lack of tail currents.

Comparing gating of TWIK-1 in different ion configurations for K^+, Rb^+ and NH_4^+, I noticed that K^+ currents were the only ones that could not easily pass through the channel. Even in absence of K^+, TWIK-1 behaves like a constantly open leak channel. Therefore I tested the inhibitory effect of K^+ ions on voltage activated Rb^+ currents from the channel and compared it with the other ions. Intriguingly, K^+ strongly inhibited the channel activity with an IC_{50} of 2.8 mM and therefore appeared to be an even more potent blocker than, Cs^+. In comparison, Rb^+ currents from TREK-1 were much less susceptible to K^+ inhibition (IC_{50} = 68 mM) and those of TREK-2 were even enhanced by K^+. These comparisons between different channels, although very interesting, are less informative. Therefore I used TREK mutants that show faster deactivation in comparison to the WT channels, i.e. ^{100}TREK-1, TREK-1 L304C and ^{T}TREK-2. Intriguingly Rb^+ currents from these channels were much more susceptible to K^+ inhibition. For instance while the currents from TREK-2 were enhanced by K^+ those of ^{T}TREK-2 were strongly inhibited (IC_{50} = 20 mM). But more interesting is to notice the correlation of K^+ inhibition with activity of the channels. While, similar to the WT, L304C despite fast deactivation and hence tiny tail currents could be voltage activated by K^+, ^{100}TREK-1 behaved similar to TWIK-1 channels, i.e. in giant patches it produced no K^+ currents recognizable from endogenous currents of oocytes, as if there is no expression. But it could be strongly

activated by Rb^+ ions. Though, upon repolarization no tail currents were observed. Therefore one can conclude that fast deactivation of the channels correlates with K^+ inhibition of Rb^+ currents, i.e. faster a channel deactivates, the more susceptible the Rb^+ currents appear to be to K^+ inhibition.

It seems that these mutations alter the structure of the filter in a way that they coordinate K^+ ions much more than the WT. It is possible that the global structure of TWIK-1 has such an influence on the filter. I therefore propose that like the mutant channels, the low activity of TWIK-1 is due to very fast deactivation of channels in presence of K^+ ions. One can think that low activity of TWIK-1 channel lies in stronger coordination and hence longer dwell times for K^+ ions in the SF, perhaps reminiscent to inhibition of K2P channels by Ba^{2+}. However, the precise mechanism of the fast deactivation will remain the subject of later studies.

4.10.3. Ion competition for binding sites within the filter

The mild decrease of Rb^+ currents in TREK-1 channels due to increasing concentrations of K^+ can be explained by the fact that if the SF allows two different ions to pass through, then competition of the two ions for simultaneous occupancy of binding sites inside the SF blocks the currents from the other ion. In this case increasing the concentration of K^+ ions in Rb^+-based solution increases the probability that binding sites are being occupied by K^+ ions rather by Rb^+ ions. Since the Rb^+ ions are more much potent at increasing the P_O of the channels during depolarization, by increasing K^+ ions in the SF the P_O of TREK-1 channels decreases, and Rb^+ currents appear to be blocked. It seems in TREK-2 SF there is no obvious competition between K^+ and Rb^+ ions and they have similar permeability in the SF, although ion binding should be different, and therefore, due to more driving force, the current amplitudes increase, as the total ion concentration increases.

4.10.4. pH-sensitivity of TWIK-1 channel

TWIK-1 channels in giant inside-out patches showed robust and reproducible inhibition by intracellular H^+ after they were activated by Rb^+. In this sense the pH-sensitivity of TWIK-1 is similar to that of TOK-1, which does not lose pH-sensitivity after patch excision [136]. This is in contrast to a previous work that proposed intracellular pH-sensitivity of TWIK-1 channels is an indirect effect that is lost after patch excision [37]. In that study the authors had used CO_2 bubbling and/or modifying the Na_2HPO_4/NaH_2PO_4 buffer ratio to obtain low pH, while I used direct HCl titration of the intracellular solutions to achieve the desired pH, which may explain the difference. Another reason could be that I measured pH-sensitivity of macroscopic currents while in the previous work the pH-sensitivity of single channels was measured.

With a high intracellular H^+ sensitivity (IC_{50} of pH 7.8) it is very improbable that TWIK-1 to function as an intracellular ion channel, where it has the highest localization. Also as it is trafficked to the plasma membrane TWIK-1 still will show low functional activity at normal physiological range.

4.10.5. TPA block

Using Rb^+ activated currents I showed that with an IC_{50} of 3.36 µM, TWIK-1 has very high affinity for TPA which is more than that of TREK-1 ($IC_{50} \approx 13$ µM) but less than that of TRESK ($IC_{50} \approx 0.3$ µM) [8]. We have also shown that in Rb^+ based solutions the affinity of TPA for TREK-1 decreases [126] which correlates with a change of ion occupancy of the SF and competition of Rb^+ ions with TPA for binding site. Therefore if ion occupancy of K^+ and Rb^+ ions in the SF follows patterns similar to that of other K2P channels, one can expect that affinity of TPA in K^+ based solution would significantly increase and yields a smaller value IC_{50}.

5. Conclusion

5.1. Summary

K2P channels are often referred to as leak channels, which are solely involved in the maintenance of resting membrane potential. However in this study I show that in their native mode, pH_{ex}-sensitive K2P channels function as voltage activated ion channels. This supports previous studies that show these channels are also involved in repolarization of the membrane after depolarization and action potential. In this context voltage activation of K2P channels has significant physiological roles, including; adjusting the heart action potential duration, hormone secretion and cell volume regulation in the kidneys.

All K2P channels except TWIK-1, regardless of degree of rectification show deactivating tail currents upon repolarization which indicates membrane depolarization beyond the reversal potential increases the channels open probability (P_O). This feature, i.e., increase from the base P_O to an upper limit enabled us to measure an equivalent gating charge which is an important criteria for studying kinetics of ion channels. To do this we used Rb^+ and Cs^+ ions as tools, which proved to be useful for further investigation of voltage activation of K2P channel. For instance Cs^+ despite being impermeable in most K2P channels, is highly potent in the voltage activation. This indicates that not ion permeation *per se*, but the binding step to the selectivity filter (SF) is the critical step in the voltage activation of K2P channels. Further study by physiological and non-physiological ions showed that the voltage activation of all K2P channels involves a one-way ion flow mechanism. We named this yet unique voltage gating mechanism; "**check-valve ion-flux**" to emphasize not only on the role of the SF but also voltage and ion gradient, i.e., the driving force. Using our data and the literature I further hypothesize that the flexibility of the SF and specific interaction of the binding sites with the flowing ions is the fundamental mechanism behind the check-valve ion-flux gating. In this work two distinct but intertwined models are introduced to explain the underlining structural mechanism of the check-valve ion-flux gating. The first; the **Pause-and-Turn model**, explains how K2P

channels sense the electro chemical driving force due to the time difference that may exist between dehydration and rehydration of ions as they interact with the SF and can cause change of ion occupancy in S1 binding site. I name the second; **Ion-Zipper model**, in which, like a three dimensional zipper, the SF goes under local structural changes as "sliders", i.e., ions move along and interact and bind to each of the binding sites. This model explains why the SF has to be fully ion-occupied before it can be open and why it would become fully ion-depleted during repolarization.

Among K2P channels TWIK-1 is an unusual one. Since its discovery as the first mammalian K2P channel several mechanisms have been proposed to explain its poor functional activity. However none of them can alone explain the TWIK-1 gating properties. In this study I showed that K^+ strongly inhibits TWIK-1. Although the exact mechanism of K^+ inhibition will be the subject of future studies, it seems in the presence of K^+, TWIK-1 goes under fast deactivation. Interestingly, some TREK-1 mutants mimic the TWIK-1 phenotype. Hence, one can assume that under certain physiological conditions or in the presence of yet undiscovered activation partners/auxiliary subunits TWIK-1 can also adopt the proper global structure compatible to voltage activation similar to the other K2P channels. Yet, in absence of such stimuli/auxiliary subunit, TWIK-1 can also be voltage activated by non-physiological ions. But it shows a modified version of the check-valve ion-flux gating. This is very probable since, in the presence of K^+, upon application of voltages beyond the physiological range TWIK-1 shows all the properties of the normal check-valve ion-flux gating, which indicates the existence of an energy barrier inside the SF. This new finding is in contrast to our previous report [126] that TWIK-1 has an open rectification behavior.

I have also demonstrated that, TWIK-1 is directly inhibited by intracellular H^+ (IC_{50} of pH 7.8). This strong inhibition implies that TWIK-1 dose not function as an intracellular channel, where it has the highest localization. Also as trafficked to the plasma membrane, TWIK-1 still will show low functional activity at normal physiological range. This makes the need for additional activating signals/ auxiliary subunits more probable.

5.2. Future outlook

We have shown that all K2P channels are voltage activated. We did our studies using homomeric K2P channels. It is believed like many other K^+ channels, K2P channels are also engaged in building heteromeric complexes. Investigating voltage activation of heteromeric K2P channels will revel if check-valve ion-flux gating and activation by non-physiological ions are similar or show deviation from that of homomeric channels and reveal more about physiological role of this family of ion channels.

I showed that TWIK-1 is strongly inhibited by K^+. Several possibilities can account for the observed results. Both very high and very low affinity of an ion for the binding sites can cause low permeation rate and hence apparent inhibition of the channel by certain ions. On the other hand a distorted arrangement of ions in the SF, as is observed for Cs^+ within TRAAK SF can reduce the ions knock-on effect and result in inhibition of the permeation. In parallel to mutations and MD simulation studies, investigation of ions interaction with the TWIK-1 SF by isothermal titration calorimetry in comparison to a channel like TREK-2 which does not show any K^+ inhibition and hence, K^+ and Rb^+ should interact with the SF similarly, can revile which scenario is true for K^+ inhibition of TWIK-1 and shed light on the unusual low activity of the channel.

In this work I have also proposed the “Pause-and-Turn” model which assumes that a time difference between dehydration and rehydration of ions at S0 binding site along the ions knock-on is the major mechanisms behind the check-valve ion-flux gating. It is possible that this proposed mechanism might be tested by MD simulation via measuring the time difference in hydration and dehydration of K^+ ions at S0 binding site and whether an ion pushed by voltage can jump out of S1 (to S2) before that at S0 becomes dehydrated and if this changes the S1 ion occupancy.

Upon activation by physiological signals, some K2P channels like TALK channels do not shift to the leak mode, but instead show higher degree of voltage activation. Investigating the mechanism behind this potentiation can reveal more details about voltage activation of K2P channels and its regulators. It is possible to see how nitric oxide-activated TALK

channels, react to activation by non-physiological ions such as Rb^+. If they do not show any further activation which suggests that the nitric-oxide activation can shift the K^+ ion occupancy of the SF to that similar to Rb^+. If further activation is observed and effect of the two activators are additive, one can conclude that nitric oxide-activation does not affect the K^+ ion occupancy within the SF. But it influences other components of the channel. In this case, mutation of cysteine residues on the transmembrane helices close to the pore, may give more information on the mechanism of activation.

References

[1] B. Hille, *Ion channels of excitable membranes*. Sinauer, ISBN. 9870878933211, 2001.

[2] B. Sakmann and G. Trube, “Conductance properties of single inwardly rectifying potassium channels in ventricular cells from guinea-pig heart.,” *J. Physiol.*, vol. 347, pp. 641–57, 1984.

[3] S. Feliciangeli, F. C. Chatelain, D. Bichet, and F. Lesage, “The family of K2P channels: salient structural and functional properties.,” *J. Physiol.*, vol. 0, no. November 2014, pp. 1–17, 2014.

[4] D. A. Doyle, J. M. Cabral, R. A. Pfuetzner, A. Kuo, J. M. Gulbis, S. L. Cohen, B. T. Chait, and R. MacKinnon, “The structure of the potassium channel: molecular basis of K^+ conduction and selectivity.,” *Science*, vol. 280, no. 5360, pp. 69–77, 1998.

[5] A. N. Miller and S. B. Long, “Crystal structure of the human two-pore domain potassium channel K2P1.,” *Science*, vol. 335, no. 6067, pp. 432–6, Jan. 2012.

[6] S. G. Brohawn, J. del Mármol, and R. MacKinnon, “Crystal structure of the human K2P TRAAK, a lipid- and mechano-sensitive K^+ ion channel.,” *Science*, vol. 335, no. 6067, pp. 436–41, Jan. 2012.

[7] R. G. Zhuo, P. Peng, X. Y. Liu, H. T. Yan, J. P. Xu, J. Q. Zheng, X. L. Wei, and X. Y. Ma, “Allosteric coupling between proximal C-terminus and selectivity filter is facilitated by the movement of transmembrane segment 4 in TREK-2 channel,” *Sci Rep*, vol. 6, no. February, p. 21248, 2016.

[8] P. L. Piechotta, M. Rapedius, P. J. Stansfeld, M. K. Bollepalli, G. Erhlich, I. Andres-Enguix, H. Fritzenschaft, N. Decher, M. S. P. Sansom, S. J. Tucker, and T. Baukrowitz, “The pore structure and gating mechanism of K2P channels.,” *EMBO J.*, vol. 30, no. 17, pp. 3607–3619, 2011.

[9] K. H. Yuill, P. J. Stansfeld, I. Ashmole, M. J. Sutcliffe, and P. R. Stanfield, “The selectivity, voltage-dependence and acid sensitivity of the tandem pore potassium channel TASK-1: Contributions of the pore domains,” *Pflugers Arch. Eur. J. Physiol.*, vol. 455, no. 2, pp. 333–348, 2007.

[10] M. Rapedius, M. R. Schmidt, C. Sharma, P. J. Stansfeld, M. S. P. Sansom, T. Baukrowitz, and S. J. Tucker, “State-independent intracellular access of quaternary ammonium blockers to the pore of TREK-1,” *Channels*, vol. 6, no. 6, pp. 473–478, 2012.

[11] Y. Y. Dong, A. C. W. Pike, A. Mackenzie, C. McClenaghan, P. Aryal, L. Dong, A. Quigley, M. Grieben, S. Goubin, S. Mukhopadhyay, G. F. Ruda, M. V Clausen, L. Cao, P. E. Brennan, N. A. Burgess-Brown, M. S. P. Sansom, S. J. Tucker, and E. P. Carpenter, “K2P channel gating mechanisms revealed by structures of TREK-2 and a complex with Prozac.,” *Science*, vol. 347, no. 6227, pp. 1256–9, 2015.

[12] S. G. Brohawn, E. B. Campbell, and R. MacKinnon, “Physical mechanism for gating and mechanosensitivity of the human TRAAK K^+ channel,” *Nature*, vol. 516, no. 7529, pp. 126–130, 2014.

[13] S. N. Bagriantsev, R. Peyronnet, K. a Clark, E. Honoré, and D. L. Minor, “Multiple modalities converge on a common gate to control K2P channel function.,” *EMBO J.*, vol. 30, no. 17, pp. 3594–606, Aug. 2011.

[14] S. G. Brohawn, E. B. Campbell, and R. MacKinnon, “Domain-swapped chain connectivity and gated membrane access in a Fab-mediated crystal of the human TRAAK K^+ channel.,” *Proc. Natl. Acad. Sci. U. S. A.*, vol. 110, no. 6, pp. 2129–34, Feb. 2013.

[15] N. Zilberberg, N. Ilan, and S. A. N. Goldstein, “KCNKØ: Opening and closing the 2-P-domain potassium leak channel entails ‘C-type’ gating of the outer pore,” *Neuron*, vol. 32, no. 4, pp. 635–648, 2001.

[16] H. Chen, F. C. Chatelain, and F. Lesage, “Altered and dynamic ion selectivity of K^+ channels in cell development and excitability,” *Trends in pharmacological sciences*, vol. 35, no. 9. Elsevier Ltd, pp. 461–469, 2014.

[17] M. L. Chapman, H. S. Krovetz, and A. M. J. VanDongen, “GYGD pore motifs in neighbouring potassium channel subunits interact to determine ion selectivity,” *J. Physiol.*, vol. 530, no. 1, pp. 21–33, 2001.

[18] L. Ma, X. Zhang, and H. Chen, “TWIK-1 two-pore domain potassium channels change ion selectivity and conduct inward leak sodium currents in hypokalemia.,” *Sci. Signal.*, vol. 4, no. 176, p. ra37, Jan. 2011.

[19] F. Duprat, F. Lesage, M. Fink, R. Reyes, C. Heurteaux, and M. Lazdunski, “TASK, a human background K^+ channel to sense external pH variations near physiological

pH," *EMBO J.*, vol. 16, no. 17, pp. 5464–5471, 1997.

[20] R. Reyes, F. Duprat, F. Lesage, M. Fink, N. Farman, and M. Lazdunski, "Cloning and expression of a novel pH-sensitive two pore domain potassium channel from human kidney," *J. Biol. Chem.*, vol. 273, no. 47, pp. 30863–30869, 1998.

[21] Y. Kim, H. Bang, and D. Kim, "TASK-3, a new member of the tandem pore K^+ channel family.," *J. Biol. Chem.*, vol. 275, no. 13, pp. 9340–7, Mar. 2000.

[22] C. Girard, F. Duprat, C. Terrenoire, N. Tinel, M. Fosset, G. Romey, M. Lazdunski, and F. Lesage, "Genomic and functional characteristics of novel human pancreatic 2P domain K^+ channels.," *Biochem. Biophys. Res. Commun.*, vol. 282, no. 1, pp. 249–256, 2001.

[23] S. Rajan, E. Wischmeyer, G. X. Liu, R. Preisig-Müller, J. Daut, A. Karschin, and C. Derst, "TASK-3, a novel tandem pore domain acid-sensitive K^+ channel. An extracellular histidine as pH sensor," *J. Biol. Chem.*, vol. 275, no. 22, pp. 16650–16657, 2000.

[24] M. J. Morton, A. D. O'Connell, A. Sivaprasadarao, and M. Hunter, "Determinants of pH sensing in the two-pore domain K^+ channels TASK-1 and -2.," *Pflugers Arch.*, vol. 445, no. 5, pp. 577–83, 2003.

[25] S. Rajan, L. D. Plant, M. L. Rabin, M. H. Butler, and S. a N. Goldstein, "Sumoylation silences the plasma membrane leak K^+ channel K2P1.," *Cell*, vol. 121, no. 1, pp. 37–47, Apr. 2005.

[26] Y. Zhou, J. H. Morais-Cabral, A. Kaufman, and R. MacKinnon, "Chemistry of ion coordination and hydration revealed by a K^+ channel-Fab complex at 2.0 A resolution.," *Nature*, vol. 414, no. 6859, pp. 43–8, 2001.

[27] Y. Zhou and R. MacKinnon, "The occupancy of ions in the K^+ selectivity filter: Charge balance and coupling of ion binding to a protein conformational change underlie high conduction rates," *J. Mol. Biol.*, vol. 333, no. 5, pp. 965–975, Nov. 2003.

[28] D. A. Köpfer, C. Song, T. Gruene, G. M. Sheldrick, U. Zachariae, and B. L. de Groot, "Ion permeation in K^+ channels occurs by direct Coulomb knock-on.," *Science*, vol. 346, no. 6207, pp. 352–5, 2014.

[29] D. Bichet, S. Blin, S. Feliciangeli, F. C. Chatelain, N. Bobak, and F. Lesage, "Silent but not dumb: How cellular trafficking and pore gating modulate expression of TWIK1

and THIK2," *Pflugers Arch. Eur. J. Physiol.*, vol. 467, no. 5, pp. 1121–1131, 2014.

[30] P. Enyedi and G. Czirják, "Molecular background of leak K^+ currents: two-pore domain potassium channels.," *Physiol. Rev.*, vol. 90, no. 2, pp. 559–605, Apr. 2010.

[31] E. M. Talley, G. Solorzano, Q. Lei, D. Kim, and D. a Bayliss, "Cns distribution of members of the two-pore-domain (KCNK) potassium channel family.," *J. Neurosci.*, vol. 21, no. 19, pp. 7491–7505, 2001.

[32] C. G. Chapman, H. J. Meadows, R. J. Godden, D. A. Campbell, M. Duckworth, R. E. Kelsell, P. R. Murdock, A. D. Randall, G. I. Rennie, and I. S. Gloger, "Cloning, localisation and functional expression of a novel human, cerebellum specific, two pore domain potassium channel," *Mol. Brain Res.*, vol. 82, no. 1–2, pp. 74–83, 2000.

[33] H. J. Meadows and A. D. Randall, "Functional characterisation of human TASK-3, an acid-sensitive two-pore domain potassium channel," *Neuropharmacology*, vol. 40, no. 4, pp. 551–559, 2001.

[34] J. Han, D. Kang, and D. Kim, "Functional properties of four splice variants of a human pancreatic tandem-pore K^+ channel, TALK-1.," *Am. J. Physiol. Cell Physiol.*, vol. 285, no. 3, pp. C529-38, 2003.

[35] N. Decher, M. Maier, W. Dittrich, J. Gassenhuber, A. Brüggemann, A. E. Busch, and K. Steinmeyer, "Characterization of TASK-4, a novel member of the pH-sensitive, two-pore domain potassium channel family," *FEBS Lett.*, vol. 492, no. 1–2, pp. 84–89, 2001.

[36] F. C. Chatelain, D. Bichet, D. Douguet, S. Feliciangeli, S. Bendahhou, M. Reichold, R. Warth, J. Barhanin, and F. Lesage, "TWIK1, a unique background channel with variable ion selectivity.," *Proc. Natl. Acad. Sci. U. S. A.*, vol. 109, no. 14, pp. 5499–504, Apr. 2012.

[37] F. Lesage, E. Guillemare, M. Fink, F. Duprat, M. Lazdunski, G. Romey, and J. Barhanin, "TWIK-1, a ubiquitous human weakly inward rectifying K^+ channel with a novel structure.," *EMBO J.*, vol. 15, no. 5, pp. 1004–11, 1996.

[38] R. B. Clark, C. Kondo, D. D. Belke, and W. R. Giles, "Two-pore domain K^+ channels regulate membrane potential of isolated human articular chondrocytes.," *J. Physiol.*, vol. 589, no. Pt 21, pp. 5071–89, 2011.

[39] O. Yarishkin, D. Y. Lee, E. Kim, C.-H. Cho, J. H. Choi, C. J. Lee, E. M. Hwang, J. Park, J.

C. Lee, E. M. Hwang, and J. Park, “TWIK-1 contributes to the intrinsic excitability of dentate granule cells in mouse hippocampus,” *Mol. Brain*, vol. 7, no. 1, pp. 1–11, 2014.

[40] P.-Y. Deng, S. K. S. Poudel, L. Rojanathammanee, J. E. Porter, and S. Lei, “Serotonin inhibits neuronal excitability by activating two-pore domain k^+ channels in the entorhinal cortex.,” *Mol. Pharmacol.*, vol. 72, no. 1, pp. 208–218, 2007.

[41] F. Lesage, R. Reyes, M. Fink, F. Duprat, E. Guillemare, and M. Lazdunski, “Dimerization of TWIK-1 K^+ channel subunits via a disulfide bridge,” *EMBO J.*, vol. 15, no. 23, pp. 6400–6407, 1996.

[42] C. M. B. Lopes, P. G. Gallagher, M. E. Buck, M. H. Butler, and S. A. N. Goldstein, “Proton block and voltage gating are potassium-dependent in the cardiac leak channel Kcnk3,” *J. Biol. Chem.*, vol. 275, no. 22, pp. 16969–16978, 2000.

[43] E. M. Talley and D. A. Bayliss, “Modulation of TASK-1 (Kcnk3) and TASK-3 (Kcnk9) potassium channels. Volatile anesthetics and neurotransmitters share a molecular site of action,” *J. Biol. Chem.*, vol. 277, no. 20, pp. 17733–17742, 2002.

[44] W. Gonzá lez, L. Zúniga, L. P. Cid, B. Arévalo, M. I. Niemeyer, and F. V. Sepúlveda, “An extracellular ion pathway plays a central role in the cooperative gating of a K2P K^+ channel by extracellular pH,” *J. Biol. Chem.*, vol. 288, no. 8, pp. 5984–5991, 2013.

[45] P. J. Stansfeld, A. Grottesi, Z. A. Sands, M. S. P. Sansom, P. Gedeck, M. Gosling, B. Cox, P. R. Stanfield, J. S. Mitcheson, and M. J. Sutcliffe, “Insight into the mechanism of inactivation and pH sensitivity in potassium channels from molecular dynamics simulations,” *Biochemistry*, vol. 47, no. 28, pp. 7414–7422, 2008.

[46] L. Ma, X. Zhang, M. Zhou, and H. Chen, “Acid-sensitive TWIK and TASK two-pore domain potassium channels change ion selectivity and become permeable to sodium in extracellular acidification,” *J. Biol. Chem.*, vol. 287, no. 44, pp. 37145–37153, 2012.

[47] K. Yuill, I. Ashmole, and P. R. Stanfield, “The selectivity filter of the tandem pore potassium channel TASK-1 and its pH-sensitivity and ionic selectivity,” *Pflugers Arch. Eur. J. Physiol.*, vol. 448, no. 1, pp. 63–69, 2004.

[48] L. Zúñiga, V. Márquez, F. D. González-Nilo, C. Chipot, L. P. Cid, F. V Sepúlveda, and M. I. Niemeyer, “Gating of a pH-sensitive K2P potassium channel by an electrostatic effect of basic sensor residues on the selectivity filter,” *PLoS One*, vol. 6, no. 1, p. e16141, Jan. 2011.

[49] M. I. Niemeyer, F. D. González-Nilo, L. Zúñiga, W. González, L. P. Cid, and F. V Sepúlveda, “Neutralization of a single arginine residue gates open a two-pore domain, alkali-activated K^+ channel.,” *Proc. Natl. Acad. Sci. U. S. A.*, vol. 104, no. 2, pp. 666–71, 2007.

[50] M. I. Niemeyer, L. P. Cid, G. Peña-Münzenmayer, and F. V Sepúlveda, “Separate gating mechanisms mediate the regulation of K2P potassium channel TASK-2 by intra- and extracellular pH.,” *J. Biol. Chem.*, vol. 285, no. 22, pp. 16467–75, May 2010.

[51] E. M. Talley, Q. Lei, J. E. Sirois, and D. A. Bayliss, “{TASK-1,} a two-pore domain K^+ channel, is modulated by multiple neurotransmitters in motoneurons.,” *Neuron*, vol. 25, no. 2, pp. 399–410, 2000.

[52] X. Chen, E. M. Talley, N. Patel, A. Gomis, W. E. McIntire, B. Dong, F. Viana, J. C. Garrison, and D. a Bayliss, “Inhibition of a background potassium channel by Gq protein alpha-subunits.,” *Proc. Natl. Acad. Sci. U. S. A.*, vol. 103, no. 9, pp. 3422–3427, 2006.

[53] B. U. Wilke, M. Lindner, L. Greifenberg, A. Albus, Y. Kronimus, M. Bünemann, M. G. Leitner, and D. Oliver, “Diacylglycerol mediates regulation of TASK potassium channels by Gq-coupled receptors.,” *Nat. Commun.*, vol. 5, no. May, p. 5540, 2014.

[54] F. Maingret, A. J. Patel, M. Lazdunski, and E. Honoré, “The endocannabinoid anandamide is a direct and selective blocker of the background K^+ channel TASK-1,” *EMBO J.*, vol. 20, no. 1–2, pp. 47–54, 2001.

[55] C. Añazco, G. Peña-Münzenmayer, C. Araya, L. P. Cid, F. V. Sepúlveda, and M. I. Niemeyer, “G protein modulation of K2P potassium channel TASK-2: A role of basic residues in the C terminus domain,” *Pflugers Arch. Eur. J. Physiol.*, vol. 465, no. 12, pp. 1715–1726, 2013.

[56] G. Peña-Münzenmayer, M. I. Niemeyer, F. V. Sepúlveda, and L. P. Cid, “Zebrafish and mouse TASK-2 K^+ channels are inhibited by increased CO2 and intracellular acidification,” *Pflugers Arch. Eur. J. Physiol.*, vol. 466, no. 7, pp. 1317–1327, 2014.

[57] S. S. Kirkegaard, I. H. Lambert, S. Gammeltoft, and E. K. Hoffmann, “Activation of the TASK-2 channel after cell swelling is dependent on tyrosine phosphorylation.,” *Am. J. Physiol. Cell Physiol.*, vol. 299, no. 4, pp. C844-53, 2010.

[58] F. Duprat, C. Girard, G. Jarretou, and M. Lazdunski, “Pancreatic two P domain K^+ channels TALK-1 and TALK-2 are activated by nitric oxide and reactive oxygen

species.," *J. Physiol.*, vol. 562, no. Pt 1, pp. 235–244, 2005.

[59] L. Ma, Y.-P. Xie, M. Zhou, and H. Chen, "Silent TWIK-1 potassium channels conduct monovalent cation currents.," *Biophys. J.*, vol. 102, no. 8, pp. L34-6, Apr. 2012.

[60] S. Feliciangeli, S. Bendahhou, G. Sandoz, P. Gounon, M. Reichold, R. Warth, M. Lazdunski, J. Barhanin, and F. Lesage, "Does Sumoylation Control K2P1/TWIK1 Background K^+ Channels?," *Cell*, vol. 130, no. 3, pp. 563–569, 2007.

[61] P. Aryal, F. Abd-wahab, G. Bucci, M. S. P. Sansom, and S. J. Tucker, "A hydrophobic barrier deep within the inner pore of the TWIK-1 K2P potassium channel," *Nat. Commun.*, vol. 5, pp. 1–9, 2014.

[62] M. Kilisch, O. Lytovchenko, B. Schwappach, V. Renigunta, and J. Daut, "The role of protein-protein interactions in the intracellular traffic of the potassium channels TASK-1 and TASK-3," *Pflugers Arch. Eur. J. Physiol.*, vol. 467, no. 5, pp. 1105–1120, 2015.

[63] S. Rinné, A. K. Kiper, G. Schlichthörl, S. Dittmann, M. F. Netter, S. H. Limberg, N. Silbernagel, M. Zuzarte, R. Moosdorf, H. Wulf, E. Schulze-Bahr, C. Rolfes, and N. Decher, "TASK-1 and TASK-3 may form heterodimers in human atrial cardiomyocytes," *J. Mol. Cell. Cardiol.*, vol. 81, pp. 71–80, 2015.

[64] K. Endo, N. Kurokawa, H. Kito, S. Nakakura, M. Fujii, and S. Ohya, "Molecular identification of the dominant-negative, splicing isoform of the two-pore domain K^+ channel K2P5.1 in lymphoid cells and enhancement of its expression by splicing inhibition," *Biochem. Pharmacol.*, vol. 98, no. 3, pp. 440–452, 2015.

[65] S. Decressac, M. Franco, S. Bendahhou, R. Warth, S. Knauer, J. Barhanin, M. Lazdunski, and F. Lesage, "ARF6-dependent interaction of the TWIK1 K^+ channel with EFA6, a GDP/GTP exchange factor for ARF6.," *EMBO Rep.*, vol. 5, no. 12, pp. 1171–5, 2004.

[66] S. Feliciangeli, M. P. Tardy, G. Sandoz, F. C. Chatelain, R. Warth, J. Barhanin, S. Bendahhou, and F. Lesage, "Potassium channel silencing by constitutive endocytosis and intracellular sequestration," *J. Biol. Chem.*, vol. 285, no. 7, pp. 4798–4805, Feb. 2010.

[67] W. Wang, C. M. Kiyoshi, Y. Du, B. Ma, C. C. Alford, H. Chen, and M. Zhou, "mGluR3 Activation Recruits Cytoplasmic TWIK-1 Channels to Membrane that Enhances Ammonium Uptake in Hippocampal Astrocytes," *Mol. Neurobiol.*, vol. 53, no. 9, pp. 6169–6182, 2016.

[68] A. P. Berg, E. M. Talley, J. P. Manger, and D. A. Bayliss, “Motoneurons express heteromeric TWIK-related acid-sensitive K^+ (TASK) channels containing TASK-1 (KCNK3) and TASK-3 (KCNK9) subunits,” *J Neurosci*, vol. 24, no. 30, pp. 6693–6702, 2004.

[69] L. D. Plant, L. Zuniga, D. Araki, J. D. Marks, and S. A. N. Goldstein, “SUMOylation Silences Heterodimeric TASK Potassium Channels Containing K2P1 Subunits in Cerebellar Granule Neurons,” *Sci. Signal.*, vol. 5, no. 251, p. ra84-ra84, Nov. 2012.

[70] S. G. Meuth, T. Budde, T. Kanyshkova, T. Broicher, T. Munsch, and H.-C. Pape, “Contribution of TWIK-related acid-sensitive K^+ channel 1 (TASK1) and TASK3 channels to the control of activity modes in thalamocortical neurons.,” *J. Neurosci.*, vol. 23, no. 16, pp. 6460–6469, 2003.

[71] E. A. Steinberg, K. A. Wafford, S. G. Brickley, N. P. Franks, and W. Wisden, “The role of K2P channels in anaesthesia and sleep,” *Pflugers Arch. Eur. J. Physiol.*, vol. 467, no. 5, pp. 907–916, 2014.

[72] D. S. J. Pang, C. J. Robledo, D. R. Carr, T. C. Gent, A. L. Vyssotski, A. Caley, A. Y. Zecharia, W. Wisden, S. G. Brickley, and N. P. Franks, “An unexpected role for TASK-3 potassium channels in network oscillations with implications for sleep mechanisms and anesthetic action.,” *Proc. Natl. Acad. Sci. U. S. A.*, vol. 106, no. 41, pp. 17546–17551, 2009.

[73] A.-M. Linden, C. Sandu, M. I. Aller, O. Y. Vekovischeva, P. H. Rosenberg, W. Wisden, and E. R. Korpi, “TASK-3 knockout mice exhibit exaggerated nocturnal activity, impairments in cognitive functions, and reduced sensitivity to inhalation anesthetics.,” *J. Pharmacol. Exp. Ther.*, vol. 323, no. 3, pp. 924–934, 2007.

[74] A. L. Gotter, V. P. Santarelli, S. M. Doran, P. L. Tannenbaum, R. L. Kraus, T. W. Rosahl, H. Meziane, M. Montial, D. R. Reiss, K. Wessner, A. McCampbell, J. Stevens, J. I. Brunner, S. V. Fox, V. N. Uebele, D. A. Bayliss, C. J. Winrow, and J. J. Renger, “TASK-3 as a potential antidepressant target,” *Brain Res.*, vol. 1416, pp. 69–79, 2011.

[75] M. T. Vu, G. Du, D. A. Bayliss, and R. L. Horner, “TASK Channels on Basal Forebrain Cholinergic Neurons Modulate Electrocortical Signatures of Arousal by Histamine.,” *J. Neurosci.*, vol. 35, no. 40, pp. 13555–67, 2015.

[76] A.-M. Linden, M. I. Aller, E. Leppä, O. Vekovischeva, T. Aitta-Aho, E. L. Veale, A. Mathie, P. Rosenberg, W. Wisden, and E. R. Korpi, “The *in vivo* contributions of TASK-1-containing channels to the actions of inhalation anesthetics, the alpha(2)

adrenergic sedative dexmedetomidine, and cannabinoid agonists.," *J. Pharmacol. Exp. Ther.*, vol. 317, no. 2, pp. 615–626, 2006.

[77] A. G. Holt, M. Asako, R. Keith Duncan, C. A. Lomax, J. M. Juiz, and R. A. Altschuler, "Deafness associated changes in expression of two-pore domain potassium channels in the rat cochlear nucleus," *Hear. Res.*, vol. 216–217, no. 1–2, pp. 146–153, 2006.

[78] K. J. Buckler, "TASK channels in arterial chemoreceptors and their role in oxygen and acid sensing.," *Pflugers Arch.*, vol. 467, no. 5, pp. 1013–25, 2015.

[79] K. J. Buckler, B. A. Williams, and E. Honore, "An oxygen-, acid- and anaesthetic-sensitive TASK-like background potassium channel in rat arterial chemoreceptor cells," *J. Physiol.*, vol. 525, no. 1, pp. 135–142, 2000.

[80] D. Kim, E. J. Cavanaugh, I. Kim, and J. L. Carroll, "Heteromeric TASK-1/TASK-3 is the major oxygen-sensitive background K^+ channel in rat carotid body glomus cells.," *J. Physiol.*, vol. 587, no. Pt 12, pp. 2963–75, 2009.

[81] S. Trapp, M. I. Aller, W. Wisden, and A. V Gourine, "A role for TASK-1 (KCNK3) channels in the chemosensory control of breathing.," *J. Neurosci.*, vol. 28, no. 35, pp. 8844–50, Aug. 2008.

[82] Y. Bando, T. Hirano, and Y. Tagawa, "Dysfunction of KCNK potassium channels impairs neuronal migration in the developing mouse cerebral cortex," *Cereb. Cortex*, vol. 24, no. 4, pp. 1017–1029, 2014.

[83] O. Barel, S. A. Shalev, R. Ofir, A. Cohen, J. Zlotogora, Z. Shorer, G. Mazor, G. Finer, S. Khateeb, N. Zilberberg, and O. S. Birk, "Maternally Inherited Birk Barel Mental Retardation Dysmorphism Syndrome Caused by a Mutation in the Genomically Imprinted Potassium Channel KCNK9," *Am. J. Hum. Genet.*, vol. 83, no. 2, pp. 193–199, 2008.

[84] I. Lauritzen, M. Zanzouri, E. Honoré, F. Duprat, M. U. Ehrengruber, M. Lazdunski, and A. J. Patel, "K^+-dependent cerebellar granule neuron apoptosis. Role of TASK leak K^+ channels," *J. Biol. Chem.*, vol. 278, no. 34, pp. 32068–32076, 2003.

[85] D. Heitzmann, R. Derand, S. Jungbauer, S. Bandulik, C. Sterner, F. Schweda, A. El Wakil, E. Lalli, N. Guy, R. Mengual, M. Reichold, I. Tegtmeier, S. Bendahhou, C. E. Gomez-Sanchez, M. Isabel Aller, W. Wisden, A. Weber, F. Lesage, R. Warth, and J. Barhanin, "Invalidation of TASK1 potassium channels disrupts adrenal gland zonation and mineralocorticoid homeostasis," *EMBO J.*, vol. 27, no. 1, pp. 179–187,

2007.

[86] L. A. Davies, C. Hu, N. A. Guagliardo, N. Sen, X. Chen, E. M. Talley, R. M. Carey, D. A. Bayliss, and P. Q. Barrett, “TASK channel deletion in mice causes primary hyperaldosteronism.,” *Proc. Natl. Acad. Sci. U. S. A.*, vol. 105, no. 6, pp. 2203–8, 2008.

[87] J. Jung, P. Q. Barrett, G. J. Eckert, H. J. Edenberg, X. Xuei, W. Tu, and J. H. Pratt, “Variations in the potassium channel genes KCNK3 and KCNK9 in relation to blood pressure and aldosterone production: An exploratory study,” *J. Clin. Endocrinol. Metab.*, vol. 97, no. 11, pp. 2160–2167, 2012.

[88] S. Muhammad, M. I. Aller, C. Maser-Gluth, M. Schwaninger, and W. Wisden, “Expression of the kcnk3 potassium channel gene lessens the injury from cerebral ischemia, most likely by a general influence on blood pressure,” *Neuroscience*, vol. 167, no. 3, pp. 758–764, 2010.

[89] J. A. Millar, L. Barratt, A. P. Southan, K. M. Page, R. E. W. Fyffe, B. Robertson, and A. Mathie, “A functional role for the two-pore domain potassium channel TASK-1 in cerebellar granule neurons,” *Proc. Natl. Acad. Sci.*, vol. 97, no. 7, pp. 3614–3618, 2000.

[90] S. G. Brickley, M. I. Aller, C. Sandu, E. L. Veale, F. G. Alder, H. Sambi, A. Mathie, and W. Wisden, “TASK-3 Two-Pore Domain Potassium Channels Enable Sustained High-Frequency Firing in Cerebellar Granule Neurons,” *J. Neurosci.*, vol. 27, no. 35, pp. 9329–9340, 2007.

[91] C. Putzke, K. Wemhöner, F. B. Sachse, S. Rinné, G. Schlichthörl, X. T. Li, L. Jaé, I. Eckhardt, E. Wischmeyer, H. Wulf, R. Preisig-Müller, J. Daut, and N. Decher, “The acid-sensitive potassium channel TASK-1 in rat cardiac muscle,” *Cardiovasc. Res.*, vol. 75, no. 1, pp. 59–68, 2007.

[92] G. Boachie-Ansah, K. A. Kane, and A. C. Rankin, “Effects of a combination of acidosis, lactate, and lysophosphatidylcholine on action potentials and ionic currents in guinea pig ventricular myocytes.,” *Journal of cardiovascular pharmacology*, vol. 20, no. 4. pp. 538–546, 1992.

[93] N. Decher, K. Wemhöner, S. Rinné, M. F. Netter, M. Zuzarte, M. I. Aller, S. G. Kaufmann, X. T. Li, S. G. Meuth, J. Daut, F. B. Sachse, and S. K. G. Maier, “Knock-out of the potassium channel TASK-1 leads to a prolonged qt interval and a disturbed QRS complex,” *Cell. Physiol. Biochem.*, vol. 28, no. 1, pp. 77–86, 2011.

[94] S. H. Limberg, M. F. Netter, C. Rolfes, S. Rinné, G. Schlichthörl, M. Zuzarte, T. Vassiliou, R. Moosdorf, H. Wulf, J. Daut, F. B. Sachse, and N. Decher, "TASK-1 channels may modulate action potential duration of human atrial cardiomyocytes," *Cell. Physiol. Biochem.*, vol. 28, no. 4, pp. 613–624, 2011.

[95] A. S. Barth, S. Merk, E. Arnoldi, L. Zwermann, P. Kloos, M. Gebauer, K. Steinmeyer, M. Bleich, S. Kääb, M. Hinterseer, H. Kartmann, E. Kreuzer, M. Dugas, G. Steinbeck, and M. Nabauer, "Reprogramming of the human atrial transcriptome in permanent atrial fibrillation: Expression of a ventricular-like genomic signature," *Circ. Res.*, vol. 96, no. 9, pp. 1022–1029, 2005.

[96] J. E. Kim, S. E. Kwak, and T. C. Kang, "Upregulated TWIK-related acid-sensitive K^+ channel-2 in neurons and perivascular astrocytes in the hippocampus of experimental temporal lobe epilepsy," *Epilepsia*, vol. 50, no. 4, pp. 654–663, 2009.

[97] C. Gestreau, D. Heitzmann, J. Thomas, V. Dubreuil, S. Bandulik, M. Reichold, S. Bendahhou, P. Pierson, C. Sterner, J. Peyronnet-Roux, C. Benfriha, I. Tegtmeier, H. Ehnes, M. Georgieff, F. Lesage, J.-F. Brunet, C. Goridis, R. Warth, and J. Barhanin, "Task2 potassium channels set central respiratory CO2 and O2 sensitivity.," *Proc. Natl. Acad. Sci. U. S. A.*, vol. 107, no. 5, pp. 2325–30, 2010.

[98] S. Wang, N. Benamer, S. Zanella, N. N. Kumar, Y. Shi, M. Bevengut, D. Penton, P. G. Guyenet, F. Lesage, C. Gestreau, J. Barhanin, and D. A. Bayliss, "TASK-2 Channels Contribute to pH Sensitivity of Retrotrapezoid Nucleus Chemoreceptor Neurons," *J. Neurosci.*, vol. 33, no. 41, pp. 16033–16044, 2013.

[99] H. Barriere, R. Belfodil, I. Rubera, M. Tauc, F. Lesage, C. Poujeol, N. Guy, J. Barhanin, and P. Poujeol, "Role of TASK2 potassium channels regarding volume regulation in primary cultures of mouse proximal tubules.," *J. Gen. Physiol.*, vol. 122, no. 2, pp. 177–90, 2003.

[100] M. I. Niemeyer, L. P. Cid, L. F. Barros, and F. V. Sepúlveda, "Modulation of the Two-pore Domain Acid-sensitive K^+ Channel TASK-2 (KCNK5) by Changes in Cell Volume," *J. Biol. Chem.*, vol. 276, no. 46, pp. 43166–43174, 2001.

[101] S. L'Hoste, H. Barriere, R. Belfodil, I. Rubera, C. Duranton, M. Tauc, C. Poujeol, J. Barhanin, and P. Poujeol, "Extracellular pH alkalinization by Cl-/HCO_3^- exchanger is crucial for TASK2 activation by hypotonic shock in proximal cell lines from mouse kidney.," *Am. J. Physiol. Renal Physiol.*, vol. 292, no. 2, pp. F628–F638, 2007.

[102] R. Warth, H. Barrière, P. Meneton, M. Bloch, J. Thomas, M. Tauc, D. Heitzmann, E. Romeo, F. Verrey, R. Mengual, N. Guy, S. Bendahhou, F. Lesage, P. Poujeol, and J.

Barhanin, “Proximal renal tubular acidosis in TASK2 K^+ channel-deficient mice reveals a mechanism for stabilizing bicarbonate transport.,” *Proc. Natl. Acad. Sci. U. S. A.*, vol. 101, no. 21, pp. 8215–8220, 2004.

[103] S. L’Hoste, M. Poet, C. Duranton, R. Belfodil, H. É. Barriere, I. Rubera, M. Tauc, C. Poujeol, J. Barhanin, and P. Poujeol, “Role of TASK2 in the control of apoptotic volume decrease in proximal kidney cells,” *J. Biol. Chem.*, vol. 282, no. 50, pp. 36692–36703, 2007.

[104] S. Bittner, N. Bobak, A. M. Herrmann, K. Göbel, P. Meuth, K. G. Höhn, M. P. Stenner, T. Budde, H. Wiendl, and S. G. Meuth, “Upregulation of K2P5.1 potassium channels in multiple sclerosis,” *Ann. Neurol.*, vol. 68, no. 1, pp. 58–69, 2010.

[105] C. P. Alvarez-Baron, P. Jonsson, C. Thomas, S. E. Dryer, and C. Williams, “The two-pore domain potassium channel KCNK5: induction by estrogen receptor alpha and role in proliferation of breast cancer cells.,” *Mol. Endocrinol.*, vol. 25, no. 8, pp. 1326–36, 2011.

[106] A. Mobasheri, R. Lewis, A. Ferreira-Mendes, A. Rufino, C. Dart, and R. Barrett-Jolley, “Potassium channels in articular chondrocytes,” *Channels*, vol. 6, no. 6, pp. 416–425, 2012.

[107] R. W. Wrenn, M. G. Currie, and L. E. Herman, “Nitric oxide participates in the regulation of pancreatic acinar cell secretion,” *Life Sci.*, vol. 55, no. 7, pp. 511–518, 1994.

[108] W. Wang, A. Putra, G. P. Schools, B. Ma, H. Chen, L. K. Kaczmarek, J. Barhanin, F. Lesage, and M. Zhou, “The contribution of TWIK-1 channels to astrocyte K^+ current is limited by retention in intracellular compartments.,” *Front. Cell. Neurosci.*, vol. 7, no. December, p. 246, 2013.

[109] X. Nie, I. Arrighi, B. Kaissling, I. Pfaff, J. Mann, J. Barhanin, and V. Vallon, “Expression and insights on function of potassium channel TWIK-1 in mouse kidney,” *Pflugers Arch. Eur. J. Physiol.*, vol. 451, no. 3, pp. 479–488, 2005.

[110] H. Sun, L. Luo, B. Lal, X. Ma, L. Chen, C. L. Hann, A. M. Fulton, D. J. Leahy, J. Laterra, and M. Li, “A monoclonal antibody against KCNK9 K^+ channel extracellular domain inhibits tumour growth and metastasis,” *Nat Commun*, vol. 7, pp. 1–12, 2016.

[111] S. Bittner, S. G. Meuth, K. Göbel, N. Melzer, A. M. Herrmann, O. J. Simon, A. Weishaupt, T. Budde, D. A. Bayliss, M. Bendszus, and H. Wiendl, “TASK1 modulates inflammation and neurodegeneration in autoimmune inflammation of the central

nervous system," *Brain*, vol. 132, no. 9, pp. 2501–2516, 2009.

[112] C. Schmidt, F. Wiedmann, N. Voigt, X.-B. Zhou, J. Heijman, S. Lang, V. Albert, S. Kallenberger, A. Ruhparwar, G. Szabó, K. Kallenbach, M. Karck, M. Borggrefe, P. Biliczki, J. R. Ehrlich, I. Baczkó, P. Lugenbiel, P. a. Schweizer, B. C. Donner, H. a. Katus, D. Dobrev, and D. Thomas, "Upregulation of K_{2P} 3.1 K^+ Current Causes Action Potential Shortening in Patients With Chronic Atrial FibrillationCLINICAL PERSPECTIVE," *Circulation*, vol. 132, no. 2, pp. 82–92, 2015.

[113] B. Liang, M. Soka, A. H. Christensen, M. S. Olesen, A. P. Larsen, F. K. Knop, F. Wang, J. B. Nielsen, M. N. Andersen, D. Humphreys, S. A. Mann, I. G. Huttner, J. I. Vandenberg, J. H. Svendsen, S. Haunsø, T. Preiss, G. Seebohm, S. P. Olesen, N. Schmitt, and D. Fatkin, "Genetic variation in the two-pore domain potassium channel, TASK-1, may contribute to an atrial substrate for arrhythmogenesis," *J. Mol. Cell. Cardiol.*, vol. 67, pp. 69–76, 2014.

[114] L. Ma, D. Roman-Campos, E. D. Austin, M. Eyries, K. S. Sampson, F. Soubrier, M. Germain, D.-A. Trégouët, A. Borczuk, E. B. Rosenzweig, B. Girerd, D. Montani, M. Humbert, J. E. Loyd, R. S. Kass, and W. K. Chung, "A Novel Channelopathy in Pulmonary Arterial Hypertension," *N. Engl. J. Med.*, vol. 369, no. 4, pp. 351–361, 2013.

[115] D. Mu, L. Chen, X. Zhang, L. H. See, C. M. Koch, C. Yen, J. J. Tong, L. Spiegel, K. C. Q. Nguyen, A. Servoss, Y. Peng, L. Pei, J. R. Marks, S. Lowe, T. Hoey, L. Y. Jan, W. R. McCombie, M. H. Wigler, and S. Powers, "Genomic amplification and oncogenic properties of the KCNK9 potassium channel gene," *Cancer Cell*, vol. 3, no. 3, pp. 297–302, 2003.

[116] S. Bittner, N. Bobak, M. Feuchtenberger, A. M. Herrmann, K. Göbel, R. W. Kinne, A. J. Hansen, T. Budde, C. Kleinschnitz, O. Frey, H.-P. Tony, H. Wiendl, and S. G. Meuth, "Expression of K2P5.1 potassium channels on CD4+ T lymphocytes correlates with disease activity in rheumatoid arthritis patients.," *Arthritis Res. Ther.*, vol. 13, no. 1, p. R21, 2011.

[117] C. Friedrich, S. Rinné, S. Zumhagen, A. K. Kiper, N. Silbernagel, M. F. Netter, B. Stallmeyer, E. Schulze-Bahr, and N. Decher, "Gain-of-function mutation in TASK-4 channels and severe cardiac conduction disorder.," *EMBO Mol. Med.*, vol. 6, no. 7, pp. 937–51, 2014.

[118] S. A. N. Goldstein, "K2P potassium channels, mysterious and paradoxically exciting.," *Sci. Signal.*, vol. 4, no. 184, p. pe35, Jul. 2011.

[119] M. Beitzinger, L. Hofmann, C. Oswald, R. Beinoraviciute-Kellner, M. Sauer, H. Griesmann, A. C. Bretz, C. Burek, A. Rosenwald, and T. Stiewe, “P73 Poses a Barrier To Malignant Transformation By Limiting Anchorage-Independent Growth.,” *EMBO J.*, vol. 27, no. 5, pp. 792–803, 2008.

[120] D. M. Bautista, Y. M. Sigal, A. D. Milstein, J. L. Garrison, J. A. Zorn, P. R. Tsuruda, R. A. Nicoll, and D. Julius, “Pungent agents from Szechuan peppers excite sensory neurons by inhibiting two-pore potassium channels.,” *Nat. Neurosci.*, vol. 11, no. 7, pp. 772–779, 2008.

[121] R. H. Chokshi, A. T. Larsen, B. Bhayana, and J. F. Cotten, “Breathing Stimulant Compounds Inhibit TASK-3 Potassium Channel Function Likely by Binding at a Common Site in the Channel Pore,” *Mol. Pharmacol.*, vol. 88, pp. 926–934, 2015.

[122] A. K. Streit, M. F. Netter, F. Kempf, M. Walecki, S. Rinné, M. K. Bollepalli, R. Preisig-Müller, V. Renigunta, J. Daut, T. Baukrowitz, M. S. P. Sansom, P. J. Stansfeld, and N. Decher, “A specific two-pore domain potassium channel blocker defines the structure of the TASK-1 open pore.,” *J. Biol. Chem.*, vol. 286, no. 16, pp. 13977–84, Apr. 2011.

[123] D. P. Flaherty, D. S. Simpson, M. Miller, B. E. Maki, B. Zou, J. Shi, M. Wu, O. B. McManus, J. Aubé, M. Li, and J. E. Golden, “Potent and selective inhibitors of the TASK-1 potassium channel through chemical optimization of a bis-amide scaffold,” *Bioorganic Med. Chem. Lett.*, vol. 24, no. 16, pp. 3968–3973, 2014.

[124] C. A. Coburn, Y. Luo, M. Cui, J. Wang, R. Soll, J. Dong, B. Hu, M. A. Lyon, V. P. Santarelli, R. L. Kraus, Y. Gregan, Y. Wang, S. V. Fox, J. Binns, S. M. Doran, D. R. Reiss, P. L. Tannenbaum, A. L. Gotter, P. T. Meinke, and J. J. Renger, “Discovery of a pharmacologically active antagonist of the two-pore-domain potassium channel K 2P9.1 (TASK-3),” *ChemMedChem*, vol. 7, no. 1, pp. 123–133, 2012.

[125] E. L. Veale, R. Buswell, C. E. Clarke, and a Mathie, “Identification of a region in the TASK3 two pore domain potassium channel that is critical for its blockade by methanandamide.,” *Br. J. Pharmacol.*, vol. 152, no. 5, pp. 778–786, 2007.

[126] M. Schewe, E. Nematian-Ardestani, H. Sun, M. Musinszki, S. Cordeiro, G. Bucci, B. L. de Groot, S. J. Tucker, M. Rapedius, T. Baukrowitz, and T. Baukrowitz, “A Non-canonical Voltage-Sensing Mechanism Controls Gating in K2P K^+ Channels,” *Cell*, vol. 164, no. 5, pp. 937–949, Feb. 2016.

[127] P. L. Smith, T. Baukrowitz, and G. Yellen, “The inward rectification mechanism of the HERG cardiac potassium channel.,” *Nature*, vol. 379, no. 6568. pp. 833–6, 1996.

[128] T. Yoshida, R. Inoue, T. Morii, N. Takahashi, S. Yamamoto, Y. Hara, M. Tominaga, S. Shimizu, Y. Sato, and Y. Mori, “Nitric oxide activates TRP channels by cysteine S-nitrosylation.,” *Nat. Chem. Biol.*, vol. 2, no. 11, pp. 596–607, 2006.

[129] F. Maingret, E. Honoré, M. Lazdunski, and A. J. Patel, “Molecular basis of the voltage-dependent gating of TREK-1, a mechano-sensitive K^+ channel.,” *Biochem. Biophys. Res. Commun.*, vol. 292, no. 2, pp. 339–346, 2002.

[130] M. Fink, F. Duprat, F. Lesage, R. Reyes, G. Romey, C. Heurteaux, and M. Lazdunskil, “Cloning, functional expression and brain localization of a novel unconventional outward rectifier K^+ channel,” *EMBO J.*, vol. 15, no. 24, pp. 6854–6862, 1996.

[131] G. MacKenzie, N. P. Franks, and S. G. Brickley, “Two-pore domain potassium channels enable action potential generation in the absence of voltage-gated potassium channels,” *Pflugers Arch. Eur. J. Physiol.*, pp. 989–999, 2014.

[132] D. Bockenhauer, N. Zilberberg, and S. a Goldstein, “KCNK2: reversible conversion of a hippocampal potassium leak into a voltage-dependent channel.,” *Nat. Neurosci.*, vol. 4, no. 5, pp. 486–91, May 2001.

[133] V. Oakes, S. Furini, D. Pryde, and C. Domene, “Exploring the Dynamics of the TWIK-1 Channel,” *Biophys. J.*, vol. 111, no. 4, pp. 775–784, 2016.

[134] C. M. B. Lopes, N. Zilberberg, and S. A. N. Goldstein, “Block of Kcnk3 by protons: Evidence that 2-P-domain potassium channel subunits function as homodimers,” *J. Biol. Chem.*, vol. 276, no. 27, pp. 24449–24452, 2001.

[135] I. Ashmole, D. V Vavoulis, P. J. Stansfeld, P. R. Mehta, J. F. Feng, M. J. Sutcliffe, and P. R. Stanfield, “The response of the tandem pore potassium channel TASK-3 (K(2P)9.1) to voltage: gating at the cytoplasmic mouth.,” *J. Physiol.*, vol. 587, no. Pt 20, pp. 4769–83, Oct. 2009.

[136] F. Lesage, E. Guillemare, M. Fink, F. Duprat, M. Lazdunski, G. Romey, and J. Barhanin, “A pH-sensitive yeast outward rectifier K^+ channel with two pore domains and novel gating properties,” *J. Biol. Chem.*, vol. 271, no. 8, pp. 4183–4187, 1996.

[137] X. Y. Ma, J. M. Yu, S. Z. Zhang, X. Y. Liu, B. H. Wu, X. L. Wei, J. Q. Yan, H. L. Sun, H. T. Yan, and J. Q. Zheng, “External Ba^{2+} block of the two-pore domain potassium channel TREK-1 defines conformational transition in its selectivity filter,” *J. Biol. Chem.*, vol. 286, no. 46, pp. 39813–39822, 2011.

[138] J. E. Contreras, J. Chen, A. Y. Lau, V. Jogini, B. Roux, and M. Holmgren, “Voltage profile along the permeation pathway of an open channel,” *Biophys. J.*, vol. 99, no. 9, pp. 2863–2869, 2010.

[139] Y. Jiang, A. Lee, J. Chen, M. Cadene, B. T. Chait, and R. MacKinnon, “The open pore conformation of potassium channels.,” *Nature*, vol. 417, no. 6888, pp 523-546, 2002.

[140] M. Pusch, L. Bertorello, and F. Conti, “Gating and flickery block differentially affected by rubidium in homomeric KCNQ1 and heteromeric KCNQ1/KCNE1 potassium channels.,” *Biophys. J.*, vol. 78, no. 1, pp. 211–226, Jan. 2000.

Appendix

Abbreviations

Abbreviation	Term
CHO	Chinese hamster ovary
COS cells	cells being CV-1 (simian) in origin, and carrying the SV40 virus
hERG	the human ether-à-go-go-related gene
IV	current voltage
K_{ir}	inwardly rectifying K^+ channels
MTS-TBAO	8-(tributylammonium)octyl methanethiosulfonate bromide
pH_{ex}	extracellular pH
PIP2	phosphatidylinositol 4,5-bisphosphate
P_O	open probability
QA	quaternary ammonium
SF	selectivity filter
siRNA	small interfering RNA
SUMO	small ubiquitin-related modifier protein
TALK	TWIK-related alkaline pH activated K^+ channel
TASK	TWIK-related acid-sensitive K^+ channel
TEA	tetraethylammonium
THA	tetrahexylammonium
THIK	tandem pore-domain halothane inhibited K^+ channel
TOK	tandem pore domain, outwardly rectifying K^+ channel
TPA	tetrapentylammonium
TRAAK	TWIK-related arachidonic acid-stimulated K^+ channel
TREK	TWIK-related (2-pore domain) K^+ channel
TRESK	TWIK-related spinal cord potassium channel
TWIK	Tandem of P-domains in a weakly inward rectifying K^+ channel
WT	wild type

Eidesstattliche Erklärung

Ich erkläre hiermit, dass

mir die Promotionsordnung der Mathematisch-Naturwissenschaftlichen Fakultät der Christian-Albrechts-Universität zu Kiel bekannt ist;

die Abhandlung mit dem Titel:

„Identification and Characterization of a Novel Voltage Gating Mechanism in Extracellular-pH-sensitive K2P Channels“

- abgesehen von der Beratung durch meinen Betreuer:

Herrn Prof. Dr. Thomas Baukrowitz – nach Inhalt und Form die eigene Arbeit ist;

weder Teile aus der Arbeit, noch die vollständige Arbeit einer anderen Stelle im Rahmen eines Prüfungsverfahrens vorgelegen hat, veröffentlicht worden ist, oder zur Veröffentlichung eingereicht wurde;

ich die Hilfe eines Promotionsberaters nicht in Anspruch genommen habe;

und die Arbeit unter Einhaltung der Regeln guter wissenschaftlicher Praxis der Deutschen Forschungsgemeinschaft entstanden ist.

Kiel, den 24.07.2017 …….....

Ehsanollah Nematian Ardestani